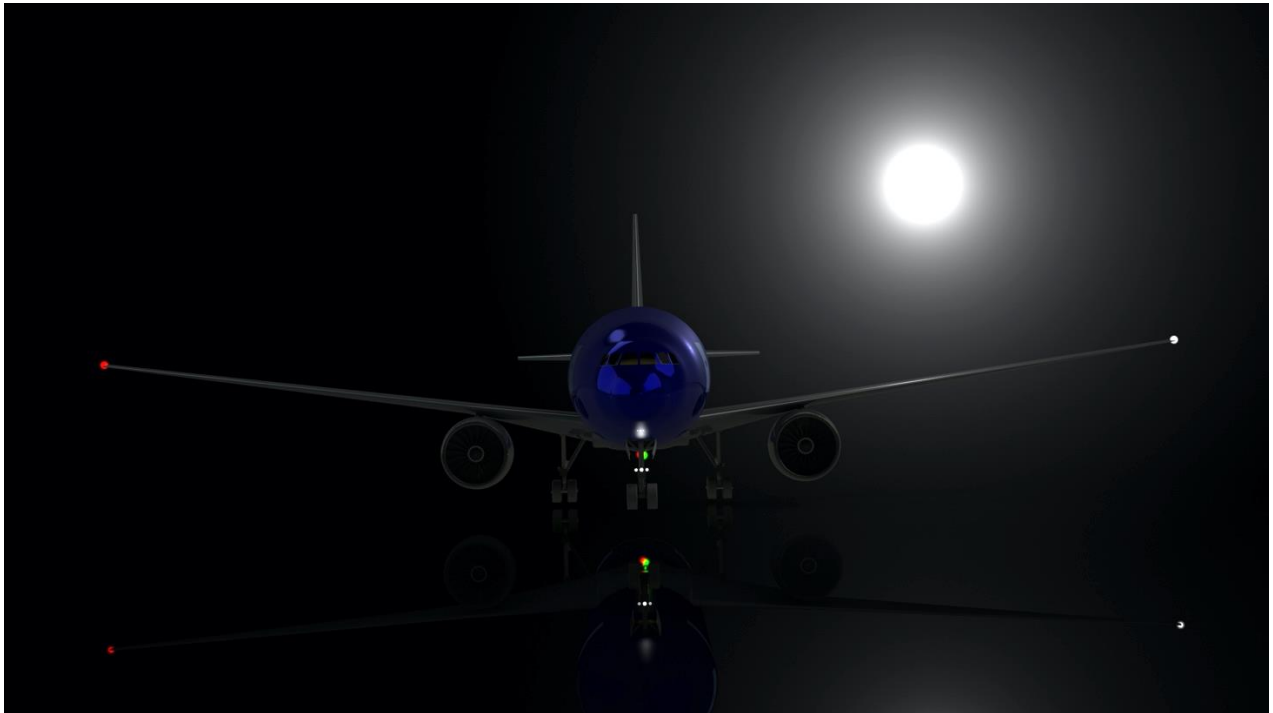# High Capacity Short Range Transport Aircraft

Final Design Report

By: Connor Flanagan, Luke DiStasio, Omar Abed, Mitchell Foster, Eitan
Ghelman, Jeffrey Hernandez, Hamid Nazemi, Eric Richter, Abdulrahman Shuraym

May 14, 2020

Condor Aviation Design Team

Omar Abed
CAD
AIAA 937419

Luke DiStasio
Aerodynamics, Materials,
Structures
AIAA 1098428
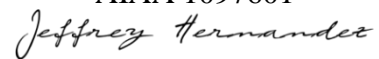
Connor Flanagan
Subsystems
AIAA 1097608

Mitchell Foster
Cost, Business Case
AIAA 1097599

Eitan Ghelman
Business Case
AIAA 1098432

Jeffrey Hernandez
Propulsion, Performance
AIAA 1097601

Hamid Nazemi
CAD, Configuration
Selection
AIAA 1098044

Eric Richter
Sizing, Performance,
CG/Stability
AIAA 1097607

Abdulrahman Shuraym
Performance, Stability
AIAA 933856

Condor Aviation Advisors

Neil Weston
Faculty Advisor

Carl Johnson
Faculty Advisor

Contents

List of Figuress

List of Tables

List of Abbreviations

APU	Auxiliary Power Unit
BOM	Mumbai airport code
CG	Center of Gravity
CASM	Cost per available seat-mile
CERs	Cost estimating relationships
CF	Complexity factor
CFRP	Carbon fiber reinforced plastic
CGK	Jakarta airport code
CJU	Jeju airport code
CTS	Sapporo airport code
$C_{L\alpha}$	Coefficient of lift derivative with respect to angle of attack
$C_{m\alpha}$	Coefficient of pitching moment derivative with respect to angle of attack
C_{mq}	Coefficient of pitching moment derivative with respect to pitch rate
$C_{S\beta}$	Coefficient of sideslip force derivative with respect to sideslip angle
$C_{n\beta}$	Coefficient of yaw moment derivative with respect to sideslip angle
$C_{l\beta}$	Coefficient of roll moment derivative with respect to sideslip angle
C_{lp}	Coefficient of roll moment derivative with respect to roll rate
C_{nr}	Coefficient of yaw moment derivative with respect to yaw rate
DEL	Delhi Indira Gandhi airport code
FL	Flight Level
FUK	Fukuoka airport code
GMP	Seoul airport code
HAN	Hanoi airport code

HKG	Hong Kong airport code
HND	Tokyo Haneda airport code
ICAO	International Civil Aviation Organization
KCAS	Knots Calibrated Airspeed
KEAS	Knots Equivalent Airspeed
MEL	Melbourne airport code
MGW	Maximum Gross Weight
MMH/FH	Maintenance-man-hours per flight hour
MTOW	Maximum Takeoff Weight
MZFW	Maximum Zero-Fuel Weight
OEW	Operating Empty Weight
OKA	Okinawa airport
PEK	Beijing Capital airport code
RASM	Revenue per available seat-mile
RDT&E	Research, development, test, and evaluation
RGF	Reference Geometry Factor
SAR	Specific Air Range
SGN	Tan Son Nhat Ho Chi Minh City airport code
SHA	Shanghai Hongqiao airport code
SUB	Juanda Surabaya airport code
SYD	Sydney Kingsford Smith airport code
WMCF	Weighted material cost factor
RFP	Request of proposal
FLOPS	Flight optimization system
M	Mach number

OEI	One engine inoperative
PA	Public Announcement
PMC	Prorate Manual – Cargo
V_a	Aircraft Maneuvering Speed`
V_b	Design Speed for Maximum Gust Intensity
V_c	Design Cruise Speed
V_d	Aircraft Dive Speed
TPE	Taiwan Taoyuan airport code

Introduction

This report is in response to a request for proposal (RFP) to design a high capacity short range transport aircraft and addresses design and technical requirements for such an aircraft. This report responds by looking at different vehicle configurations and picking one that makes the most sense for this use case. Based on the vehicle configuration, a variety of technical tasks such as detailed sizing, aerodynamics, structural, cost analysis and subsystems selection were performed. The report also demonstrates how certain parameters for the proposed aircraft were selected with different sensitivity studies to ensure that the aircraft is optimized for the specified mission designated in the RFP. The RFP indicated that the aircraft should be able to carry 400 passengers, have a range of 3,500 NM which places this aircraft in a size comparable to a Boeing 777 or Airbus A350, however, with significantly reduced range. The aircraft proposed in this report, named the Condor X, is similarly sized albeit in a much smaller weight class and with much lower acquisition and operating costs.

The demand for such an aircraft in today's world is very clear. For example, Emirates, now operates scheduled A380 Service between Dubai and Muscat, a mere 184 NM away. In the airline's configuration, the aircraft is used to haul 517 passengers on a 40-minute flight. Further, Emirates airlines operated this route with a 777-300ER which is itself a giant also designed for long-haul flights [1]. This popular route is clearly much shorter than what these aircraft are designed to fly (7000 – 8000 NM). So, the demand for a high passenger capacity optimized for short-haul routes becomes very clear. Within the gulf, the use of such aircraft is not unique to the Dubai-Muscat route as Emirates operated the A380 between Dubai and Kuwait City (461 NM), and now operates 777s on the same route. Beyond Emirates, other carriers like Turkish Airlines and Qatar Airways also operate long-range aircraft such as the A330 and 777 on their short-haul routes. The trend expands well beyond the gulf carriers to east Asia where domestic Japanese demand for short-haul high capacity airliners led Boeing to design the 747-400D, a denser version of the 747-400 without the winglets as the benefits of winglets would not even be realized on such short-haul routes. Similar routes are prevalent in China as well, where flights between Guangzhou and Beijing are often operated with 777-300s. This report aims to introduce an aircraft better suited for such missions and show what the optimal characteristics of such an aircraft would be.

Design Process

The design process of the Condor X aircraft is outlined in Figure 1. The first major steps were to review the aircraft system requirements from the RFP and develop an understanding of the market the requested aircraft fits into. From the market study, a detailed list of design criteria and performance indicators were identified as a baseline for what the aircraft should meet or exceed. These performance requirements were used in the initial configuration selection process. The starting point for weight sizing of the Condor X aircraft was a calibrated model of a Boeing 777-300ER in NASA's FLOPS tool. This provided a benchmark to allow sizing and performance comparisons to be verified between the designed Condor X aircraft and existing aircraft. Technology improvements in the areas of materials and sybsystems were factored into the Condor X model to reduce weight relative to the baseline. After calibrating the FLOPS model, trade studies were performed to optimize aircraft geometry as well as cruise altitude and Mach number. Component locations were altered as needed to meet aerodynamic stability and landing gear tip-over requirements. Aerodynamic and structural analyses were performed in parallel and the results were used in calibrating the FLOPS model to the final aircraft design. Various production and operations costs were then computed and compared to those of existing aircraft in order to assess the likely economic performance of the Condor X design.
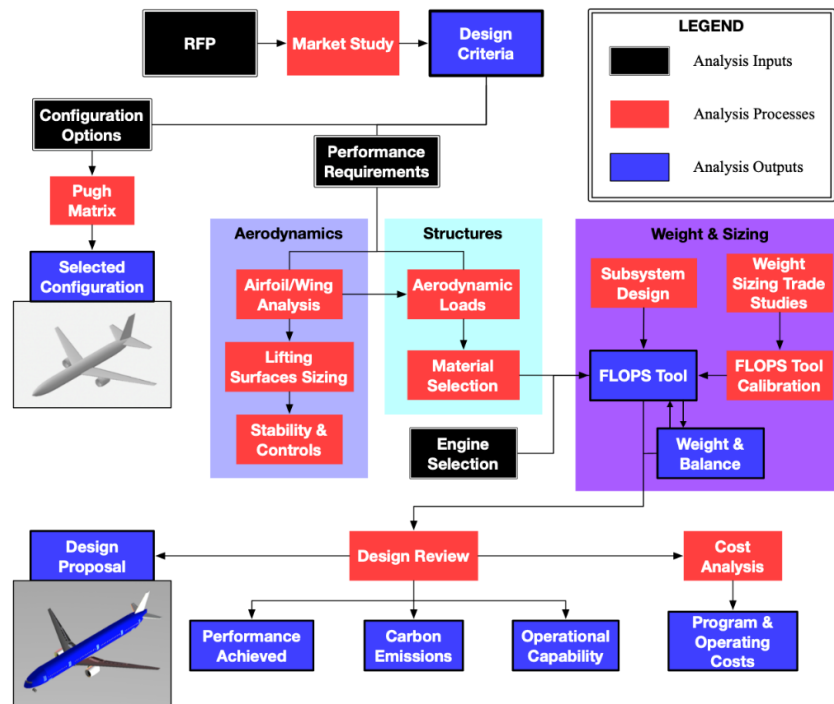
Figure 1. Condor X design process outline

The proposed design, rendered in Figure 2 and Figure 3, is a traditional airline transport aircraft configuration featuring two engines, a low two-section wing and a conventional tail stabilizer.

Figure 2. Condor X aircraft landing render

Figure 3. Condor X on the tarmac render

Concept of Operations

The Condor X is a high capacity, short range transportation aircraft that addresses the congestion of major commercial airports due to increase demand in air travel. The concept of the Condor X is to take 406 passengers in dual configurations to decrease the high-frequency of flying a specific route, such as the flight between Melbourne and Sydney in Australia or Jeju-si and Seoul in South Korea. These two routes have short range of less than 400 NM along with a high demand of more than 9 million passengers, which shows the demand for high capacity, short range aircrafts. The RFP objective is to design a transport aircraft capable of flying 3500 NM without the operation cost of long-range high-capacity transport aircraft. Thus, the Condor X is designed to travel 3500 NM with 406 passengers in dual configurations (56 business class and 350 economy class). Table I shows that the Condor X fulfills the mandatory and tradable requirements highlighted in the RFP.

Table I. Compliance matrix

Mandatory/ Tradable	Requirement description	Met Y/N
M	Capable of taking off and landing from runways (asphalt or concrete)	Y
M	Capable of VFR and IFR flight with an autopilot	Y
M	Capable of flight in known icing conditions	Y
M	Meets applicable certification rules in FAA 14 CFR Part 25	Y
M	Engine/propulsion system assumptions documented for engine entering service in 2029	Y
M	Price of Jet-A Fuel is $3.00 / Gallon + $3.00 / Gallon Carbon Tax	Y
M	400 passengers in a dual class: 50 Business 36" by 21", 350 Econ 32" by 18", 5 ft^3 baggage storage volume	Y
M	Galleys, Lavatories, and Exits layout that meets 14 CFR Part 25 requirement.	Y
M	Passenger/pilot/attendant weight 200 lb and baggage weights 30 lb	Y
M	3,500 NM. design range mission with reserve energy to meet 14 CFR Part 25 requirements	Y
M	Max takeoff length of 9,000' over a 35' obstacle at MTOW and sea level ISA + 15 degrees C	Y
M	Maximum Landing field length of 9,000' at Sea Level ISA +15 degrees C	Y
T	Approach speed 145 KCAS at the end of the design range mission	Y
T	Cabin pressurized to 8,000 ft pressure altitude at maximum flight altitude	Y
T	Crew: 2 pilots, 8 flight attendants	Y

Mission Profile

The Condor X was analyzed using two missions: the design mission shown in Figure 4 and a reference mission, which is shown in Figure 5. The purpose of the design mission is to define the aircraft's sizing and geometric parameters. An example of a flight resembling this mission is a direct flight from Los Angeles to New York. The reference mission was used to optimize the aircraft based on operation cost and maintenance and is analogous to frequently flown routes such as the route between Jeju-si and Seoul. The mission profiles were assembled by finding the optimum cruise altitude and the Mach number that consumed the least amount of fuel with the minimum required takeoff weight. The trade study section below details the results of changing the Mach number in both the reference and design mission. In FLOPS, climb and cruise is defined as a step block with a maximum and minimum altitude and Mach number, and the reserve mission was constructed to satisfy the NBAA requirement with a 200 NM cruise to an alternative airport and a 30 minute loiter. For detailed information about the design mission, see Table II.
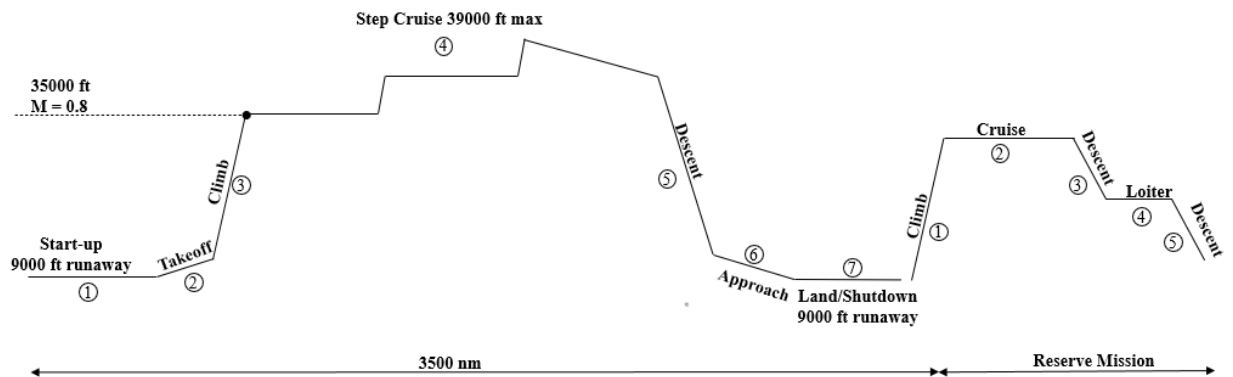
Figure 4. Design mission profile

Table II. Detailed design mission profile parameters

	Segment	Initial Weight (lb)	Fuel (lb)	Time (MIN)	Distance (NM)	Altitude (FT)	
1	TAXI OUT	421,026	652	14	~	0	0
2	TAKE OFF	420,373	1,165	2	~	0	0
3	CLIMB	419,209	7,403	19.3	127.4	0	35,000
4	CRUISE	411,806	29,816	182.6	1,403.6	35,000	35,000
3a	CLIMB	381,990	577	2.6	20.2	35,000	37,000
4a	CRUISE	381,413	27,078	176.7	1,351.6	37,000	37,000
3b	CLIMB	354,335	631	3.2	24.3	37,000	39,000
4b	CRUISE	353,704	8,182	55.6	425.1	39,000	35,098
5	DESCENT	345,521	1,288	28.4	148	35,098	1,500
6	APPROACH	344,234	373	4	~	~	~
	RESERVES	343,861	14,192	~	~	~	~
7	TAXI IN		233	5	~	~	~
	ZERO FUEL	329,669	~	~	~	~	~
	Total	~	**91,590**	**493.4**	**3,500.2**	~	~
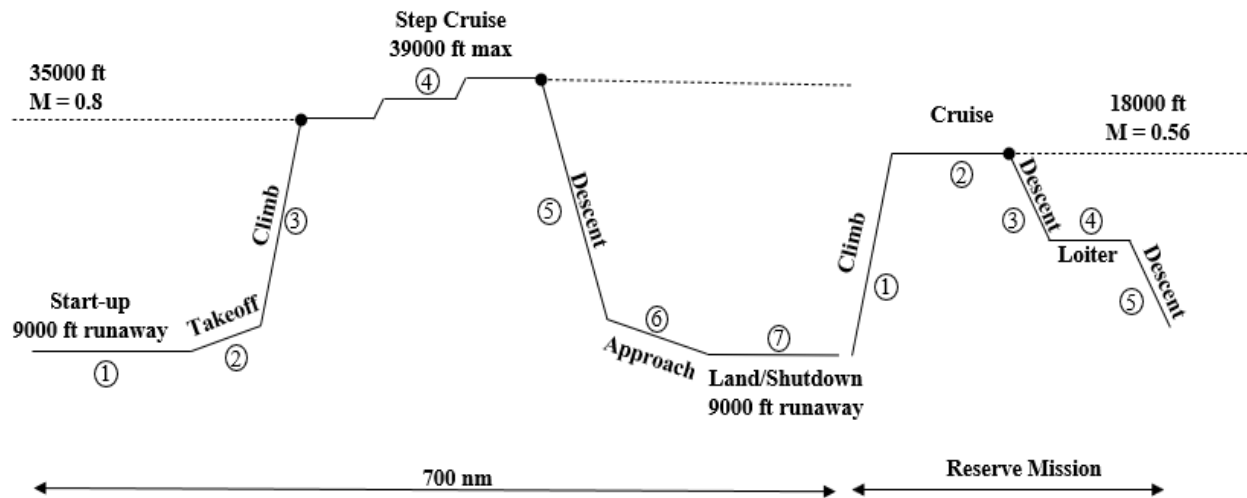
Figure 5. Reference mission profile

Business Case

Figure 6 contains a plot of relevant Boeing and Airbus aircraft mapped by range and passenger capacity. There are several existing aircraft that can meet the design requirements set in the RFP, but as can be seen in the figure, the design requirement sits in a space of its own. Aircraft that can meet the passenger requirements are overbuilt for long range and aircraft that are built for short range simply do not have the passenger capacity. The Condor X has no single direct competitor and clearly sits in a market niche.
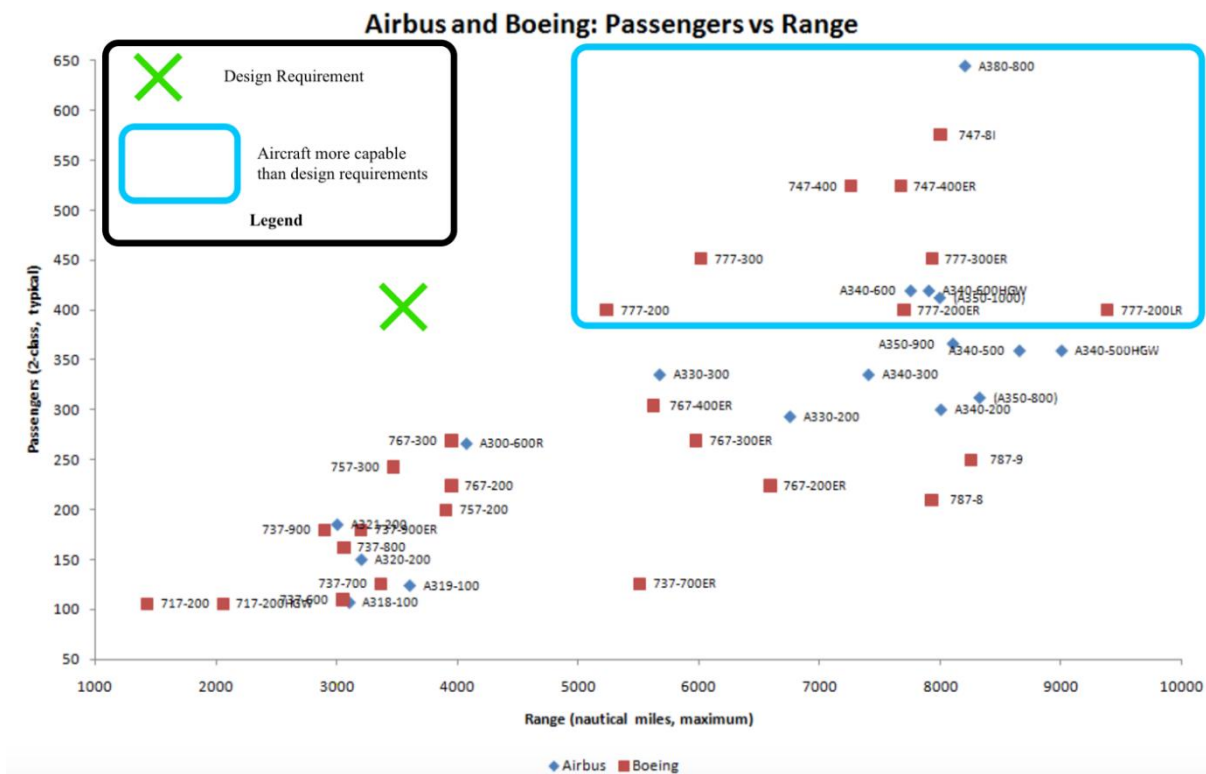
Figure 6. Aircraft viability map

While the Condor X may not seem to directly compete with any single aircraft, it is useful to compare it to other large jet aircraft to establish its superiority within the design requirements. The low weight to passenger capacity is an early indicator of the excellence of the Condor X in this market space.

Table III. Comparison between Condor X and comparable aircraft serving similar markets

	A330-300	A340-600	A350-1000	A380	747-400	757-300	767-400	777-200	777-9	787-10	Il-96-400M	Condor X
Capacity	300	380	350-410	400-550	408	243	296	313	426	330	370	406
Range (NM)	6,350	7,550	8,700	8,000	6,209	3,400	5,625	5,240	7,285	6,430	4,725	3,500
MTOW (tons)	267	380	319	575	430	137	225	273	388	280	270	211
Cruise Speed (M)	.82	.82	.85	0.85	0.86	0.8	0.8	.84	~	0.85	0.84	0.8

Another useful metric for determining the market viability is to determine the coverage of the Condor X. For Figure 7, Figure 8, and Figure 9, three sections were chosen: less than 1000 miles or approximately within economic mission range, 1000-4000 miles or within design mission range, and greater than 4000 miles which is outside the range. The charts below demonstrate the almost complete coverage of the American domestic market in terms of passenger and cargo flights. The data for the following three charts was collected from the Bureau of Transportation Statistics [2].
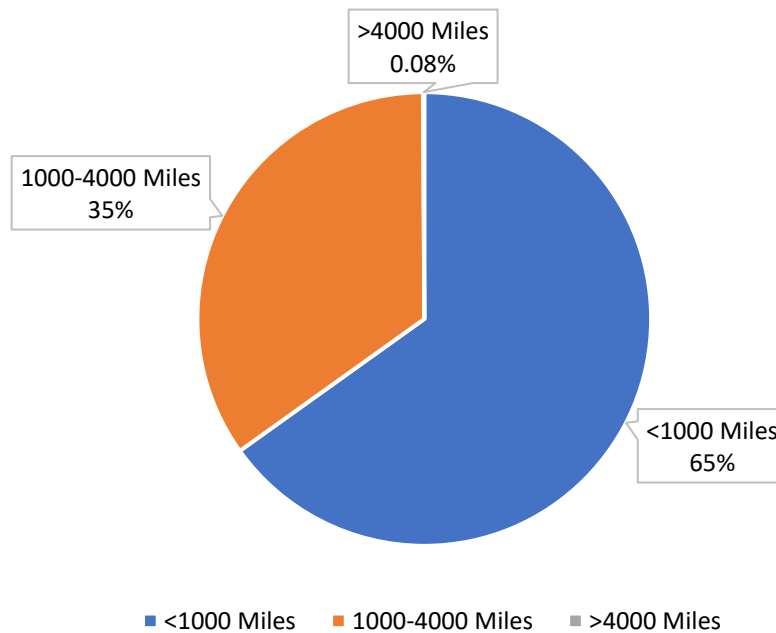
Figure 7. Passengers flying within Condor X range

Just over one billion passengers flew domestically in the United States in 2018. Approximately 65% of those passengers flew on flights that lay within or just outside of the economic mission range. Another approximately 35% of passengers fall within the extended 4,000-mile design range. Less than 1% of passengers will fly domestic flights where the Condor X would not be viable. Considering a flight from New York City to Los Angeles is just over 2000 nautical miles it should be clear that the Condor X is optimized for domestic travel.
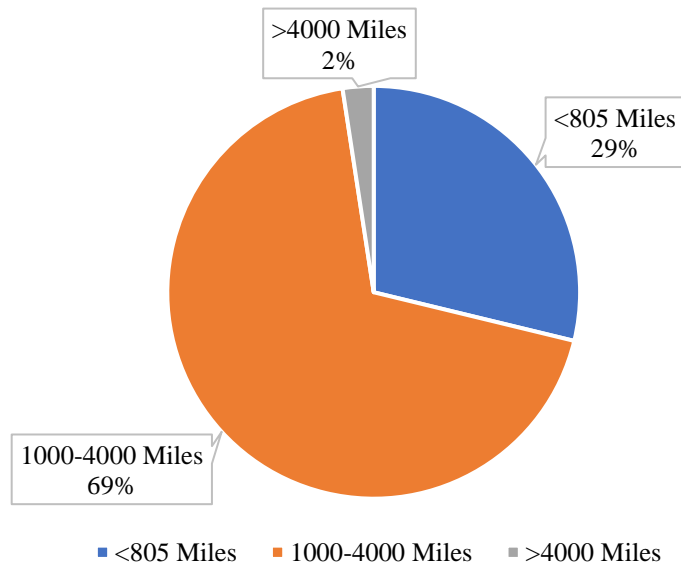
Figure 8. Fair paid for flights within Condor X range

Continuing this line of thinking, approximately 98% of domestic fare revenue in 2018 came from flights within the design mission range. The extra 1500 nautical miles in range required to capture the fares from passengers flying from New York City to Honolulu is not worth the added weights and costs that come with that overbuilding.
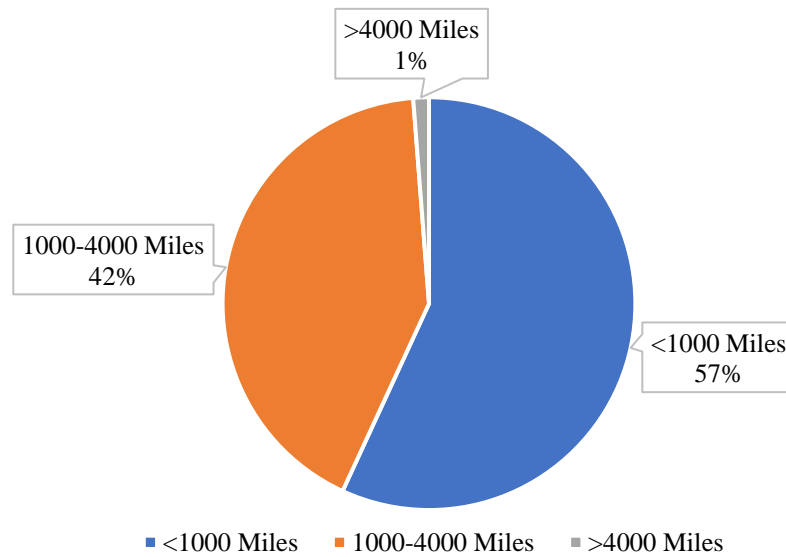
Figure 9. Cargo flown within Condor X range

Alternatively, the Condor X can also be viable as a cargo plane. Approximately 57% of all cargo by weight is flown within the economic mission range and another 42% within the design range. The high passenger capacity converts smoothly to more cargo weight delivery per flight.

The American market is obviously not the only available market for the Condor X. As shown in Figure 10, there is large market for short haul high capacity flights in the Asia-Pacific region. With 25% of world air travel now and 35% of world air travel in the next 20 years, this is a growing region with many ideal routes for the Condor X. For example, domestic routes in larger countries like China and Australia, or routes over water going to or coming from Japan and South Korea. India also boasts a 68% domestic flight rate, or 170 million seats in 2019. [3]
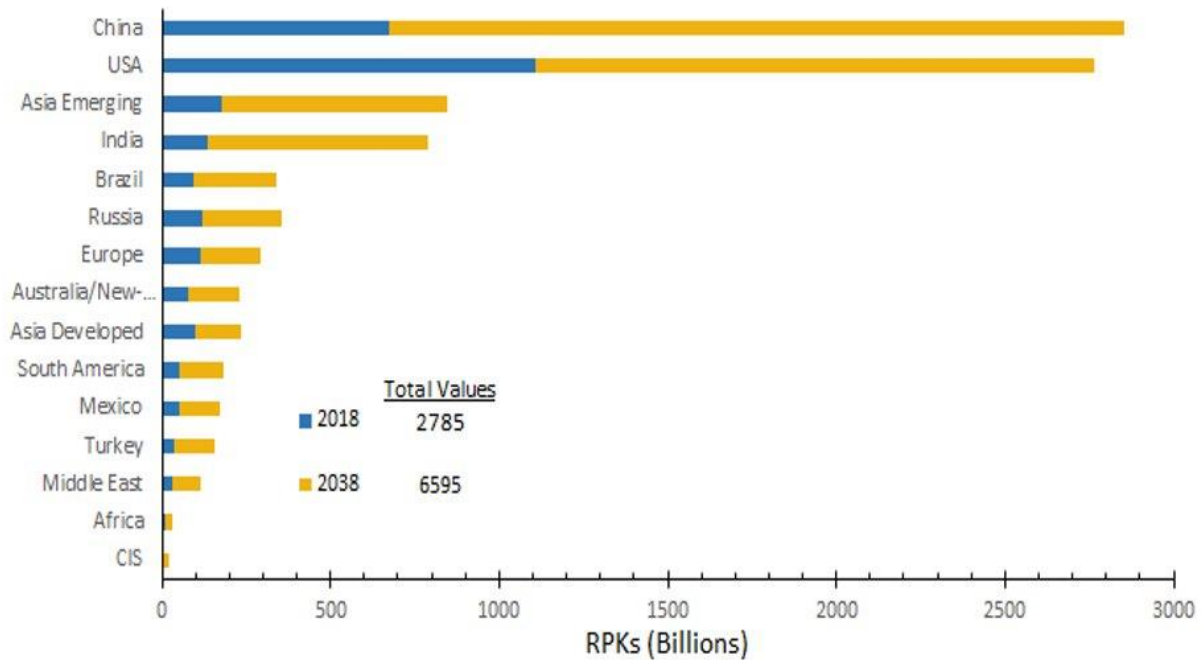
Figure 10. Short-haul route creation by market region

Short haul markets have also seen some of the largest growth, especially in markets such as domestic China, across the Mediterranean between Africa and Europe, and within Europe. Some of the busiest routes in the world fall within the range of the Condor X's economic mission. Nine of the top ten busiest routes have distances below 700 nautical miles [4]. The route between Tokyo and Okinawa is approximately 840 nautical miles. Substituting standard sized jet aircraft for the Condor X with double the passenger capacity could reduce much of the heavy traffic beginning to plague some of these airports. These routes can be viewed on Figure 11.

Table IV. Top ten busiest flight routes: Global

Route	CJU-GMP	MEL-SYD	CTS-HND	FUK-HND	BOM-DEL	PEK-SHA	HAN-SGN	HKG-TPE	CGK-SUB	HND-OKA
People per Year (millions)	13.46	9.09	8.726	7.864	7.13	6.833	6.77	6.719	5.271	5.67
Distance (NM)	237	381	442	477	613	580	623	436	374	839

Figure 11. Top ten busiest flight routes: Global

The busiest American domestic routes trend longer than those in the Pacific region, predominantly due to travel between the east and west coasts. However, six of the top ten still fall within the Condor X's economic range and the remainder still fall within its design mission range. These are all major airports with the capability to handle a larger aircraft like the Condor X and may greatly benefit from the reduced traffic that would come with fewer flights at a much higher capacity. A map of these routes can be seen in Figure 12.

Table V. Busiest flight routes: American Domestic

Route	JFK-LAX	LAX-SFO	LGA-ORD	LAX-ORD	ATL-MCO	LAS-LAX	LAX-SEA	DEN-LAX	ATL-JFK	ATL--FLL
People per Year (millions)	3.532	3.507	3.119	2.927	2.836	2.823	2.768	2.520	2.388	2.361
Distance (NM)	2151	293	637	1516	351	205	829	749	662	505
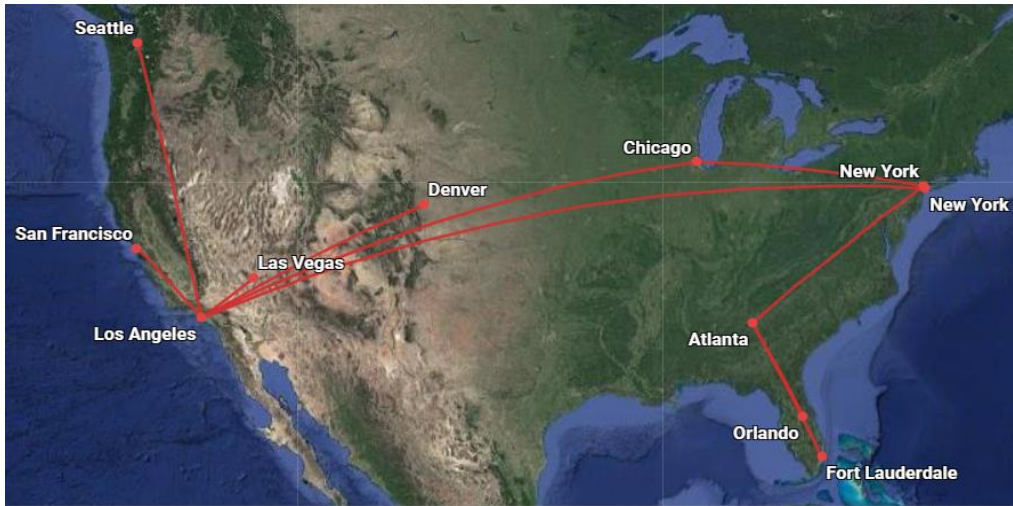
Figure 12. Busiest flight routes: American Domestic

The Condor X would be also flying much more than the just the top routes. The design range of the aircraft allows it to make some very common transatlantic flights. Many of these flights are highlighted in Figure 13. While clearly designed for short, efficient flights, the Condor X is still versatile and could be used for medium range international flights as well.
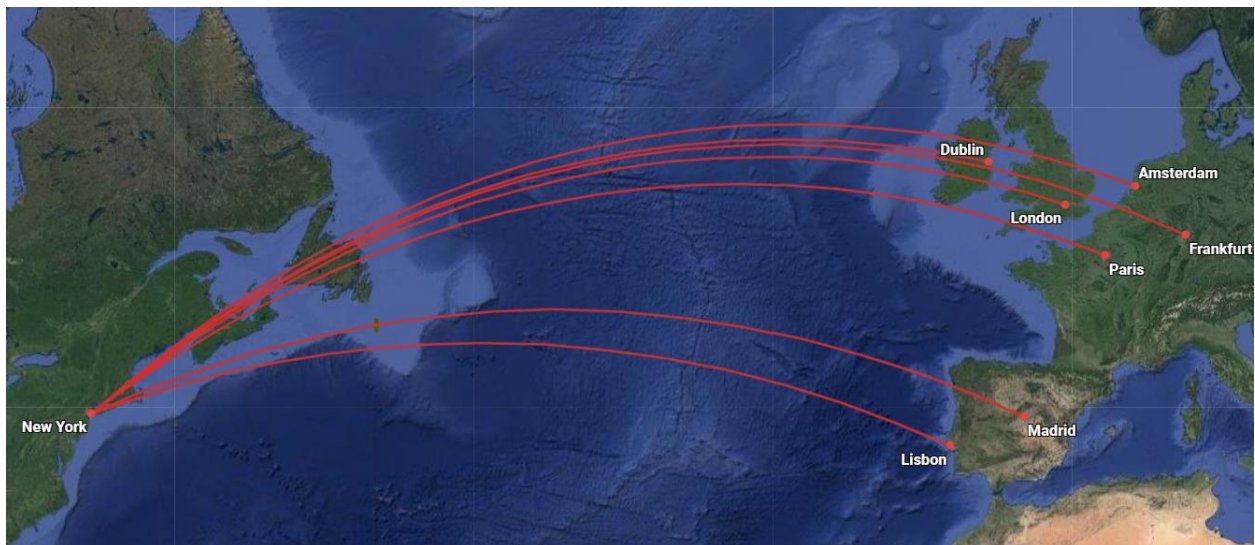
Figure 13. Transatlantic flights out of JFK within range

Estimates had previously shown an air traffic increase of 4.3% annually. Airbus estimates that this increased traffic would require thousands of new passenger and freight aircraft. In 2020, with the onset of COVID-19, it looks like projections are showing airlines having a massive $314 billion loss in revenue as forecasters believe the return to normalcy in airline flight may be slow [5]. Boeing is also taking a large hit on top of their troubles with the 737 Max, with some analysts predicting it may take until 2023 to reach the levels seen in 2019 [6]. Ultimately, the Condor X team is not composed of economists and because of the long-term development of large jet aircraft, the current situation should not affect the long-term outlook and viability of the Condor X and the analysis conducted in this report.

Configuration Selection

Several different configurations for this aircraft were considered and four were selected for further study. The four options were then compared using a Pugh matrix, Table VI, to select a final configuration. Option 4 had the highest score on this Pugh matrix and as such was selected as the final configuration for the Condor X aircraft.

Table VI. Pugh matrix of aircraft configuration
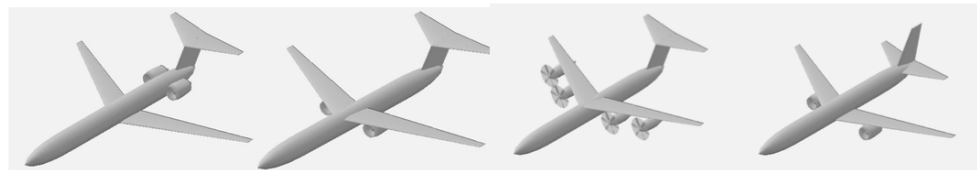
	Weight	Option 1	Option 2	Option 3	Option 4
Fuel Efficiency	0.9	8	8	10	8
Public Perception/Design Appeal	0.5	7	5	4	10
Serviceability	0.8	9	8	8	10
Manufacturability	0.7	8	10	10	10
Compatibility with Infrastructure	0.8	10	3	3	10
Comfort	0.4	9	7	6	8
Total	4.1	35.1	28.3	29.2	38.4

The strengths of the final configuration chosen, Option 4, are numerous. As a baseline, it would be easier to sell to airlines as it would not sacrifice passenger appeal. It is a traditional configuration and one that passengers are comfortable with, used to seeing, and like flying on. Furthermore, given this conventional configuration, it would be readily compatible with airports without any need for special equipment, procedures, or training.

Given the missions that this aircraft is supposed to fly, it is also natural to consider a turboprop option, Option 3 in the Pugh matrix, as they are more efficient at slower cruise speeds and lower altitudes, both sacrifices that can be made on short routes. However, three main considerations prevented the selection of Option 3. One factor going against the decision to select a turboprop was that the aircraft has a range of 3,500 NM, meaning it could fly routes from New York City to London or transcontinental routes such as New York City to Los Angeles. In these routes it could serve as a replacement for the Boeing 757, 747, and 767 along with the Airbus A330 and A340. A turboprop aircraft making transcontinental or transatlantic flights would be sacrificing too much speed and consequently time, and as such, it would unnecessarily limit the market of this aircraft to ultrashort haul routes. Another consideration was the fact that the aircraft in question would benefit from a traditional turbofan configuration is that a turboprop would be unnecessarily loud and as such uncomfortable for longer flights. Lastly, passenger appeal should also be considered. Passengers are comfortable and used to flying in conventionally configured turbofan aircraft, a large turboprop aircraft would not have the same appeal. Passengers are more reluctant to fly on aircraft with exposed props and unconventional designs and associate them with smaller, less safe aircraft [7].

Some discussion of the first option with fuselage-mounted engines is also warranted. This configuration might lead to lower noise in the majority of the cabin. However, this is offset by two disadvantages. One is the reduction in passenger appeal as passengers seem to prefer a conventional configuration. Large 400-person aircraft with fuselage mounted engines do not exist and having them would be a great departure from the norm. This combined with the fact that passengers already prefer to fly on conventional aircraft makes this configuration rather unfavorable. Second, the configuration might lead to unnecessary weight in the wings along with additional complications associated with mounting large high-bypass turbofans on the fuselage of an aircraft.

Lastly, to further justify this configuration, consideration was made as to where the market has converged after decades of aircraft development. While in the early days of jet aviation four-engine aircraft were common, they

have gradually been replaced with three-engine, and now two-engine variants. The two-engine Boeing and Airbus aircraft are very successful while the four-engine Boeing 747 and Airbus A380 and A340 have proven to be incompatible with what the airlines want today. This can also be seen by the fact that the McDonnel Douglas MD-11 (and its predecessor the DC-10) along with the Lockheed L-1011 were both long-term failures, showing that three-engine configurations are also unnecessarily complex and inefficient. As a result, the choice for two engines becomes increasingly clear. As for the question of whether to have them fuselage-mounted or under the wing, that also becomes very clear when looking at the market. Commercial aircraft with Fuselage-mounted engines are becoming less and less common, the McDonnell Douglas MD-80 series of aircraft are no longer in production with no successors adopting that configuration. Furthermore, even regional jets are moving towards a more conventional configuration as evident with the Bombardier CS100/Airbus A220 and the Embraer E-jet family of aircraft. Therefore, the configuration for the Condor X is not only shown to be best suited by out Pugh matrix, but also by decades of results that can be drawn upon from the aviation industry and the market. While this design might appear to be too conventional, there is a reason that the convention has converged on being aircraft with two wing mounted engines for this class of transport. The three-view engineering drawing is presented in Figure 14.
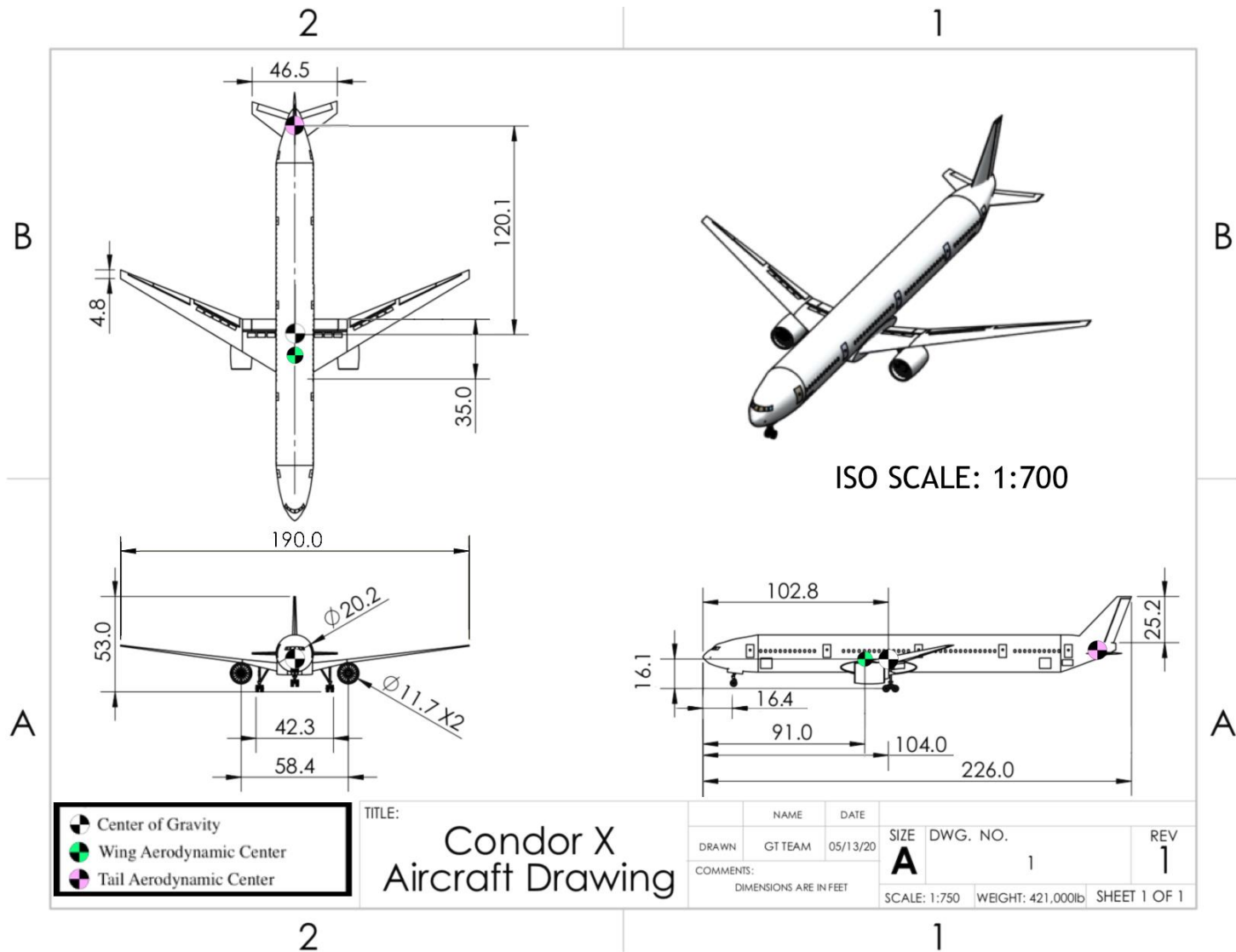
Figure 14. Three-view engineering drawing of the Condor X aircraft

Interior Layout

The aircraft was designed with the goal of maximizing passenger capacity while also allowing for easy conversion into a freighter. The fuselage, shown in Figure 15, has a diameter of 20.34 ft, allowing the accommodation of a large number of passengers in a shorter layout while also offering a competitive replacement for the aging aircraft in cargo service today. This section will provide a summary of the interior layout of the passenger and cargo variants.
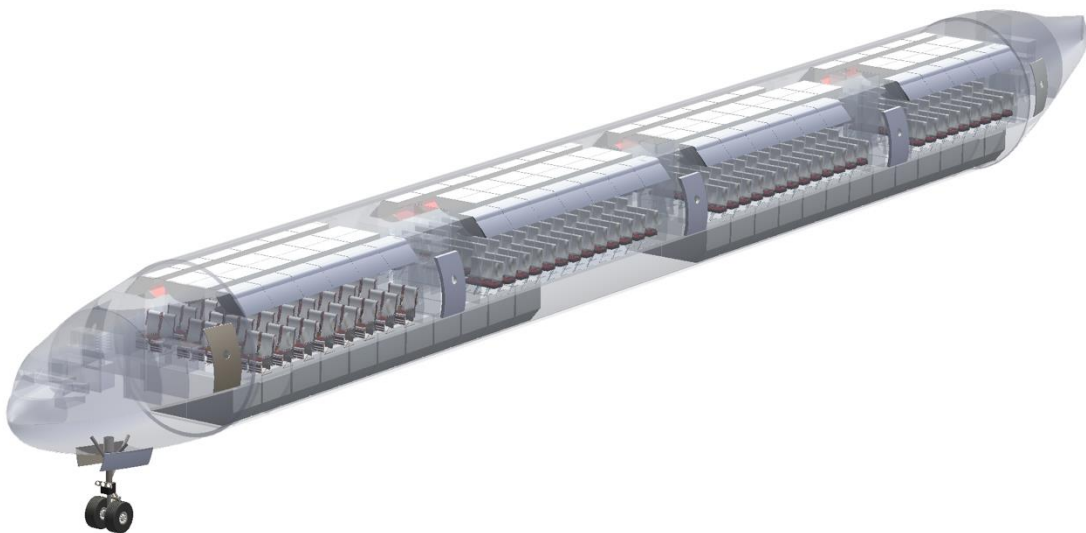
Figure 15. Fuselage and interior layout of Condor X passenger variant

Passenger

As configured, the passenger variant of the Condor X will be able to carry a total of 406 passengers in a two-class configuration. This configuration also includes 13 lavatories and 3 galleys and as such, passenger comfort, especially on routes making use of the full range of the aircraft is not compromised. However, the amenities on board along with the seat pitch can be adjusted to enable denser configurations. Figure 16 shows one of the three onboard galleys.
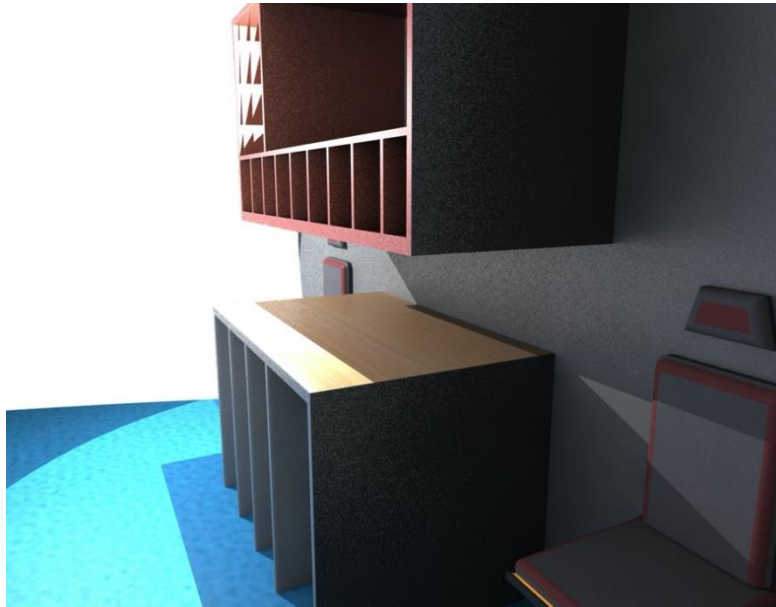
Figure 16. Rendering of aft galley of aircraft - one of three total galleys.

Figure 17 shows the layout of the Condor X in its 406 passenger, two-class, configuration. It is important to note that even in its passenger variant, the Condor X can hold 50 LD3 unit load devices in its cargo hold with space left over for bulk cargo. Comparable aircraft in this cabin class can carry 44 in the case of the Boeing 777-300 or 48 in the case of the Boeing 777-9 [8]. As such, airlines will not only be able to rely on their passenger revenue, but also enjoy the benefits of flying more cargo.
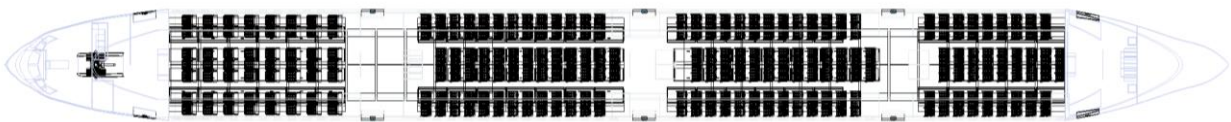
Figure 17. Interior layout of Condor X in passenger configuration

The RFP required that the business class seat pitch be 36 in, however, this requirement was exceeded to provide a more accurate representation of the market. The required seat pitch was simply too small for a business class configuration on an aircraft of this size, as such it was increased to 46 inches. The initial requirement of 36 in was shorter than the pitch on some domestic premium economy seats within the United States and fell well below business class seat pitches. The 46-inch pitch falls on the low-end of business class seat pitches and is comparable to the seat

pitch on low-budget high capacity airliners such as Norwegian Air's Boeing 787 while falling well short of business class seat pitches of global carriers on longer flights. These global carriers often have business-class seat pitches ranging between 60 to 90 inches. The selected 46 inches allows for passenger comfort that is suitable for the maximum 3,500 NM range of this aircraft without sacrificing unnecessary comfort. Figure 18 shows the spacing between the seats as well as the seven-abreast seating configuration. Much like the seat pitch, the seven-abreast layout was selected to maximize passenger capacity while also retaining a suitable level of comfort. Figure 19 shows a rendering of what the business class cabin would look like.
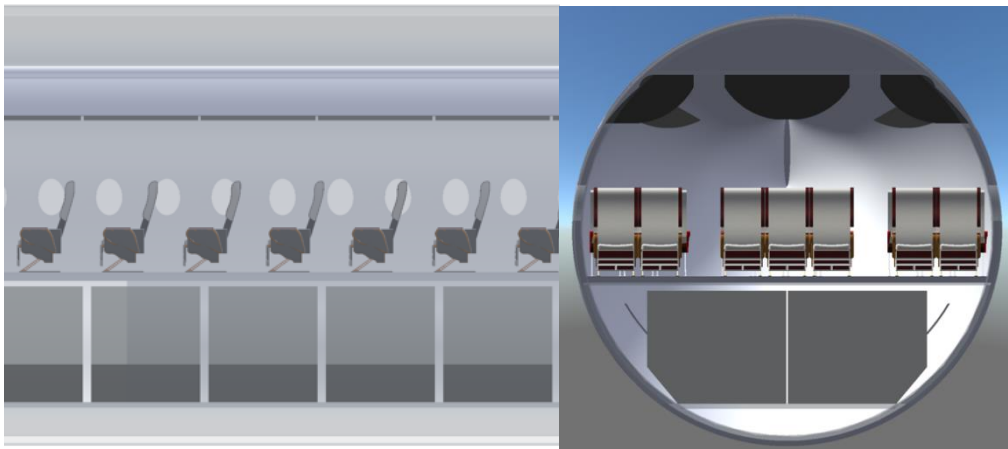
Figure 18. Business class seating configuration

Figure 19. Business cabin interior render

The economy seat pitch was kept at the RFP designated 32 inches as it was appropriate for this market segment. With a 32-inch pitch and 10-abreast seating the Condor X is able to accommodate 350 passengers. Figure 20 shows the economy class seating arrangement of the Condor X while Figure 21 shows rendering of the economy class cabin.
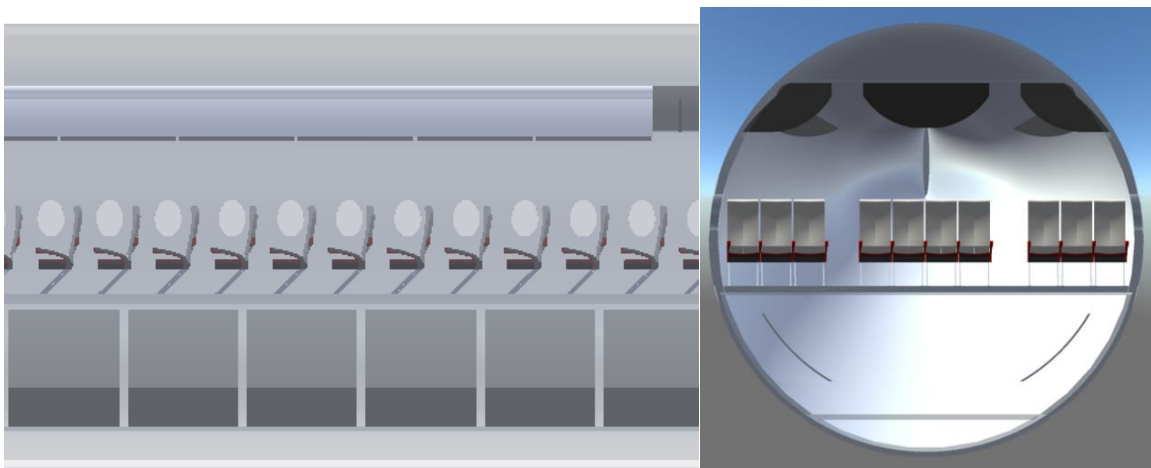
Figure 20. Economy class seating configuration

Figure 21. Economy cabin interior render

Cargo

To maximize the use cases of the Condor X, particular attention was paid to making sure it can serve as a viable cargo aircraft during design. The lower deck of the cargo variant remains the same, being able to accommodate a class-leading 50 LD3 containers. Its main cargo deck can accommodate PMC pallets (96in x 125in) in two formats depending on the height of the load. Figure 22 shows the main deck configuration with 32 low-height PMC pallets and a full lower cargo deck. Currently, a comparable cabin class aircraft, the 777F can accommodate up to 27 pallets. [9] These PMC pallets can also be substituted with M-1 or M1-H unit load devices as they have the same footprint.
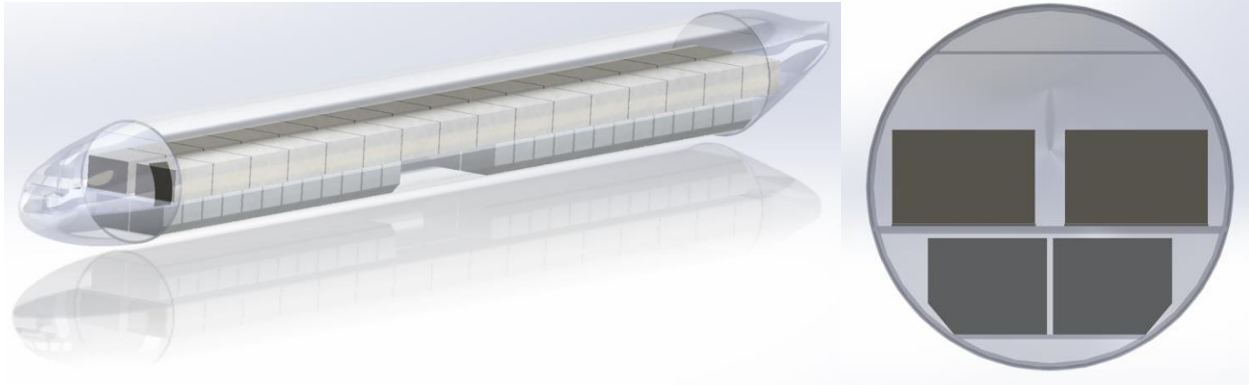
Figure 22. Cargo configuration with main deck low-height PMC pallets

For flying larger cargo, the PMC pallets can be rotated and accommodate taller cargo. With the maximum height allowed by PMC pallets, the Condor X can accommodate 21 units. Figure 23 shows such a configuration.
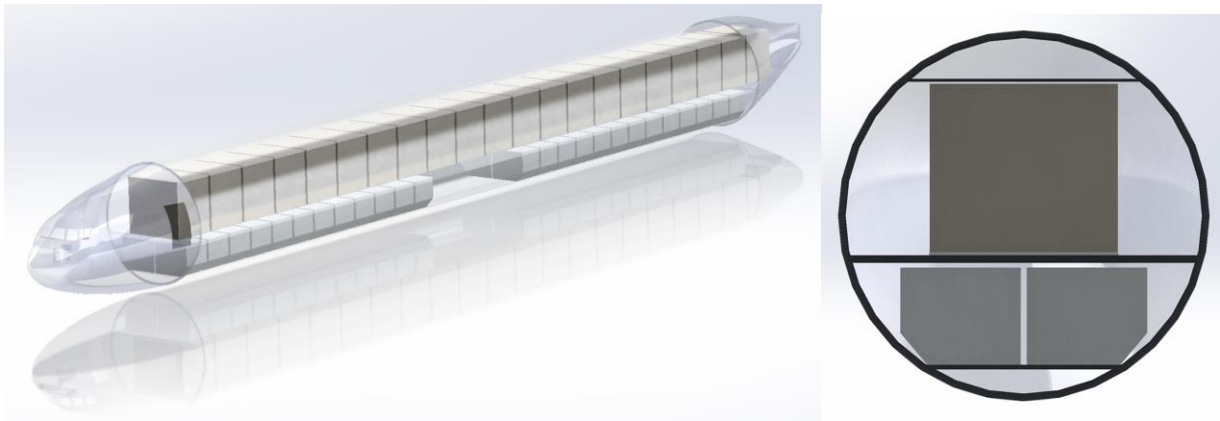
Figure 23. Cargo configuration with main deck high PMC pallets

Performance

FLOPS

To conduct most of the aircraft sizing and performance analysis, the FLOPS sizing tool was used [10]. FLOPS (Flight Optimization System) is an aircraft sizing tool developed at NASA Langley that was built primarily for sizing commercial transport aircraft. Inputs are read in the form of a text file by the FLOPS executable and a corresponding output text file is produced including everything from weight analysis to takeoff and landing performance. Sizing an aircraft with FLOPS however typically requires a baseline aircraft that is already calibrated to ensure the output model is sized reasonably. An input file was first created and calibrated to the Boeing 777-300ER, a similarly sized wide-body aircraft typically found flying routes similar to those defined in the RFP. The Boeing 777-300ER was selected as the ideal 777 variants as it is the newest to be certified and is the product of decades of iteration and improvement, thus creating a baseline aircraft model that is closer in technology level to the present. From this baseline model, changes in everything from mission profile to aircraft geometry were adjusted to arrive at a newly sized aircraft.

An overview of the changes made within FLOPS to arrive at the final iteration of the Condor X can be found in Figure 24 and Figure 25. The calibrated baseline 777-300ER model had a MTOW of just under 777,000 pounds in a two-class configuration with 50 business-class passengers and 300 economy-class passengers.
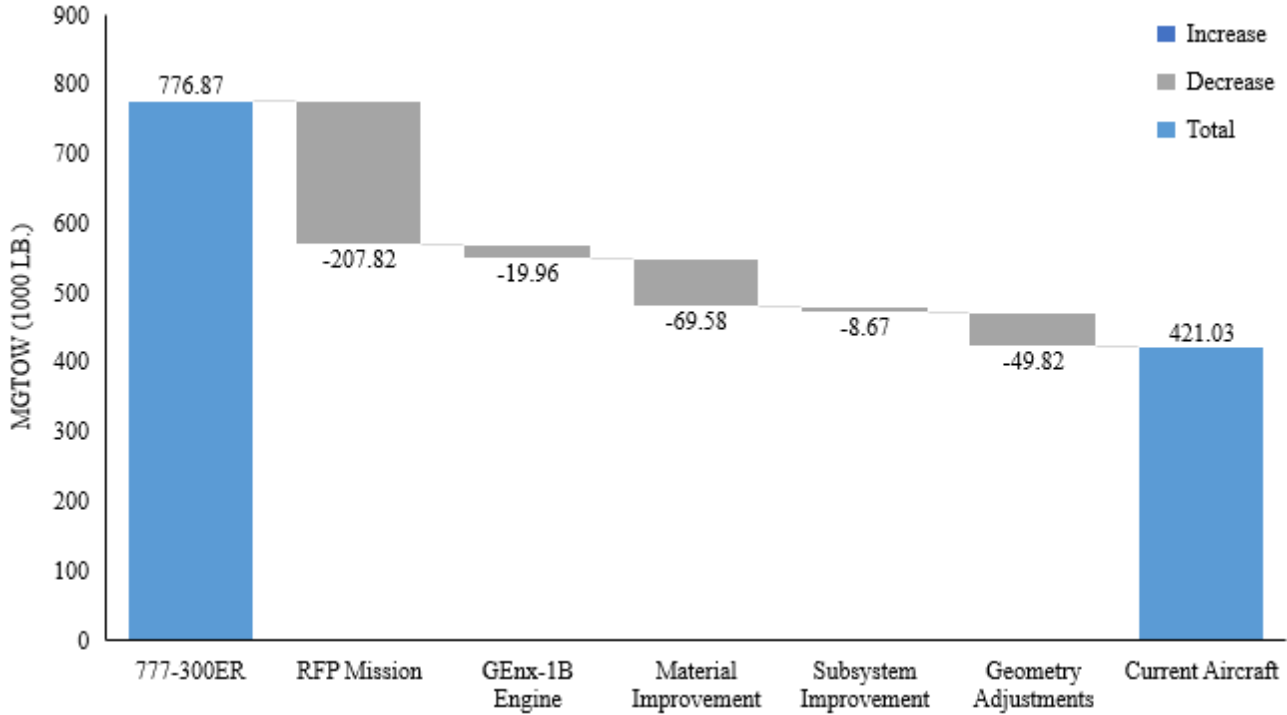
Figure 24. Change in Max Gross Takeoff Weight from resulting design changes
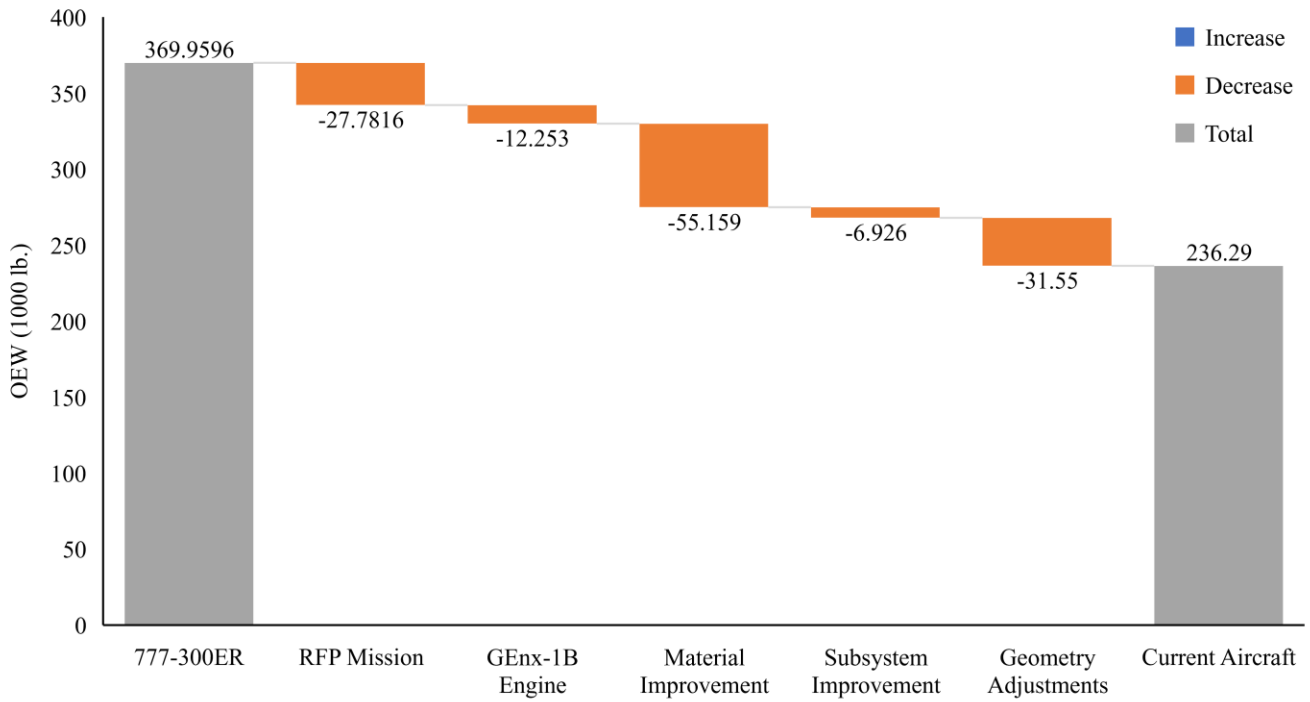
Figure 25. Change in Operating Empty Weight from resulting design changes

The first set of changes made to the input model were related to the mission profile set by the RFP given; mission range, business/economy-class seating, and baggage weight per passenger were adjusted to fit the sizing mission set forth. By reducing the mission range within FLOPS from 7880 NM to 3500 NM, the MTOW of the aircraft changed dramatically; even with the increased passenger count and higher payload, the unnecessary fuel removed from the longer mission saved more than 50 tons alone. As fuel storage was removed from the aircraft, the empty weight decreased significantly due to the reduction in structural weight and landing gear weight required to support the massive MTOW of the 777-300ER. The next significant change made input change made within FLOPS was to replace the powerplant with one better suited to the RFP mission and lower aircraft weight. The 777-300ER is currently equipped with the GE90-115b engine, a massive high-bypass turbofan capable of producing ~115,300 pounds of thrust. Though FLOPS does include the ability to scale a provided engine deck to better suit the inputted mission, scaling down an engine the size of the GE90-115b by ~55-65% would prove unrealistic; small changes in engine performance on the order of ~10-15% are significantly more plausible and could realistically be achieved through re-fanning the engine. As a result, a smaller turbofan engine better suited to the weight class of the Condor X was needed. The engine selected was the GEnx-1b, the current powerplant used on several Boeing 787 variants. More details regarding this powerplant can be found later in the Propulsion section. As shown in Figure 24 and Figure 25, inputting the GEnx-1b calibrated engine deck into FLOPS resulted in a noticeable decrease in both OEW and MTOW, primarily due to both the weight savings from a smaller engine and the improved fuel burn when compared to the -115b.

Materials selection and improved aircraft technologies were then considered to further reduce aircraft weight. The most significant change made to the aircraft model was the introduction of composite materials in the fuselage, wing, and horizontal/vertical tail. As shown in Figure 25, introducing new materials such that most of the airframe is composite results in a sizeable reduction in operating empty weight. Specific details on the material changes made are discussed later. Improved subsystem/interior technologies were then implemented to further reduce aircraft weight. These technologies include things like lighter seat fixtures and higher-pressure hydraulic systems. The final set of changes to the FLOPS aircraft model included geometry changes to both the fuselage and the wing. As a result of the configuration selection and preliminary sizing analysis, a passenger compartment length that comfortably fit the required amount of business and economy-class passengers was derived and implemented into the FLOPS model. Wing aspect ratio was also increased to further improve efficiency in flight, with supported analysis discussed later.

While these changes in airframe geometry resulted in a slight increase in OEW, the reduction in fuel burn found during both the reference mission and the sizing mission more than compensate this.

Trade Studies

To better understand the impact of cruise Mach number on the fuel burn and efficiency of the aircraft in flight, analyses were performed on the Condor X FLOPS model for Mach numbers ranging from 0.75-0.85. These values were based on the typical cruise speeds achieved by turbofan passenger transports. However, altitude is also a significant factor in analyzing how cruise speed effects fuel burn and cruise performance; to optimize cruise performance, the analysis carried out in FLOPS to evaluate the effects of cruise Mach number were performed such that the optimal initial and final cruise altitude were solved for automatically during the FLOPS cruise analysis. Potential step altitudes were defined in 2000 ft. increments between FL310 and FL410. When conducting the cruise segment analysis, the optimal initial and final altitudes were selected at each Mach number analyzed. The resulting change in block fuel and block time as a function of cruise Mach number for the sizing mission can be found in Figure 26 and Figure 27, respectively.
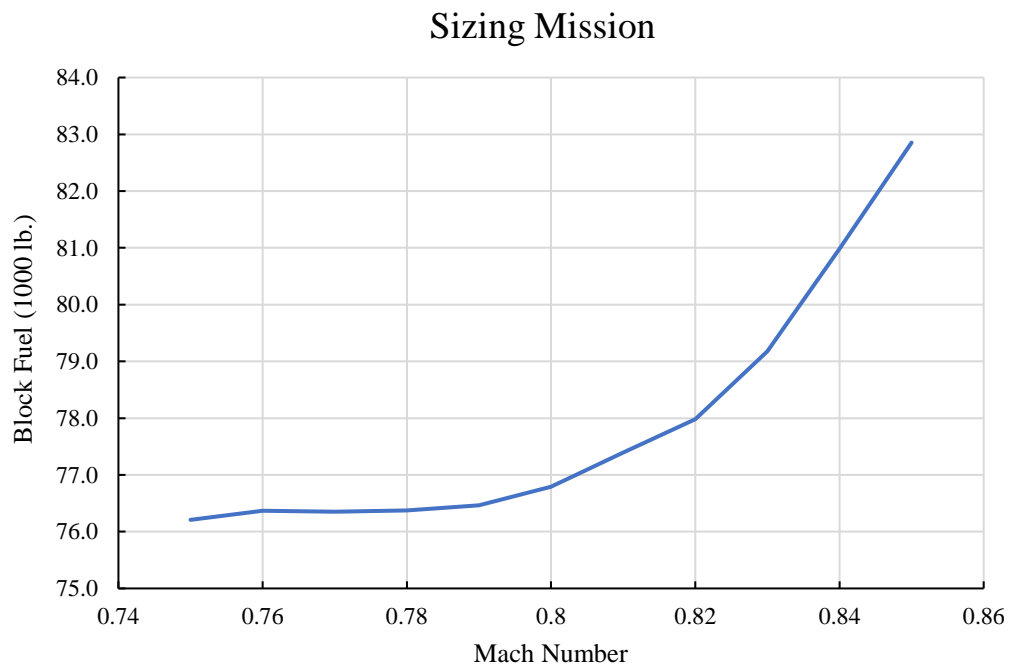
Figure 26. Block fuel as a function of Mach Number with optimized altitude selection – Sizing mission
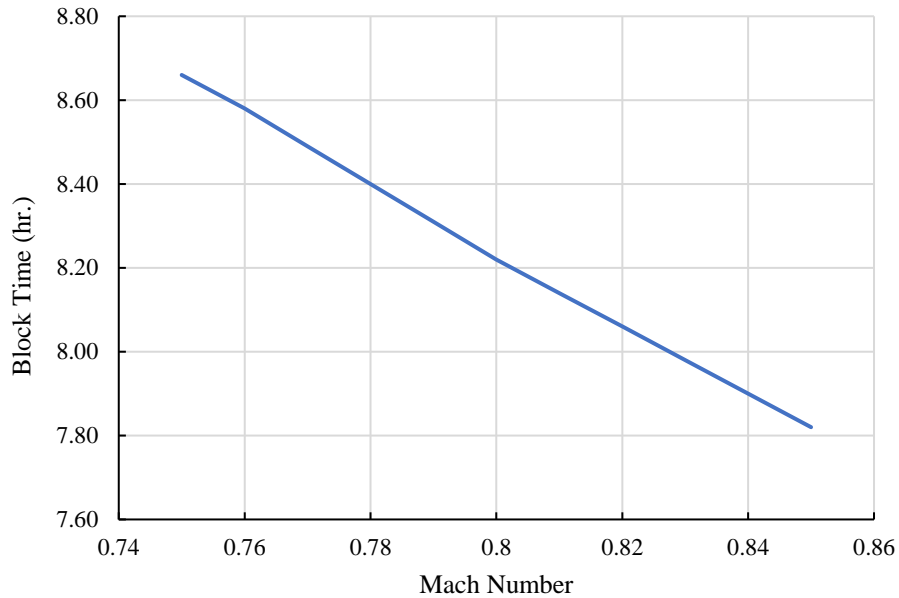
Figure 27. Block time as a function of Mach Number with optimized altitude selection – Sizing mission

Similarly, the resulting change in gross weight and block time as a function of cruise Mach number for the economic mission can be found in Figure 28 and Figure 29, respectively.
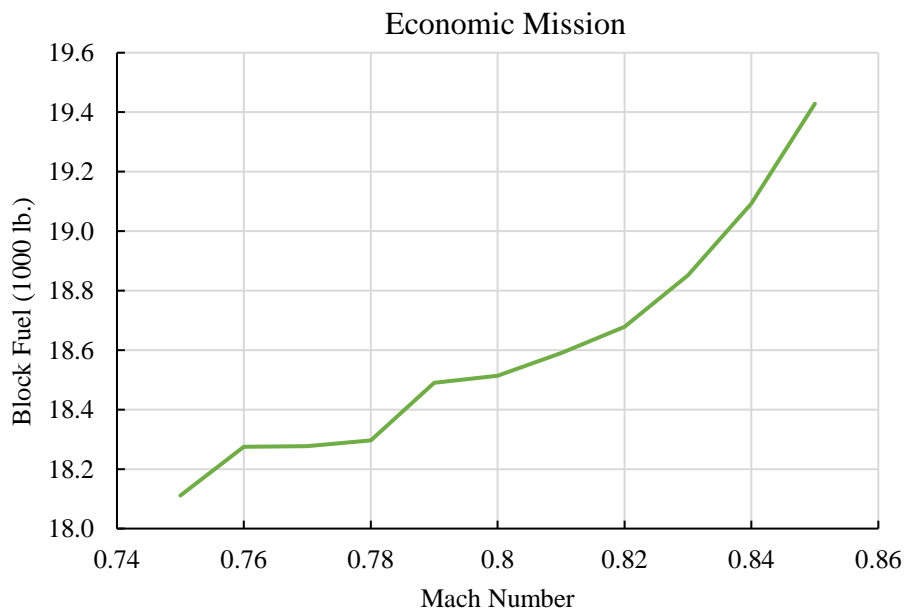
Figure 28. Block fuel as a function of Mach Number with optimized altitude selection – Economic mission
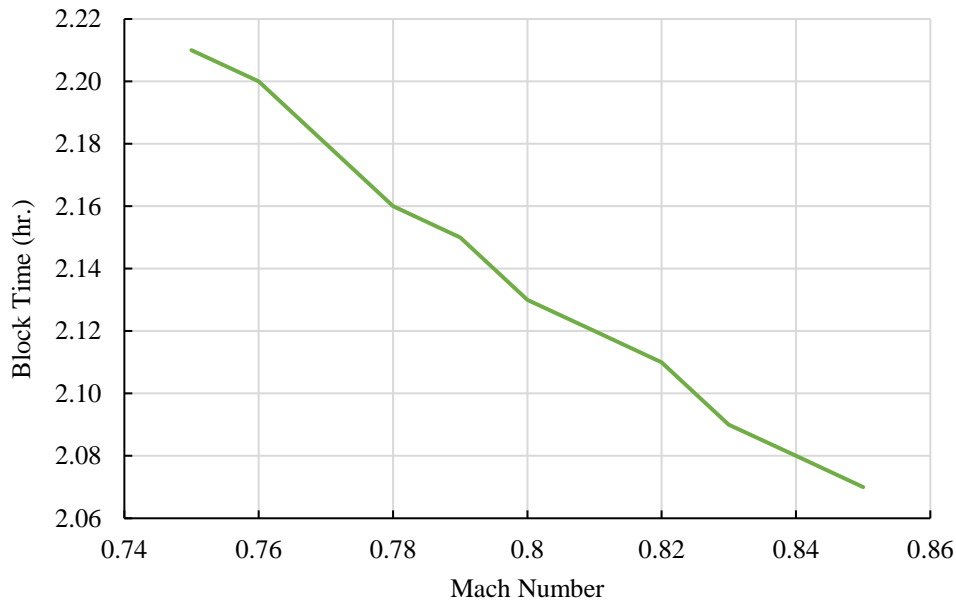
Figure 29. Block time as a function of Mach Number with optimized altitude selection – Economic mission

A cruise Mach number of 0.80 was selected for a combination of two main reasons: time savings during the economic mission combined with improved fuel efficiency. Although cruising at Mach 0.80 resulted in *slightly* higher fuel burn during the sizing and economic mission, the slightly reduced block time and increased number of trips per week make up for the small increase in operating cost with a greater increase in revenue. This was determined to be the 'sweet spot' to reduce block time such that revenue can be noticeably increased at a small penalty to fuel burn.

Various wing geometries were also analyzed to determine mission fuel burn sensitivity to aspect ratio and quarter-chord sweep angle. These values were adjusted simultaneously within FLOPS to perform a multi-dimensional analysis. An aspect ratio of 12 was selected as the maximum allowable aspect ratio given traditional values found in already- existing passenger transport aircraft; although an aspect ratio of 12 is high, use of modern composite materials and a lower overall wing area than similarly sized aircraft were deemed sufficient reasons to allow for the maximum value to be set as such. The primary focus of the multi-dimensional wing study was to understand the impact of wing geometry on mission fuel burn during both the sizing mission and the economy mission. The sensitivity of MGW to

aspect ratio can be found in Figure 30, while the sensitivity of block fuel for both missions can be found in Figure 31 and Figure 32.
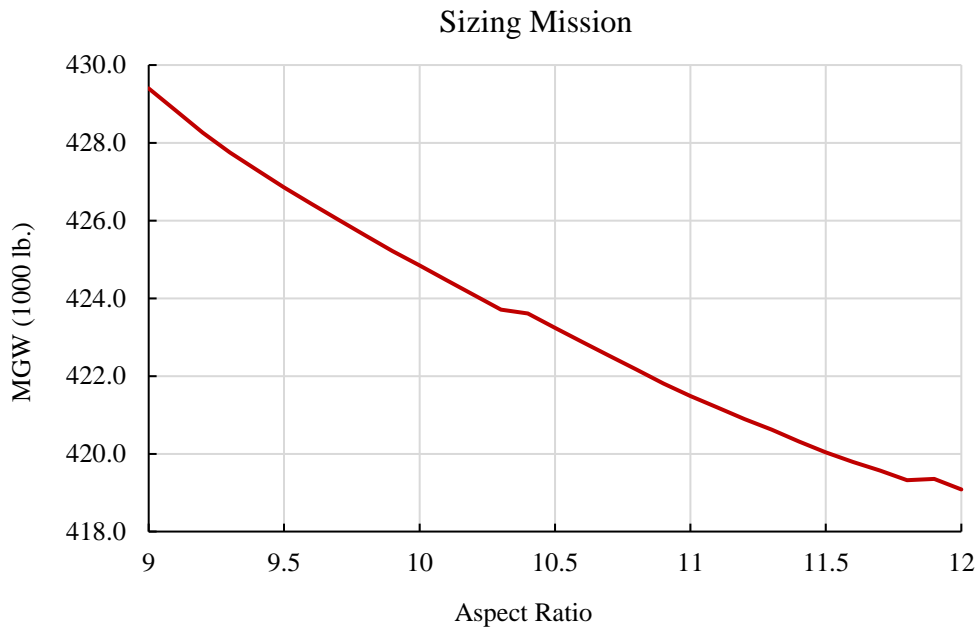
Sizing Mission

Figure 30. Max Gross Weight sensitivity to aspect ratio – Sizing mission
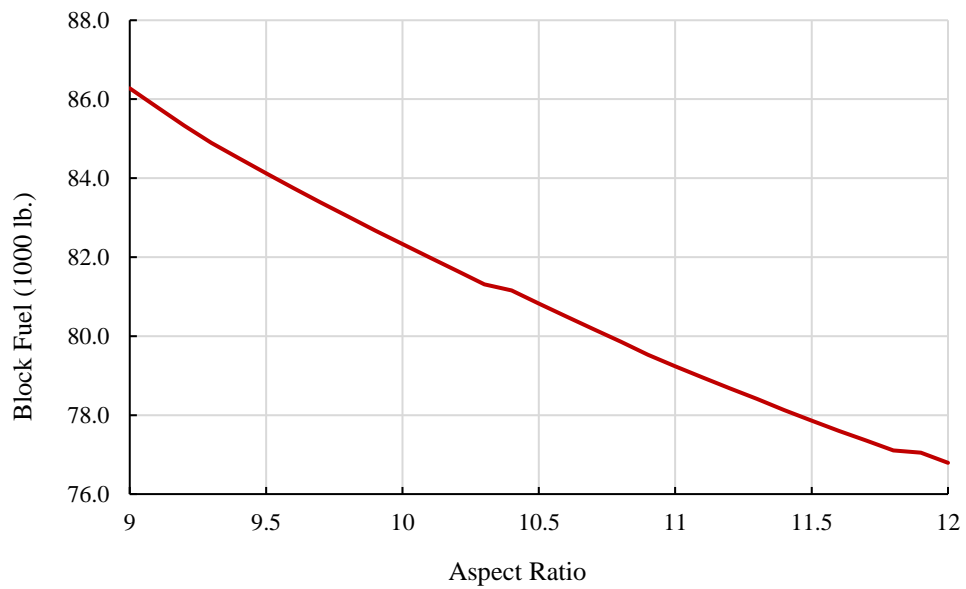
Figure 31. Block fuel sensitivity to aspect ratio – Sizing mission
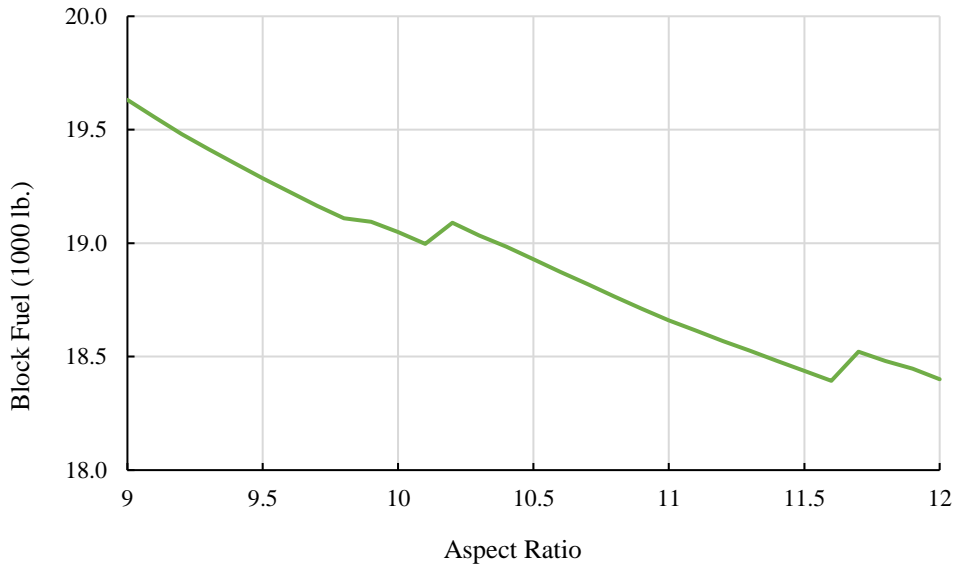
Figure 32. Block fuel sensitivity to aspect ratio – Economic mission

Similarly, the sensitivity of MGW to quarter-chord sweep angle can be found in Figure 33, while the sensitivity of block fuel for the sizing mission can be found in Figure 34.
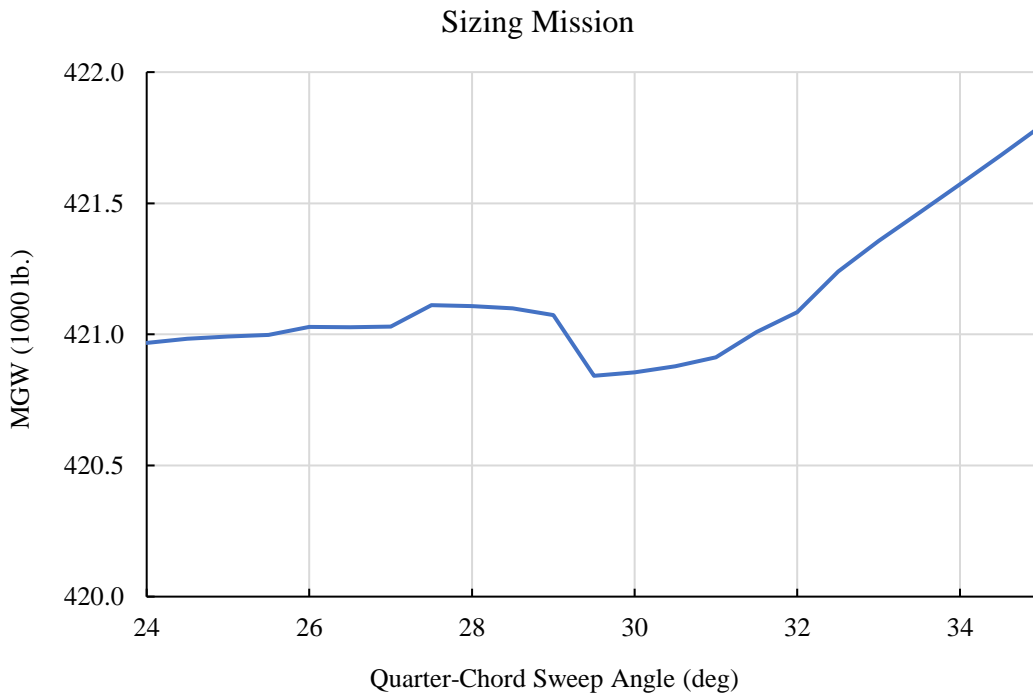
Sizing Mission

Figure 33. Max Gross Weight sensitivity to quarter-chord sweep angle – Sizing mission
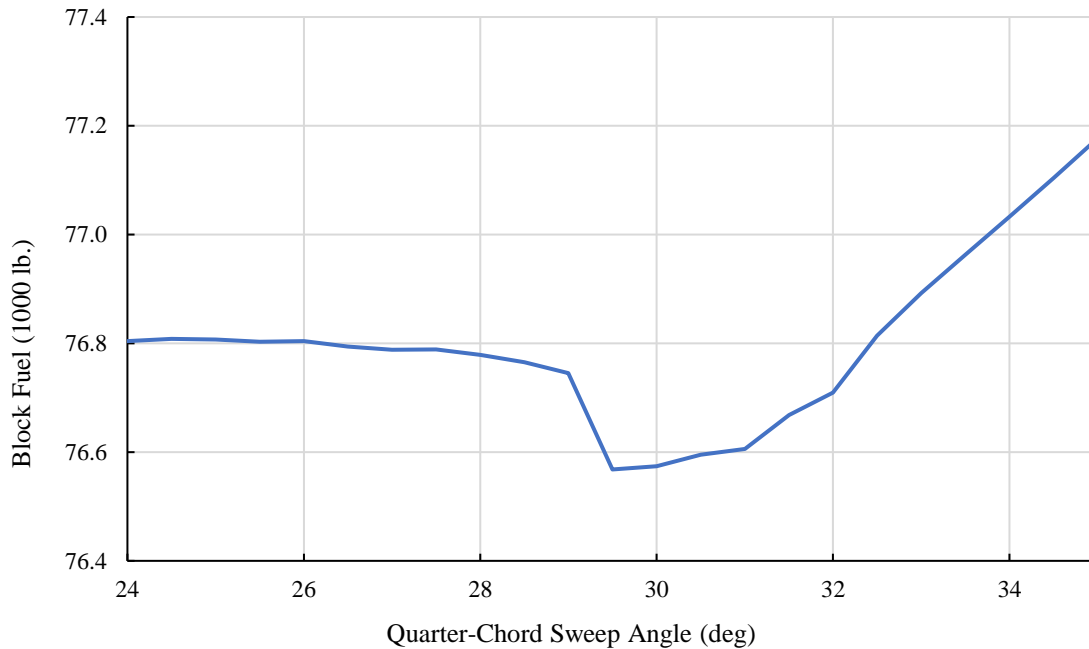
Figure 34. Block fuel sensitivity to quarter-chord sweep angle – Sizing mission

A noticeable decrease in fuel burn was observed during both the sizing and economic mission as a result of increasing wing aspect ratio, though the change was more pronounced during the sizing mission. The optimal aspect ratio proved to be the maximum allowable limit of 12 set before the analysis. With an aspect ratio of 12, fuel burn during the sizing mission decreased by more than 2,000 pounds when compared to a wing with an aspect ratio of 11 conducting the same flight. A quarter-chord sweep angle of 26.6 degrees was selected to prevent the CG from shifting too far aft, however the study above confirms that the selected sweep angle will not negatively impact mission fuel burn noticeably. Compared to the optimal quarter-chord sweep angle of 29.5 degrees, the fuel burn across the sizing mission increases by just ~0.29%. The penalty in fuel burn was therefore not very significant compared to the improvement in CG location and landing gear sizing.

Arriving at a combination of thrust loading and wing loading to satisfy the requirements given in the RFP involved significant iteration and multi-dimensional analysis. Initially, a series of two-dimensional trade studies were performed within FLOPS to understand the sensitivity of wing loading and thrust loading on the sizing and performance of the aircraft. To map the sensitivity, wing loading was varied from 120 to 150 pounds per square foot

while thrust loading was varied from 0.27 to 0.36. These ranges cover typical values found for large transport category aircraft. The results were then sorted in ascending order of MTOW to evaluate the "ideal" combinations resulting in the lowest weight. The MTOW of the model was evaluated during the sizing mission given that the takeoff and landing requirements defined by the RFP are most difficult to achieve at the MTOW as opposed to a lighter weight during the shorter economic mission. The results were then plotted in a 3D surface plot to illustrate the viable wing and thrust loading design space. The results can be found in Figure 35.
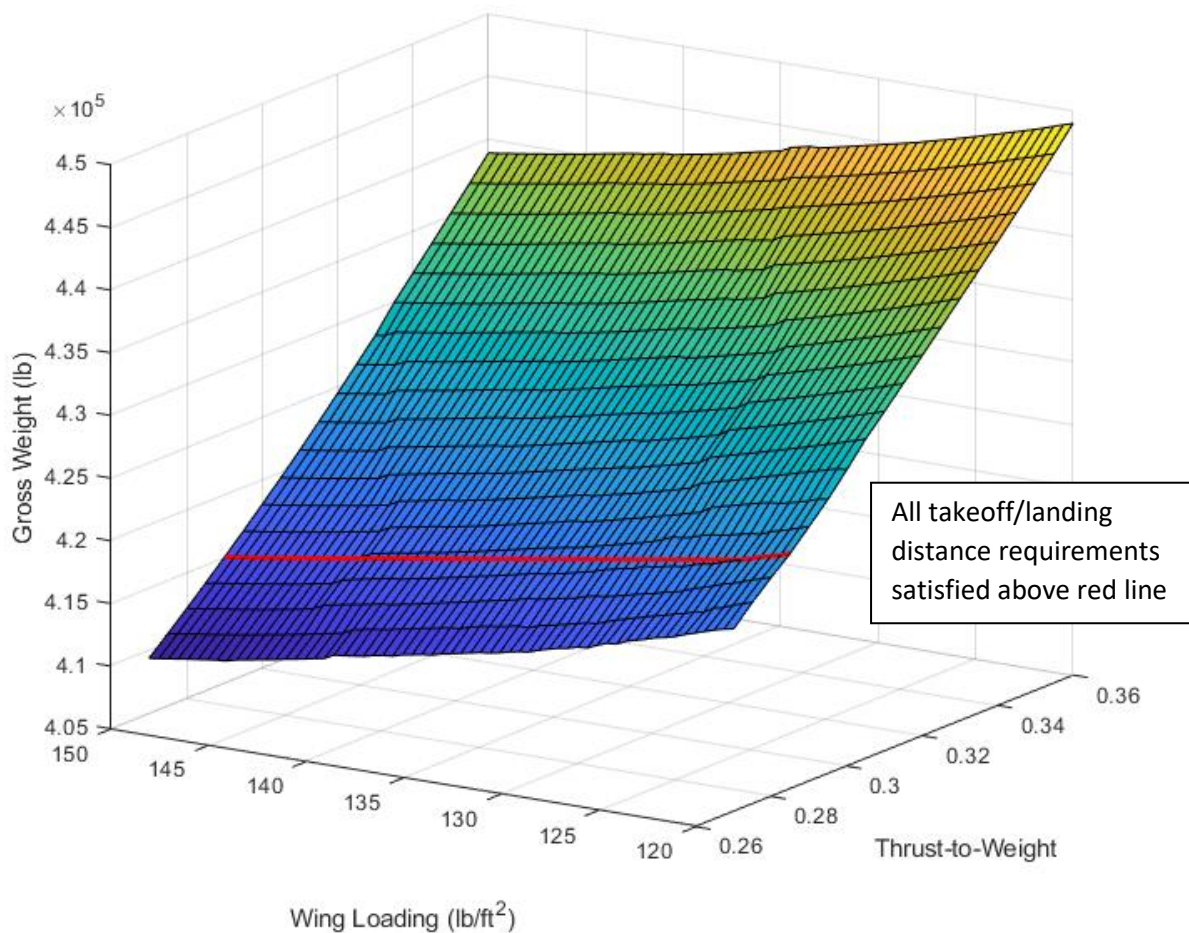
Figure 35. Feasible design space as a function of wing and thrust loading

Although an ideal range of wing loading and thrust loading appeared, the aircraft model proved not very sensitive to smaller changes in wing loading and thrust loading. The results with the lowest MTOW were then further analyzed and rerun to determine the corresponding takeoff and landing performance. The combination of wing loading

and thrust loading that achieved the lowest MTOW, while also achieving the necessary takeoff and landing requirements with enough margin was then selected. The range of thrust loading and wing loading value that were deemed viable design points are those that appear above the red line in Figure 35. A thrust loading of 0.30 and a wing loading of 139.8 pounds per square foot was selected, corresponding to the takeoff and landing performance discussed in the next section. The constraining requirement driving the thrust loading was thrust required during missed approach execution, which was achieved with sufficient margin in excess thrust of approximately 2000 pounds with the selected thrust loading and wing loading values.

Takeoff/Landing Performance

Takeoff and landing performance were both analyzed in FLOPS to predict FAR Part 25 takeoff and landing field length requirements. Takeoff performance was analyzed for the following scenarios:

- Aborted Takeoff – All Engines Operating

- Aborted Takeoff – One Engine Inoperative

- One Engine Inoperative Takeoff – 2.4% Flight Path Angle/35-foot Obstacle

- All Engines Operating Takeoff – 35ft Obstacle

The takeoff distances calculated for each scenario above were then increased by 15%. The longest takeoff distance of the four scenarios is therefore the certified takeoff distance. A summary of takeoff performance can be found in Table VII.

Table VII. Calculated takeoff distance for required takeoff scenarios

Takeoff Condition	Distance (ft)
Aborted Takeoff - All Engines Operating	7,687
Aborted Takeoff - One Engine Inoperative	7,685
Takeoff - One Engine Inoperative	8,087
Takeoff - Nominal	6,779
FAR Field Length	8,087

Landing performance was analyzed for a normal approach with a 3 degree glideslope clearing a 50 ft. obstacle coupled with a missed approach go-around. A thrust margin of ≥2000 pounds during the missed approach go-around was deemed enough to ensure the aircraft can complete the maneuver at the calculated approach speed of 139.3 KCAS. The required landing distance was than extended by 60% to provide a suitable safety margin. The calculated landing distance can be found in Table VIII.

Table VIII. Calculated landing distance breakdown by phase of approach

Standard Approach	Velocity (KCAS)	Distance (ft)
50 Foot Obstacle	139.3	0
Flare	139.3	659
Touchdown	138.2	1,029
Spoiler Actuation	133.4	1,487
Brakes Applied	128.4	1,929
End of Landing	0	3,614
FAR Field Length	~	6,022

Payload Range

The payload-range diagram for the Condor X can be found in Figure 36. The payload-range diagram includes range values for a maximum allowable payload matching that of the RFP with a slight increase in the number of passengers; 406 passengers with baggage equates to 93,380 pounds of payload. The ferry range of the Condor X was calculated to be 5065 NM, achievable with zero payload and a maximum fuel capacity of 15,095 US gallons. As illustrated in diagram, the line representing MTOW is atypically short; because the Condor X was designed specifically for the sizing/economic mission, there is little onboard fuel storage available for any mission designed beyond the sizing mission. All fuel storage on the Condor X is contained inside the wings, with no additional onboard fuel storage available. The required fuel capacity to complete the sizing mission is therefore very close to the fuel storage capacity, resulting in a narrow operating line between MZFW and MFW. However, operating with zero payload still results in a lengthy ferry range, capable of ferrying from the east coast of the United States to much of Eastern Europe.

PAYLOAD/RANGE FOR MACH 0.80 CRUISE
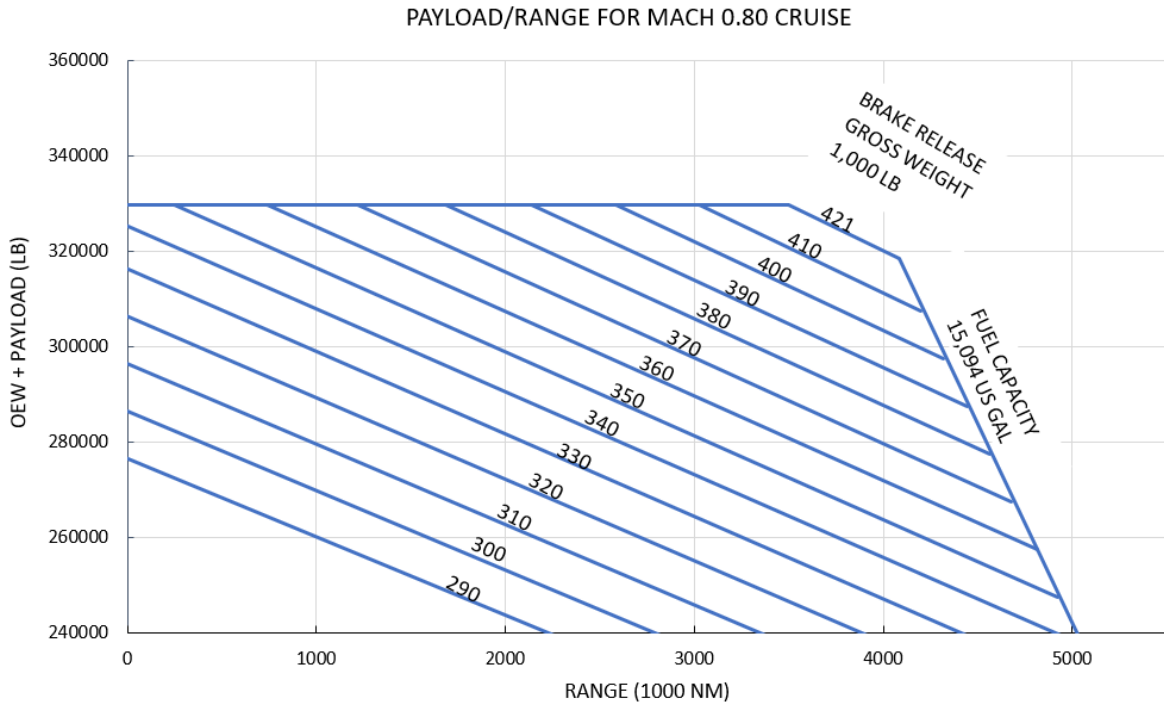
Figure 36. Condor X Payload-Range diagram with optimized step cruise

Structural Envelope

An important consideration for any prospective pilot or purchaser of the Condor X is the structural envelope. This illustrates under what condition the aircraft will be able to fly without exceeding speed or structural limitations. It is shown in the form of a V-n diagram, shown in Figure 37. This diagram shows the several important characteristics of the aircraft, which are detailed in Table IX.
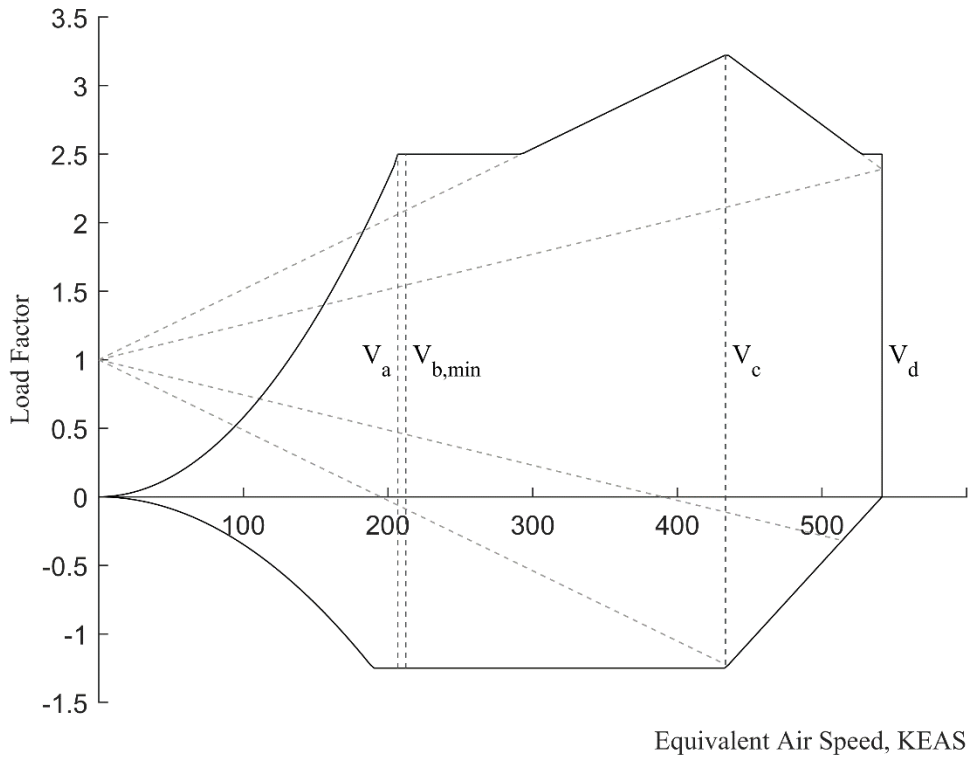
Figure 37. V-n diagram for the Condor X

The speeds shown in the table are normalized using a thrust lapse to represent conditions at the cruise altitude. The gust values are FAR25 requirements and the loads applied from them are represented via the dashed lines in Figure 37. As can be seen in Table IX, the load factor seen by the aircraft will only ever reach a factor of 3.22, at cruise speed with the strongest gust require. This will be the maximum load factor designed to in terms of structure placement, and the cruise speed is sufficiently far from V_b. This is to avoid any speed related complications that arise from the force of the gust acting on the aircraft's performance parameters.

Table IX. Relevant airspeeds and load factors from the V-n Diagram

	Airspeed (KEAS)	Load Factor
V_a	206.80	2.50
V_b	212.32	2.50
V_c	433.19	3.22
V_d	541.49	2.50
Gust 1	56.91	3.22
Gust 2	28.46	2.50

Constraint Analysis

After the weight sizing gave the result of the takeoff weight, a constraint diagram was made to validate the selected thrust loading and the wing loading from the FLOPS. Initially, the aspect ratio was selected to as Boeing 777-300ER, but the Condor X showed with aspect ratio of 9 the aircraft would require more thrust. Thus, the aspect ratio was increased to 12, which showed decreased the thrust by 6.5%. Thus, the result in the Figure 38 shows the constraint diagram for the Condor X with aspect ratio of 12. The Condor X thrust loading selected is 0.3 and 140 pound per square foot wing loading. The design mission and FLOPS values were used to construct the constraint diagram.

The takeoff performance was constructed based on the semi-empirical relationship for FAR 25 certified aircraft from Roskam Part I. Field length required by RFP is 9000 ft and since the aircraft have the double slot flap, the lift coefficient was chosen to by 2.39. [11] The climb performance was constructed by one-engine-inoperative with the landing gears retracted as stated by FAR 25. The climb was performed after the takeoff passed the 35 ft obstacle at speed of 161 knots. The approach speed given by the RFP is 145 knot and the lift coefficient used in this segment was 3.09 [11].
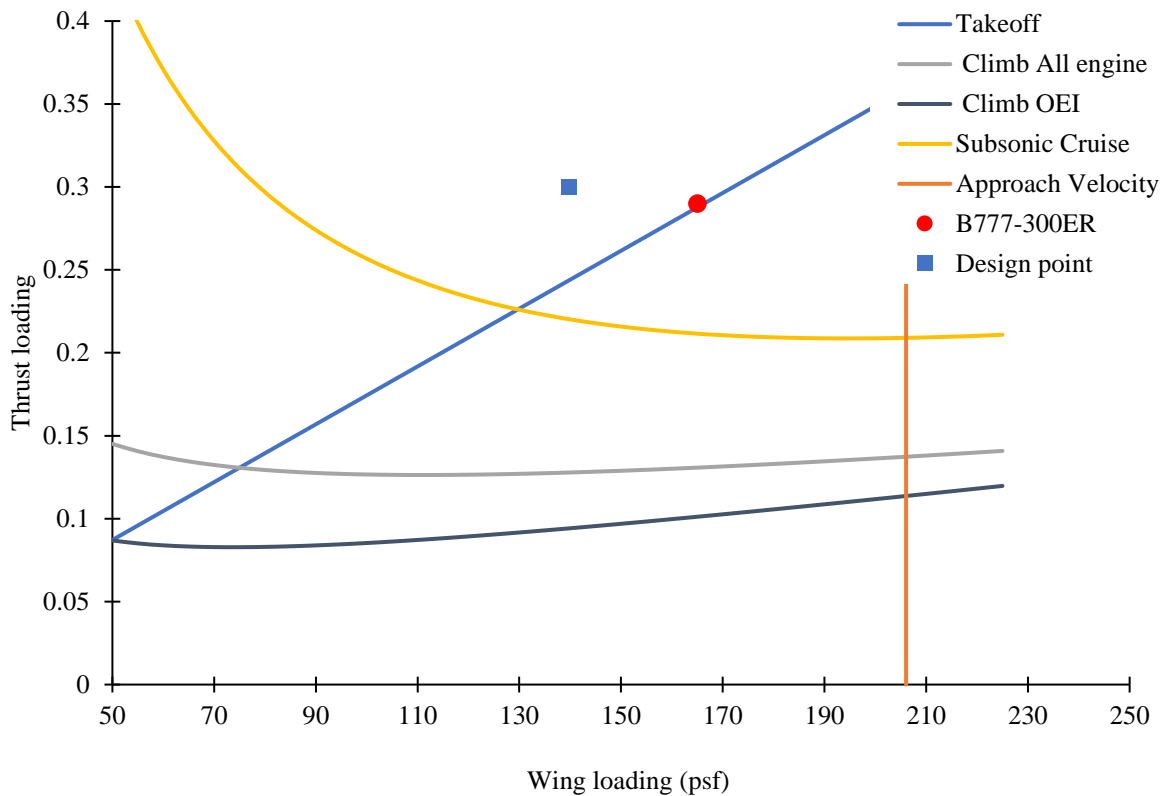
Figure 38. Constraint diagram

Propulsion

The engine selection for the Condor X began with establishing that the thrust required for the aircraft would need to be approximately 63,153 pounds. With this parameter, the engines of the Boeing 747, 767, and 787 were considered. The engines shown in Table X meet the required thrust levels and were quantitatively based on their thrust to weight ratios and their overall diameters. In addition, various parameters such as relative noise emission and fuel consumption were also qualitatively compared.

Table X. Compared engine parameters

Engine	Take-off Thrust	Dry Weight	T/W	Diameter (ft)
GEnx-1B [12]	72,300	13,552	5.34	11.43
CF6-80E1 [13]	69,800	11,225	6.22	9.43
GE90-110B1 [14]	110,760	19,316	5.73	12.88
GP7270 [15]	74,735	14,810	5.05	10.31
PW4164 [16]	64,500	12,900	5.00	10.25
Trent 1000-A [17]	69,194	13,087	5.29	12.47

The chosen engine is the GEnx-1B due to its relative interchangeability with the Trent 1000-A, the size of the fan, and the fuel benefits over the CF6-80E1. In terms of the thrust to weight ratio, the only engines that outperform the GEnx were the CF6 and the GE90. Although the GEnx has a larger weight and diameter than the CF6, it compensates for this by being a more fuel-efficient replacement for the CF6. As compared to the GEnx, the GE90 is severely overdesigned for this aircraft, and would not be suited for the current set up of the Condor X. As for the comparisons to the GP7270 and the PW4164, the GEnx was chosen over them because of the increased thrust to weight ratio seen in the chart, even though they are smaller engines. When comparing to the Trent 1000-A, the smaller engine was selected due to the similar thrust to weight ratios.

For the selected metrics, the CF6 has better performance parameters than the GEnx. However, the GEnx has several advantages over the CF6 in terms of other parameters, such as 15% improved fuel efficiency, 15% less CO_2 produced, 30% more use and 30% fewer parts, meaning its maintainability is greatly improved, as stated by GE [18]. GE goes on to state that the GEnx is the quietest engine that they have ever produced, based on a thrust per decibel rating, and that it has a higher durability and lower operating costs than comparable engines in its class. The combination of all these factors is ultimately why the GEnx was chosen for the Condor X.

For technical considerations as the GEnx was integrated into the designed aircraft, it became relevant through FLOPS that the engine could be sized down. This was because the thrust values given by the engine deck were more than enough for the aircraft. The engine was optimized by being scaled down to 93.7% of its values, resulting in desired thrust value and a total dry weight of the engine to 12,698 pounds. This optimization makes it so that the engine is powerful enough to meet requirements for the most strenuous flight conditions.

Cost Analysis

The cost analysis performed on the Condor X was done using the DAPCA IV model from the RAND Corporation [19]. The DAPCA IV model uses a series of CERs to determine estimations for RDT&E costs. It uses CERs to estimate flyaway and operating costs as well. While the original model uses labor rates from 1986, Condor Aviation used the U.S. Bureau of Labor Statistics inflation calculator to determine the approximate labor rates in 2020 dollars. The model encompasses a variety of factors including size, performance, construction, and various others. A few key factors primarily drive the cost estimation: weight, speed, and material composition. Consequently, Condor Aviation sought to minimize the cost of the aircraft primarily around these factors. The following sections break down the overall program, flyaway, and operating costs.

Program Cost

The program cost can be broken down into two sections: non-recurring and recurring. Non-recurring costs are the costs of development for the aircraft. This concerns the costs of engineering, tooling, quality control, development support, and flight testing. These costs are minimal in terms of the overall program cost. The bulk of the program cost stems from the recurring costs. Recurring costs are the costs of producing the aircraft. This concerns the costs of engineering, tooling, manufacturing, and quality assurance. Condor Aviation has also accounted for the cost of avionics and engines as well. Avionics cost assumptions are taken from Raymer [20], while the GEnx engine cost assumptions are taken from General Electric [21].

Where material composition is concerned, Advanced Airframe Structural Materials by the RAND Corporation [22] was used. The cost of advanced materials is factored in by applying a WMCF to each component of the development and production costs. The WMCF is built from three main factors: the structural cost fraction, the CF, and the component structural weight. Some components are weighted more heavily than others when it comes to factoring in advanced materials. For example, the recurring manufacturing materials CF is more than five times larger for composite materials than for aluminum, whereas the non-recurring engineering CF is barely larger than the baseline. The application of advanced materials mainly affects the recurring cost elements such as tooling and manufacturing. A complete list of the final non-recurring, recurring, and total program costs after the application of the WMCF is shown in Table XI. Note that the DAPCA IV model assumes a production run of 100 aircraft, therefore

the values seen within this table only reflect the cost of producing 100 aircraft. Larger production numbers are accounted for in the later sections where units produced is a factor.

Table XI. Development and production program costs for 100 unit production run.

Non-Recurring		
Engineering	$	3,799,000,000
Tooling	$	2,935,000,000
Development Support	$	698,000,000
Flight Test Cost	$	120,000,000
Non-Recurring Total	**$**	**7,552,000,000**
Recurring		
Engineering	$	3,053,000,000
Tooling	$	1,800,000,000
Manufacturing Labor	$	11,279,000,000
Manufacturing Materials	$	9,037,000,000
Quality Assurance	$	1,961,000,000
Avionics	$	1,344,000,000
Engines	$	57,000,000
Recurring Total	**$**	**28,531,000,000**
Sum Total	**$**	**36,083,000,000**

Flyaway Cost

Flyaway costs include all the costs of producing the aircraft, including the engines and avionics. For the purpose of this analysis, Condor Aviation chose to model the flyaway cost analysis off a three-year production run averaging 14 aircraft per month, totaling to 500 units produced. While this tends to increase the program cost by a large amount, it brings the flyaway cost to a much more reasonable amount. When compared to other aircraft of similar specifications, the Condor X has a much lower flyaway cost than its competitors, as illustrated in Figure 39.
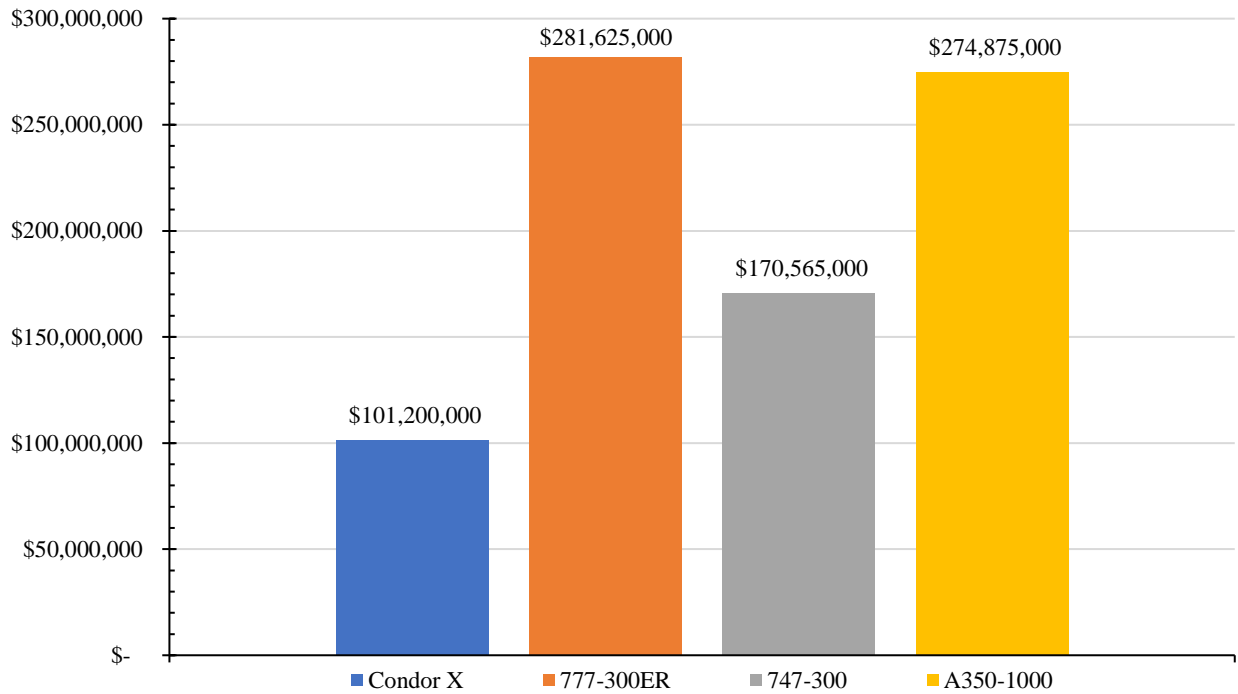
Figure 39. Similar aircraft flyaway cost comparison.

For the Condor X to truly be successful, it would need to make a profit. The RFP states a need for a 15% profit, so this number was kept in mind when calculating a purchasing price for the Condor X. When determining a purchasing price, the total cost of the program was taken into consideration. Comparing the purchase price to that of its competitors, it is obvious that the Condor X is a much more profitable option. Figure 40 shows the unit price for the Condor X alongside similar aircraft. While the 747-300 is the closest in terms of unit price, it is a much older and inefficient aircraft. This is further looked at in the operating cost section. For an overall look at the costs of the program see Table XII.
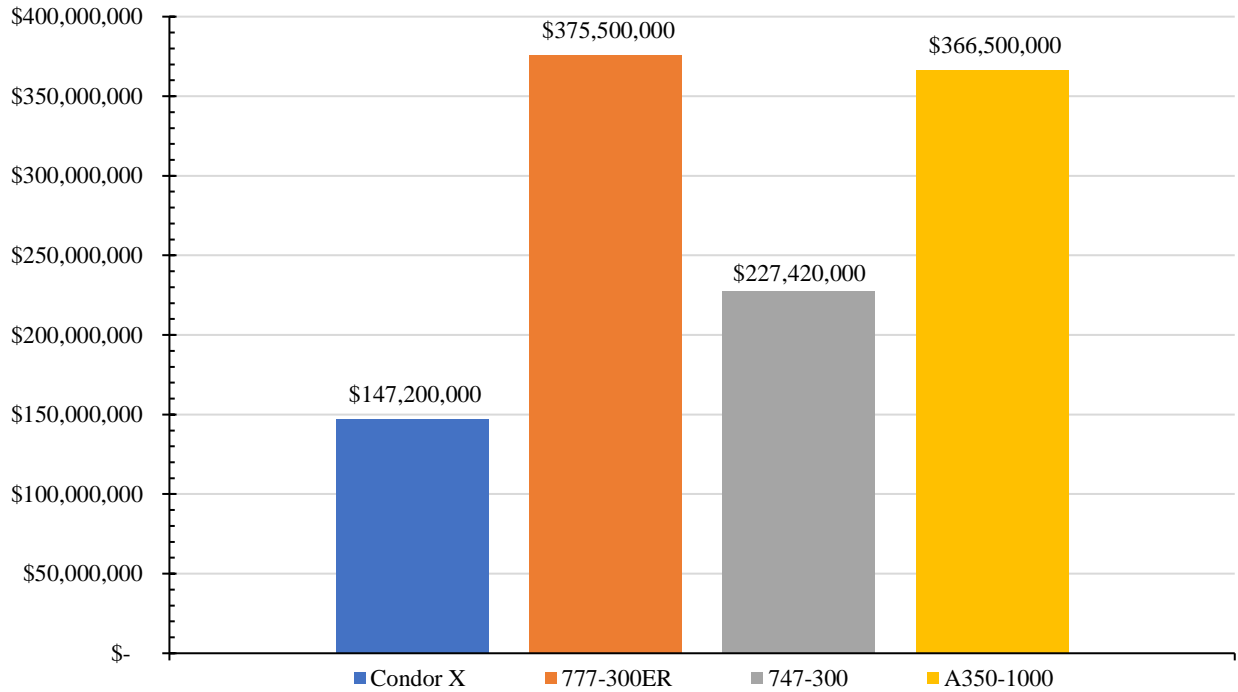
Figure 40. Similar aircraft unit cost comparison.

Table XII. Cost analysis evaluated with a 15% profit margin.

Units Produced	Program Cost	Flyaway Cost	Purchase Price	Profit
100	$ 36,084,000,000	$ 285,300,000	$ 415,000,000	$ 5,413,000,000
200	$ 46,183,000,000	$ 182,600,000	$ 265,600,000	$ 6,927,000,000
300	$ 53,354,000,000	$ 140,600,000	$ 204,500,000	$ 8,003,000,000
400	$ 59,108,000,000	$ 116,800,000	$ 169,900,000	$ 8,866,000,000
500	$ 63,995,000,000	$ 101,200,000	$ 147,200,000	$ 9,599,000,000
600	$ 68,286,000,000	$ 90,000,000	$ 130,900,000	$ 10,243,000,000
700	$ 72,138,000,000	$ 81,500,000	$ 118,500,000	$ 10,821,000,000
800	$ 75,650,000,000	$ 74,800,000	$ 108,700,000	$ 11,348,000,000
900	$ 78,890,000,000	$ 69,300,000	$ 100,800,000	$ 11,834,000,000
1000	$ 81,905,000,000	$ 64,800,000	$ 94,200,000	$ 12,286,000,000

Figure 41 gives a more in-depth look at the production run chosen. At 14 units a month for three years, a little over 500 units will be produced. As seen in the figure, the break-even point is 292 units produced after 1.75 years. The total profit at the end of the production run is $9.6 billion, as shown in Table XII.
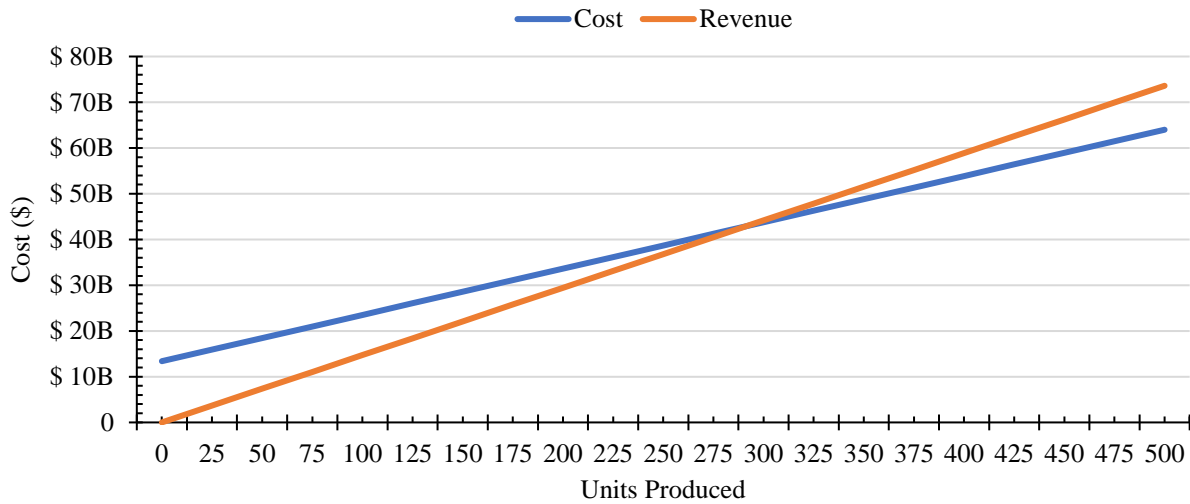
Figure 41. Cost versus revenue for a 3-year, 500-unit production run.

Operating Cost

As per the RFP, the operating costs were determined based on the 700 nautical mile reference mission. The operating cost analysis takes several factors into consideration.

- Fuel and gallon Carbon tax

- Maintenance and materials (oil, tires, etc.)

- Flight and cabin crew

- Insurance

- Depreciation

For the Condor X and the 777-300ER, Condor Aviation used FLOPS output files to get more accurate flight characteristics, most importantly for fuel burn. Maintenance cost approximations are based on MMH/FH, maintenance rates, and materials costs. MMH/FH are based on similar aircraft from Nicolai and Carichner [23], maintenance rates are taken from FAA [24], and maintenance materials are from Raymer [20]. Flight crew rates are also taken from Raymer [20], and cabin crew rates are taken from the U.S. Bureau of Labor Statistics [25]. Insurance rates are taken from Oliver Wyman [26]. Depreciation rates are taken from GRA Incorporated [24]. A comparison of operating costs of the Condor X to competitors is shown in Figure 42 . Note that the insurance cost is so low that it is not visible on

the graph. The Condor X is obviously the best choice across the board, only being beaten commonly in the insurance and depreciation categories. The 747-300 is also slightly cheaper in terms of maintenance, but this is likely due to the engines of the older aircraft being much simpler and therefore easier to maintain.
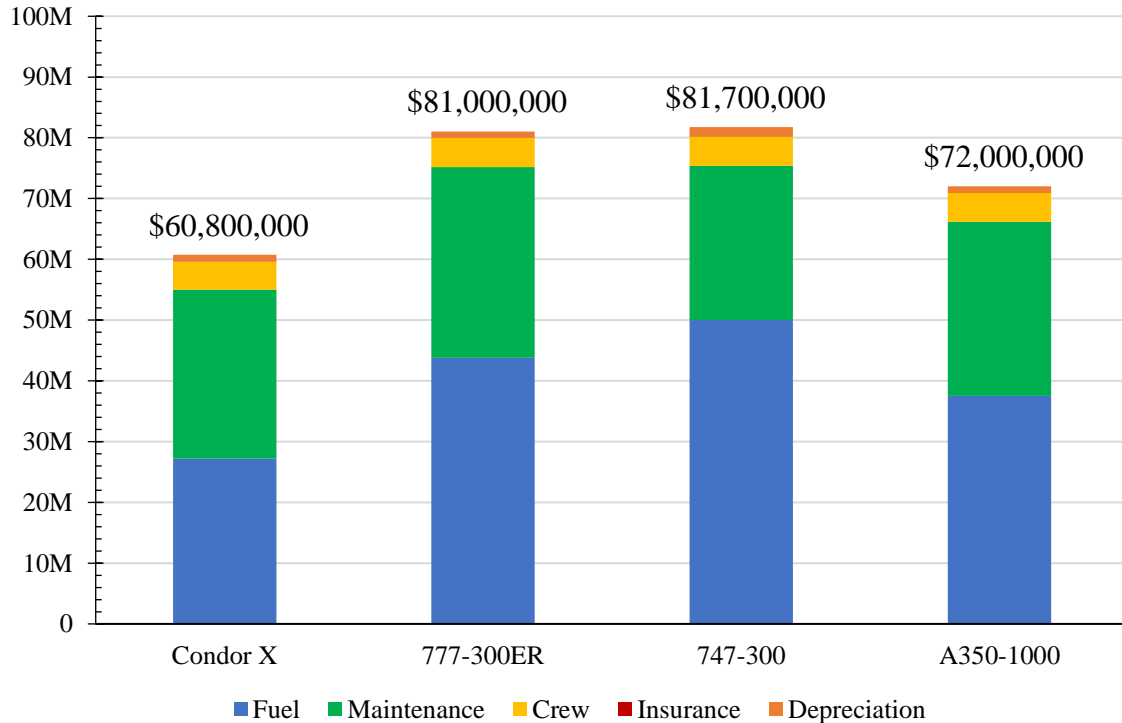
Figure 42. Similar aircraft yearly operating cost comparison based on 700 nautical mile reference mission.

The operating cost for the Condor X is expanded upon in Figure 43 , giving values for each component. The reason the maintenance cost is so high is because the Condor X is expected to be taking off and landing more frequently than the average aircraft. This is to be expected because the aircraft is built for short haul flights.
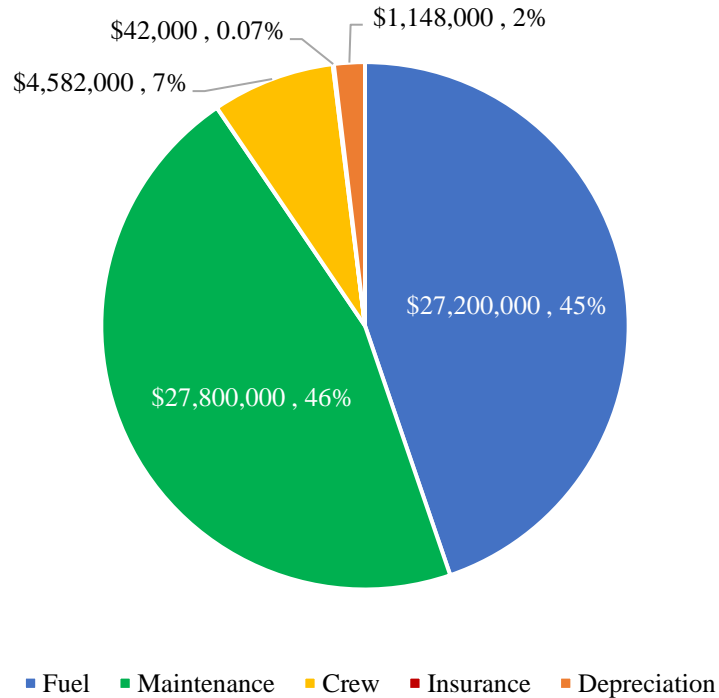
Figure 43. Portion breakdown of operating cost.

One important measure of the operating cost of an aircraft is the CASM. Generally, this is the cost incurred to fly a single seat one mile. It serves as a good measure of the efficiency of various airlines. An analysis was performed on the CASM for the Condor X and its competitors using the 700 nautical mile reference mission. Table XIII shows the results of this analysis. As seen in the table, the Condor X is significantly cheaper to operate than the other aircraft. Depending on the carrier, the 11 percent CASM of the Condor X could be quite profitable. This is dependent on carrier because some carriers can expect larger RASM values than others. According to the Airline Economic Analysis [27], major carrier such as Delta, American, and United had an average RASM of 15.7 cents in 2018, whereas smaller carrier such as Southwest, JetBlue, and Virgin see an average RASM of 12.9 cents. When compared to the Condor X, aircraft like the 777 and 747 cannot be run profitably by smaller carriers where the 700 nautical mile reference mission is concerned.

Table XIII. Similar aircraft CASM comparison based on 700 nautical mile reference mission.

	Condor X	777-300ER	747-300	A350-1000
Fuel	$ 16,579.16	$ 25,288.12	$ 28,855.38	$ 21,641.53
Main.	$ 12,213.59	$ 12,732.31	$ 11,033.95	$ 11,836.70
Crew	$ 1,775.99	$ 1,759.08	$ 1,784.83	$ 1,726.21
Insurance	$ 25.56	$ 22.22	$ 20.20	$ 23.23
Depreciation	$ 698.64	$ 587.66	$ 835.40	$ 633.75
Total	$ 31,292.94	$ 40,389.40	$ 42,529.77	$ 35,861.43
CASM	$ 0.11	$ 0.16	$ 0.15	$ 0.14

Carbon Emissions

Emissions from Operation

CO_2 emissions for the Condor X were estimated during both the 3500 NM sizing mission and the 700 NM economic mission using the carbon dioxide emission coefficient published by the U.S. Energy Information Administration [28]. This coefficient is published as 21.10 pounds per gallon of jet fuel. The CO_2 output for each mission was then normalized by passenger count so that the CO_2 emissions from several aircrafts flying similar length missions could be compared. These comparisons for the sizing and economic mission can be found in Table XIV and Table XV respectively.

Table XIV. CO_2 emissions and fuel efficiency comparison – Sizing mission

Airplane	# of Pax	Sector (nm)	Fuel Burn (lb/nm)	Fuel Efficiency (seat-nm/gal)	CO_2 (lb/seat-nm)
Condor X	406	3500	22.11	124.85	0.169
747-8 [29]	467	3500	40.86	76.46	0.276
777-200ER [30]	301	3500	28.76	69.65	0.303
787-9 [31]	304	3500	23.51	86.25	0.245
A330neo-900 [32]	310	3500	24.47	84.07	0.251

Table XV. CO$_2$ emissions and fuel efficiency comparison – economic mission

Airplane	# of Pax	Sector (nm)	Fuel Burn (lb/nm)	Fuel Efficiency (seat-nm/gal)	CO$_2$ (lb/seat-nm)
Condor X	406	700	26.45	104.39	0.202
737-MAX 9 [33]	180	700	13.28	90.82	0.232
757-300 [34]	243	700	20.37	80.14	0.263
A319-neo [35]	144	700	13.29	74.26	0.284
A220-300 [36]	160	700	11.16	95.74	0.220

As shown in Table XIV and Table XV, the Condor X maintains the lowest CO$_2$ emissions across the board when flying both the smaller regional mission and the longer sizing mission. The Condor X achieves significantly higher fuel-efficiency per passenger than other common short haul aircraft in addition to larger wide-body aircraft while carrying more passengers.

The low overall in-flight carbon footprint relative to its size means that the Condor X is also well-positioned to satisfy the ICAO CO$_2$ emissions standards set forth in ICAO Annex 16, Vol. 3 [36]. These new ICAO standards amended in 2017 clearly define a CO$_2$ evaluation metric based on the size and specific air range (SAR) of a newly certified aircraft to ensure aircraft adhere to stricter carbon emissions standards. The evaluation metric can be found in Equation 1, where SAR is in units of kilometer per kilogram and reference geometry factor (RGF) is in unitless. RGF is defined as the area of the passenger compartment at the midsection of the fuselage parallel to the floor of the aircraft interior.

$$CO_2\ emissions\ evaluation\ metric\ value = \frac{\left(1/SAR\right)_{AVG}}{-RGF^{0.24}} \tag{1}$$

$$Maximum\ Value = 10^{-1.412742+\left(-0.020517*log_{10}(MTOM)\right)+\left(0.0593831*(log_{10}(MTOM))^2\right)} \tag{2}$$

The maximum metric value allowed in the ICAO standards varies by aircraft type/weight but is typically defined by an equation that depends on MTOW. Because of the weight category of the Condor X, the maximum allowable metric value was calculated using Equation 2. Using Equations 1 and 2, the maximum allowable metric value was calculated to be 1.3664, while the actual CO$_2$ emissions evaluation metric value was calculated to be 1.2049.

The Condor X therefore satisfies the most recent ICAO carbon emission standards and even maintains a noticeable margin such that it should continue to satisfy future emission standards as well.

Emissions from Production

Emissions from production stem mainly from the CO_2 emissions of the manufacturing process of various metals used in the airframe. The metal with the highest carbon footprint is titanium, at 36 pounds CO_2 per pounds of material. Fortunately, this only accounts for a small portion of the Condor X airframe. In comparison, steel has the lowest carbon footprint, at 2.35 pounds CO_2 per pound material. Where the Condor X shines in terms of the carbon footprint is the high percentage of composite materials. As seen later in the Materials section, the Condor X uses more composite materials than competitors, lowering the carbon footprint considerably. The carbon footprint of composite materials is also relatively small, being only 4.79 pounds CO_2 per pound material. Values for these carbon ratios are taken as an average from ARPA-E and Ziadeh [37] [38]. For a complete list of the amount of emissions of production, see Table XVI.

Table XVI. Carbon emissions from production.

Material	lb CO_2/lb Material	lb CO_2 per Plane
Aluminum	16.10	400,979
Titanium	36.00	647,544
Steel	2.35	19,509
Composites	4.79	364,520

Aerodynamics

Airfoil Selection

The most important airfoil requirement for a transonic commercial transport aircraft is a critical Mach number higher than the cruise Mach number. If this is not met, the aircraft will experience significant wave drag, reducing both fuel efficiency and range. This requirement limits the range of possible airfoils to those which are supercritical and designed for existing transonic aircraft. One example is the Common Research Model (CRM) wing, which was jointly designed and tested by Boeing and NASA between 2007 and 2009. The CRM wing was designed for a Mach 0.85 cruise, so its airfoils have a critical Mach number well above the Mach 0.8 cruise speed of the Condor X [39].

Because of the extensive experimental testing done on the CRM wing, drag polars are available over a range of flight conditions [40]. Figure 44 compares the CRM drag polar at Mach 0.8 and 0.85 to the Boeing 747 at its cruise condition of Mach 0.84 [41]. This comparison and the reliability of the CRM data led to the decision to use the CRM airfoils.
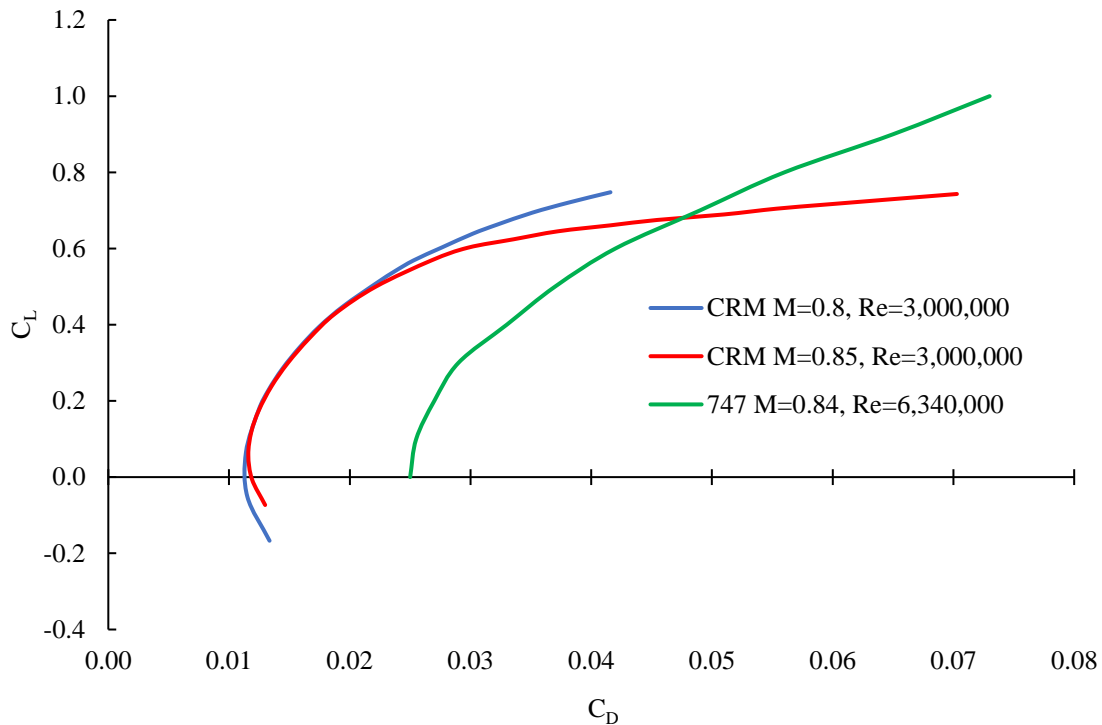
Figure 44. CRM and 747 drag polar comparison

Once the CRM wing was chosen as a model, three airfoil sections were extracted from the publicly available geometry of the wing [42]. These three sections are located at the root, 37% of semi-span, and the tip. Each of the three airfoils were scaled such that their chord lengths matched the design chords of the Condor X at each section location. Figure 45 shows the untwisted geometry of each scaled airfoil.
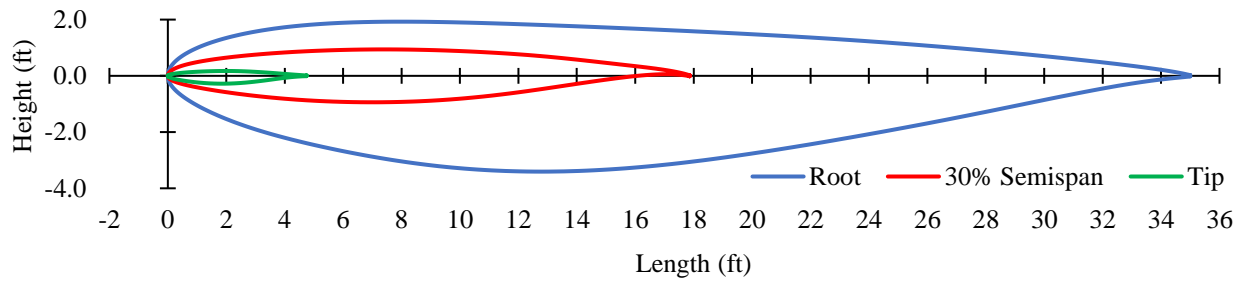
Figure 45. Condor X airfoil sections

Wing Geometry

The twist of the root and tip airfoils were not changed from their values in the CRM wing because these airfoils were designed to perform with the twist distribution of the CRM wing. Twist and thickness were both increased in the mid-span section in order to make the wing more closely match the CRM twist and thickness distributions. This was necessary because the Condor X midspan section is located at 30% of semi-span compared to 37% for the CRM mid-span section. The CRM and final Condor X airfoils with twist and thickness adjusted are both shown in Figure 46. The final twist and thickness distributions of the Condor X wing are shown in Figure 47 and Figure 48, respectively.
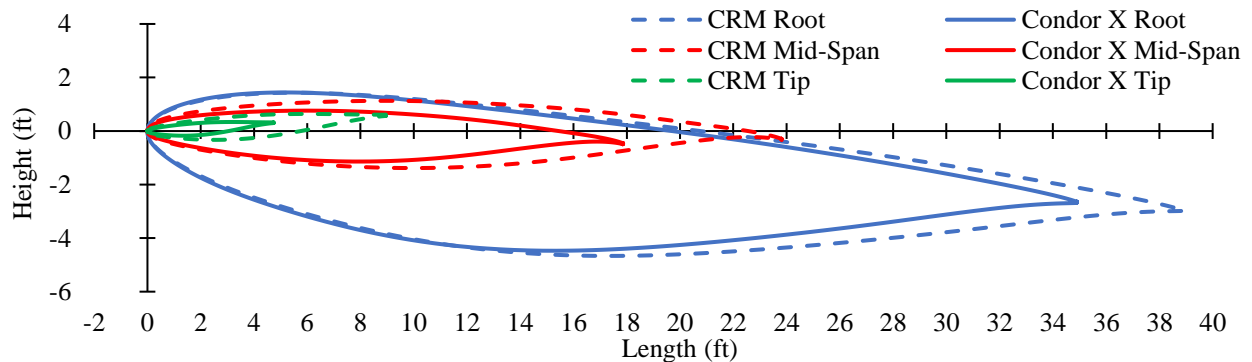
Figure 46. Condor X airfoils before and after adjustment
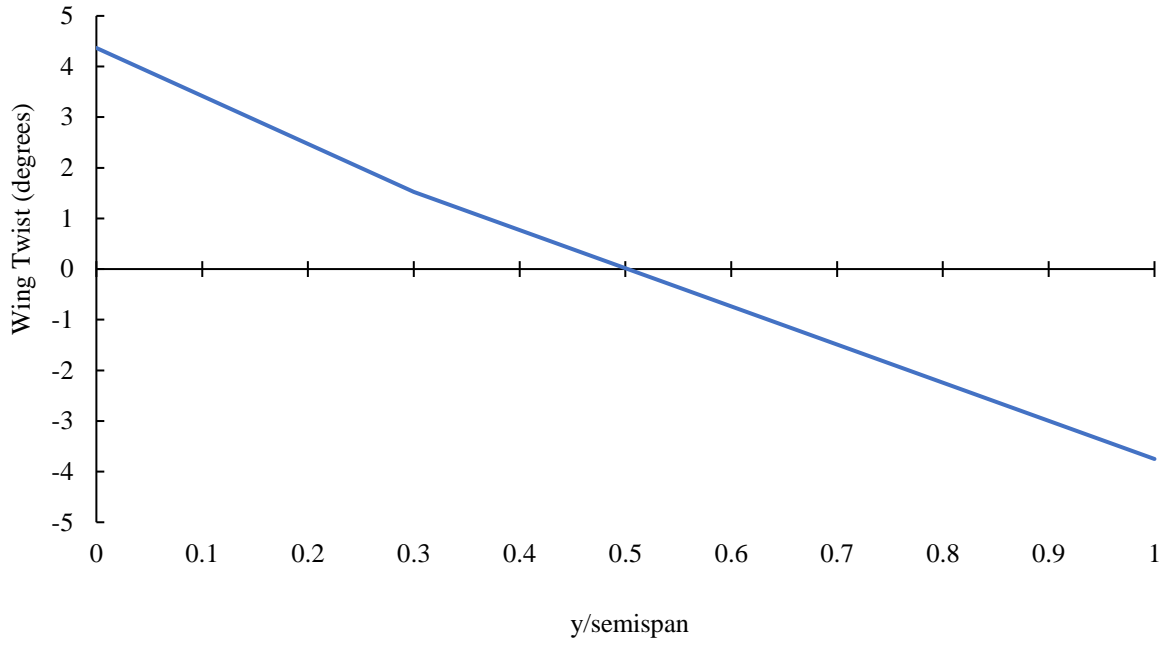
Figure 47. Wing twist distribution
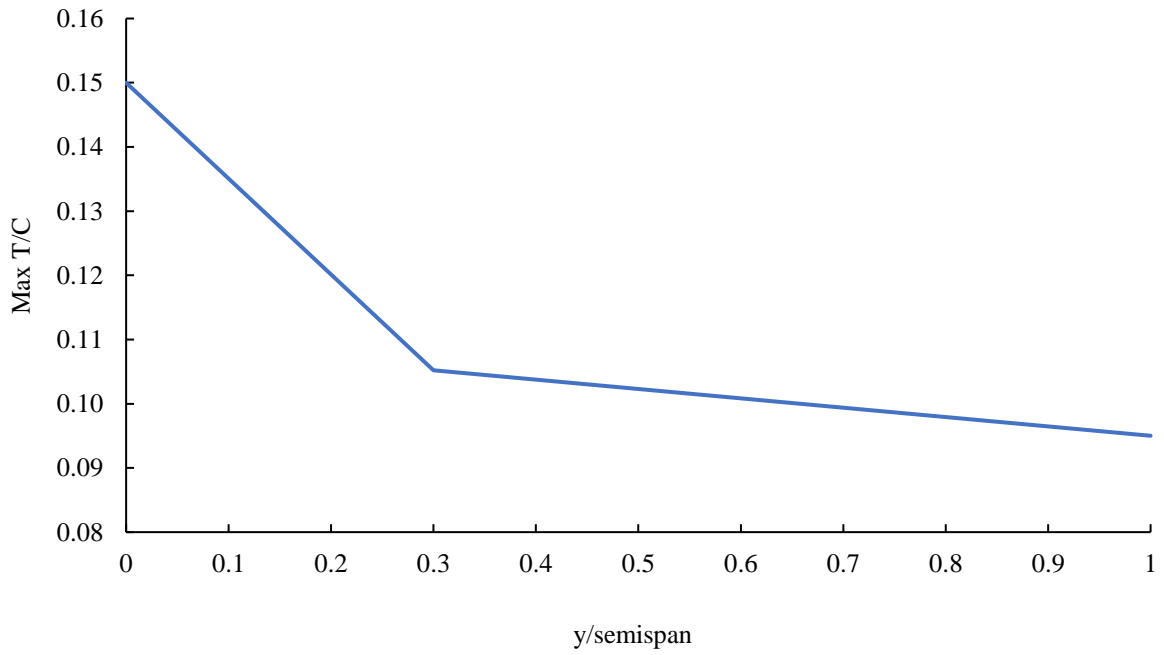
Figure 48. Wing thickness distribution

The Condor X wing has a constant leading-edge sweep of 31-degrees and an average quarter-chord sweep of 26.57 degrees. This sweep can be smaller than the 35-degree CRM sweep without causing wave drag issues because the Condor X cruises at Mach 0.8 compared to 0.85 for the CRM [39]. A top view of the wing geometry is shown in Figure 49 with the quarter-chord highlighted in purple, and general wing geometric parameters are listed in Table XVII.
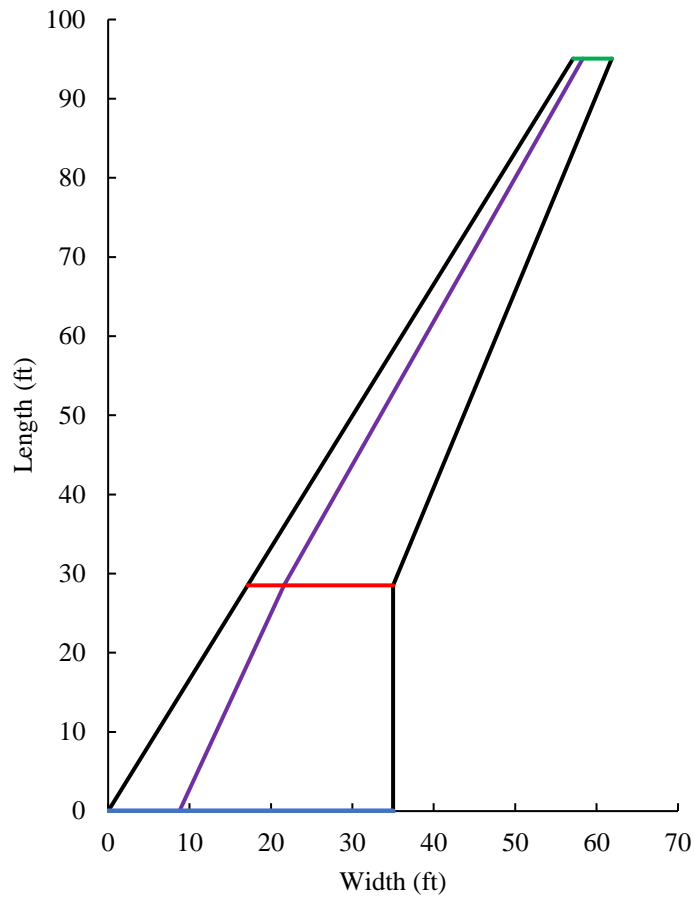
Figure 49. Top view of wing geometry

Table XVII. Major geometric wing parameters

S_{ref} (ft^2)	b (ft)	AR	Dihedral (deg)	Taper Ratio	(t/c)$_{avg}$	$\Lambda_{c/4}$ (deg)
3,012	190.12	12	7	0.19	10.8%	26.57

Stability Results and Tail Sizing

The Condor X utilized a conventional tail configuration and the Figure 50 shows the configuration. The tails were sized using the volume coefficient based on the Boeing 777-300ER. FLOPS has its own volume coefficient equation [43], and it showed that the Boeing 777-300ER has a horizontal and vertical tail volume coefficient of 1.942 and 0.171, respectively. Table XVIII lists the major geometric tail parameters.
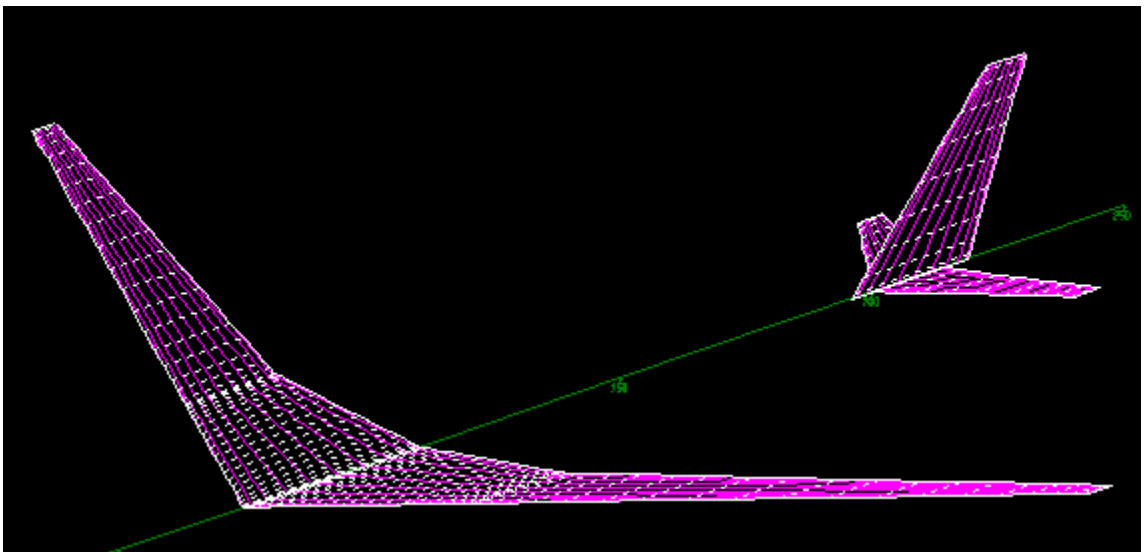
Figure 50. AVL lift surfaces model

Table XVIII. Horizontal and vertical tail geometry

	Horizontal	Vertical
Reference area (ft^2)	410	432.9
Reference span (ft)	43	27.9
Quarter-chord sweep (deg)	37.5	40
Aspect ratio	4.5	1.8
Taper ratio	0.35	0.33

The wing surface was modeled in AVL using the set of three airfoils and the twist distribution defined in the aerodynamic section, zero incident angle and a seven-degrees dihedral. The wing leading edge is 75 feet behind the

nose. The horizontal and vertical tails used NACA 0010 and NACA 0011 airfoils with zero incident angle and twist, and their leading edges were placed at 196 feet and 201 feet behind the nose. AVL showed that for this configuration, the horizontal tail must be reduced to have an acceptable static margin. Thus, the horizontal tail area was reduced to 410 square feet. The static margin that corresponds to this area is 22% and the tip-over angle is 15 degrees. The neutral point is the x-direction lays 108 feet from the nose. The Table XVIII and Table XIX shows the stability derivative for this configuration at Mach 0.2. The result shows that at low speed the Condor X is stable and has a reasonable response to perturbation compared to the Boeing 747-100.

Table XVIII. The longitudinal stability derivative at M=0.2

Stability derivative (1/rad)	Condor X	B747-100 [44]
$C_{L\alpha}$	5.50	5.67
$C_{m\alpha}$	-1.08	-1.45
C_{mq}	-26.5	-21.4

Table XIX. The lateral stability derivative at M=0.2

Stability derivative (1/rad)	Condor X	B747-100 [44]
$C_{Y\beta}$	-0.374	-1.08
$C_{n\beta}$	0.167	0.184
$C_{l\beta}$	-0.113	-0.281
C_{lp}	0	-0.502
C_{nr}	-0.233	-0.36

Subsystems

The design of the Condor X included an analysis of all major aircraft subsystems that are required to ensure the safety of passengers as well as the functionality of the aircraft. The choices made in the design ensured that all systems would mesh and work together in a practical manner. After the innovations outlined in the following sections

were applied to the Condor X, the weight of the aircraft was reduced by over 6,000 pounds compared to the reference Boeing 777-ER.

Hydraulics

While technology in the electric space for the manipulation of control surfaces is advancing, it was decided that the Condor X would make use of traditional hydraulics. This decision was made with cost in mind, as reinventing the wheel is expensive for both development and regulatory reasons. The Condor X does improve on the designs of most current aircraft, taking a page from the Airbus A380, Boeing 787, and many military aircraft by using high pressure 5,000 psi hydraulic fluid [45]. The use of eight hydraulic pumps, as seen in Figure 51, includes redundancy to ensure that in the event of a pump failure on taxi or takeoff, the airline will not need to reschedule up to 400 passengers onto other flights. This advancement in technology helps to reduce weight of the system as a whole by allowing for the use of less fluid and smaller diameter tubing throughout the aircraft. The weight savings from the use of high-pressure hydraulics was estimated to be a 20% over the use of a typical 3,000 psi system [45]. The reduction in tubing diameter will also allow the space saved to be used for uses such as additional fuel capacity.
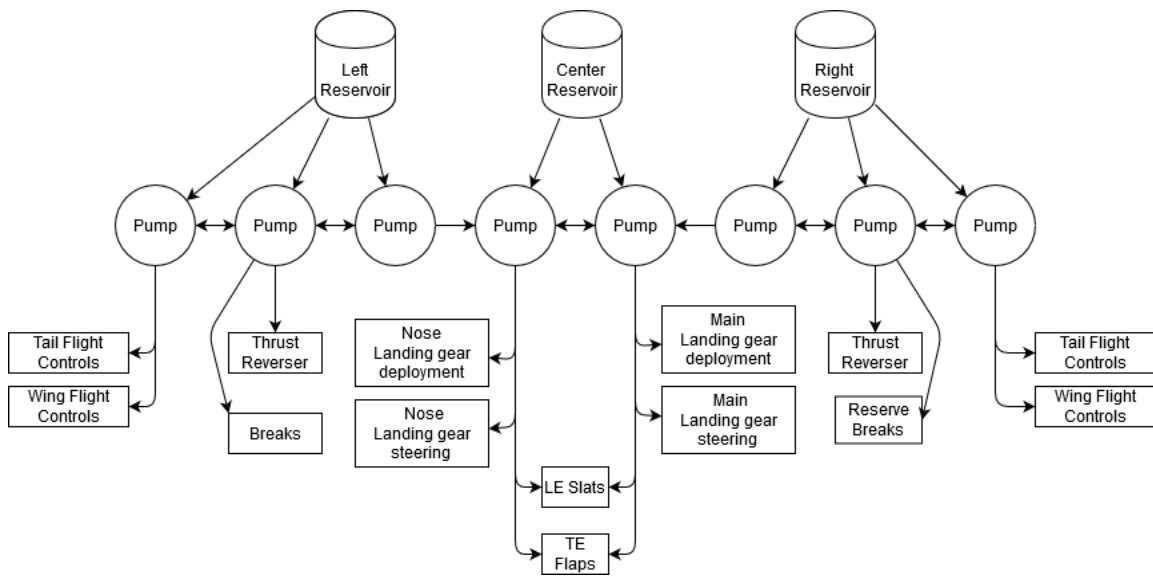
Figure 51. Hydraulic System Schematic

Furnishings

Figure 52 shows the seats chosen for economy class are the Recaro SL3710 seats. These were chosen as they are lightweight seats, coming in at just over 17 pounds each [46], but still allow all the comforts that are needed for the shorter-range flights that the Condor is expected to make.

Figure 52. *Render of Recaro SL3610 economy class seating [46]*

Figure 53 shows the business class seats were also chosen from Recaro, their CL4400 models. These seats are much more luxurious than the economy models, coming equipped with TV screens, extendable footrests, and room enough for both passengers to rest their arms. [47]

Figure 53. Render of Recaro CL4400 business class seating [47]

In addition to the seats there will be four exit doors on each side which comply with FAR 25 Type 1 emergency exit requirements. There will also be floor lighting and emergency exit signs powered by auxiliary batteries, not dependent on engine power. In the case of a cabin depressurization oxygen will be delivered to the masks through a chemical oxygen generator. This system was chosen over the gaseous manifold system due to its much smaller form factor for the volume of oxygen required by 400 passengers and crew. The furnishings of the aircraft will be similar to most other similar aircraft, the overhead bins will be made from sturdy, lightweight plastics.

In-Flight Entertainment

To keep up with its competition, the Condor will be equipped with in-flight entertainment systems for all passengers. This business class passengers will have the ability to choose from a curated list of TV shows, movies, and music on the display in the headrest in front of their seat. The economy class passengers will have this same luxury, although they will need to access the media through their mobile device. All the media that can be streamed to both the in-seat TV's and mobile devices will be stored locally, on the aircraft on a media server. This will allow the media to be streamed out to passengers while avoiding the need to access the internet. The rest of requests, such as web browsing, messaging, and other communication, will be served through a satellite internet connection. As both a service to the passengers and to reduce bandwidth on the satellite connection, malware, ads, and tracking will be run though a DNS sinkhole.

Fuel System

The Condor, like all commercial aircraft, is a wet winged aircraft that has fuel lines running from the in-wing fuel tanks to the engines. The engine fuel delivery system is powered by four 28V pumps, a forward and aft pump on each side. These four pumps are aligned such that they are feeding their respective sides engine, although in the case of engine or pump failures there will be cross feed valves in between the pumps that will allow the left side pumps to feed the right engine and vis versa. There will also be one pump that feeds fuel into the APU as well as a left and right jettison pump for a total of seven fuel pumps.

Electrical and Power Generation

As the Condor X is an all-electric aircraft besides the anti-icing system, it has higher electrical power usage and draw than similar classes aircraft. The Condor X would require about 900 kVA of power if all systems were all running at the same time. The electrical system on the Condor X shares similarities with that of the Boeing 787. On most traditional commercial aircraft, the power is generated by the engines and then immediately stepped down to a 115V AC signal to be distributed to other subsystems all other AC subsystems, only changed when a device required a DC signal. The Condor's power generation and delivery system creates a baseline 230V variable frequency signal that is directly passed on to components that can receive higher powered, less regulated currents. For components that are not able to receive the unregulated signal, or need even higher voltages, the signal is stepped up or down to the required levels to be used. A visual representation of how this works is shown in Figure 54.
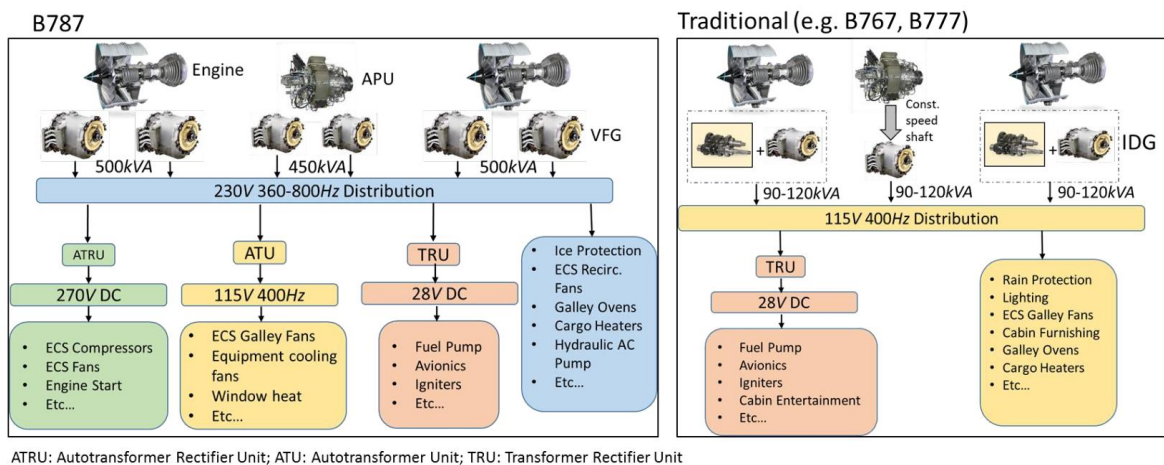
Figure 54. Diagrams of electrical distribution systems for the Boeing 787 and Condor vs traditional systems [48]

This method of power delivery is superior to the traditional model for several reasons. First the complexity of the power generation system is reduced, as the variable frequency generators can be attached directly to the engine instead of needing to have the shaft geared down to a constant speed. This reduction in complexity increases efficiency on the power generation side. Second the reduction in number of components reduced the points of failure, increasing the reliability of the system.

Avionics and Communication

To ensure the safety of passengers and compliance with FAA Part 25 standards, the avionics of the Condor X will be custom designed for the aircraft. This decision was made due to the complexity of the Condor X's control systems and the size of the aircraft. The avionics will be comprised of five large touchscreen displays similar to the Rockwell Collins ProLine Fusion line in the 777X, four across the dash behind the yokes and one lower and centered between the pilot and copilot.

Fiber optic cables were chosen as the transmission method inside the aircraft as much of the aircraft as possible as they are both lighter, faster, and higher bandwidth than their copper counterparts. The main passenger cabin will be equipped with a PA system that will allow pilots or flight attendants to address passengers at any time; this system will also disrupt and music or movies that are being watched through the in-flight entertainment systems.

Environmental Controls

The Condor X will have an environmental controls system that will allow the for passengers to control personal air conditioning as well as temperature regulation in the cabin of the aircraft. This system will be powered electronically instead of through bleed air. This decision was made for two main reasons. First, to reduce the need for bleed air to just the anti-icing ssystem. This will allow for greater cruise fuel efficiency, as less airflow will be diverted and wasted on non-propulsion systems. Second, electrical air conditioning and environmental control systems weigh less than their bleed air counterparts. Due to the high altitudes that the Condor will be flying at a pressurization altitude of 8,000 feet was chosen.

Due to the large amounts of sound generated by both the engines and the aircraft physically moving though the sky, the Condor is equipped with sound insulation between the outer and inner shell of the aircraft in the form of carbon fiber mesh dampeners. These dampeners absorb the vibrations within the panels that make up the shell of the aircraft. In addition to the carbon fiber, overhead bins and wall panels will have vibration dampeners integrated to where they attach to the walls of the aircraft.

Cargo Container

The Condor X can use either two single or one double contoured unit load device to maximize the amount of storage capacity in the cargo bay of the aircraft in a passenger configuration. The lower deck can accommodate 50 LD3 unit load devices in both the passenger and cargo configurations. The plane can also be retrofitted after it is retired from passenger flights to be a cargo aircraft. In this configuration, there is still the same amount of room in the lower cargo bay, but there is also room enough for the tallest PMC pallet configurations (118 inches). The main cargo deck can hold 21 118-inch high PMC pallets, or 32 low-height PMC, M-1, or M-1H unit load devices.

Anti-icing system

While there is research into electronic anti icing systems on GA aircraft, the Condor's anti-icing system is powered by bleed air. This decision was chosen because the weight and complexity disadvantages of running conductive material under the surface of every area that would need to be deiced was found to be heavier and less efficient than the bleed air alternative. Conversely, having hot engine bleed air run through piccolo tubes at all the leading edges on the plane is more efficient as the tubes are hollow instead of solid.

Materials

Condor Aviation aimed to maximize aircraft performance by utilizing the best available technology. Two of the aircraft most representative of the state of the art in the area of materials are the Boeing 787 and the Airbus A350. The material composition of both aircraft was studied, and a reasonable estimate for improvement upon the materials and building techniques utilized in their designs was produced.

The Boeing 787, certified in 2011, was the first wide-body commercial airliner comprised of 50% composite materials by weight [49]. This was accomplished in large part due to advanced building techniques which allowed Boeing to produce large, single-piece fuselage barrel sections with carbon fiber laminate. Similar laminate techniques were also used to construct large sections of the wings, control surfaces, and empennage. Carbon composite sandwich panels were used on the nacelles, wing body and wingtips, and the empennage control surfaces due to their high bending stiffness [50]. Other composites were used around the wing and empennage leading edges as well as the wing attachment points to resist compression loading [51]. The 787 also minimized aluminum usage by incorporating 15%

titanium by weight in areas like the tail cone. Overall, these design improvements resulted in a weight savings of up to 20% compared to a traditional aluminum airframe according to Boeing, although this estimate is unverified [49].

The Airbus A350, which was certified in 2014 three years after the 787, raised the use of composites from 50% to 53% by weight [52]. Although Airbus chose to construct the fuselage out of separate panels instead of using Boeing's single-barrel approach, they also used carbon fiber reinforced plastic (CFRP) materials in their fuselage [53]. Benefits of this decision include a better strength to weight ratio and increased resistance to fatigue and corrosion compared to metals. The A350 achieved a reduction in structural maintenance tasks of 50% and an increase in the time threshold between airframe checks of 50% compared to the A380 [53]. Another benefit of using CFRPs in construction is their ability to be melted down and recycled, which makes the aircraft more sustainable [53]. Airbus managed to reduce the percentage use by weight of steel, titanium, and aluminum alloys compared to the 787 despite using mostly aluminum in the cockpit [52]. They also set a goal weight reduction of 20% compared to an aluminum design, although this is also not verified for the final design [54].

The Condor X materials selection combines the most successful aspects of both of these designs. It will consist of single-barrel CFRP fuselage sections similar to those used in the 787, maximize the utilization of composites in the wings and empennage, and minimize the use of steel to a level comparable to the A350. To be conservative, it was assumed that the 787 and A350 achieved a final weight savings of 15% compared to equivalent aluminum airframes because the 20% goal of both was unverifiable. By maximizing composite use in structural components and minimizing the use of metals, it was assumed that weight savings in the Condor X would be approximately 18% compared to an equivalent aluminum airframe. Because this estimate is still below the 20% claimed by Boeing and Airbus for their designs and the Condor X will enter service a full 18 years after the 787 and 14 years after the A350, it is viewed by Condor Aviation as a reasonably conservative estimate. A materials breakdown for both existing aircraft and the Condor X is shown in Figure 55.
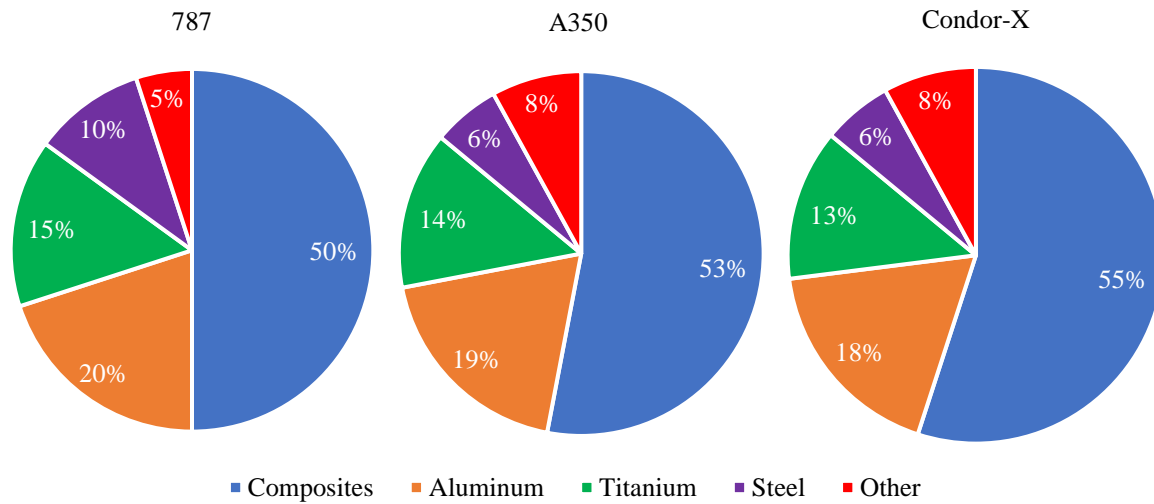
Figure 55. Material composition comparison between the Boeing 787, Airbus A350, and Condor X

The 18% weight reduction estimate was used to reduce specific component weights in the FLOPS model during weight sizing. Because the base model was a Boeing 777-300ER, it was assumed that the airframe was nearly entirely aluminum. For this reason, the wing and both the horizonal and vertical tail weight multipliers were reduced by 18%. Because the 777-300ER used composites in its floor panels, the overall fuselage weight reduction was assumed to be only 15%. Landing gear weight was assumed to be less flexible due to the use of steel which cannot be replaced with composites due to the load requirements, so the landing gear weight multiplier in FLOPS was left unaltered. Figure 56 shows the weight reduction of different components. Note that the component differences in gross weight between the Condor X and a 777-300ER would be larger than the percentage differences shown in Figure 56 because the Condor X airframe is smaller.
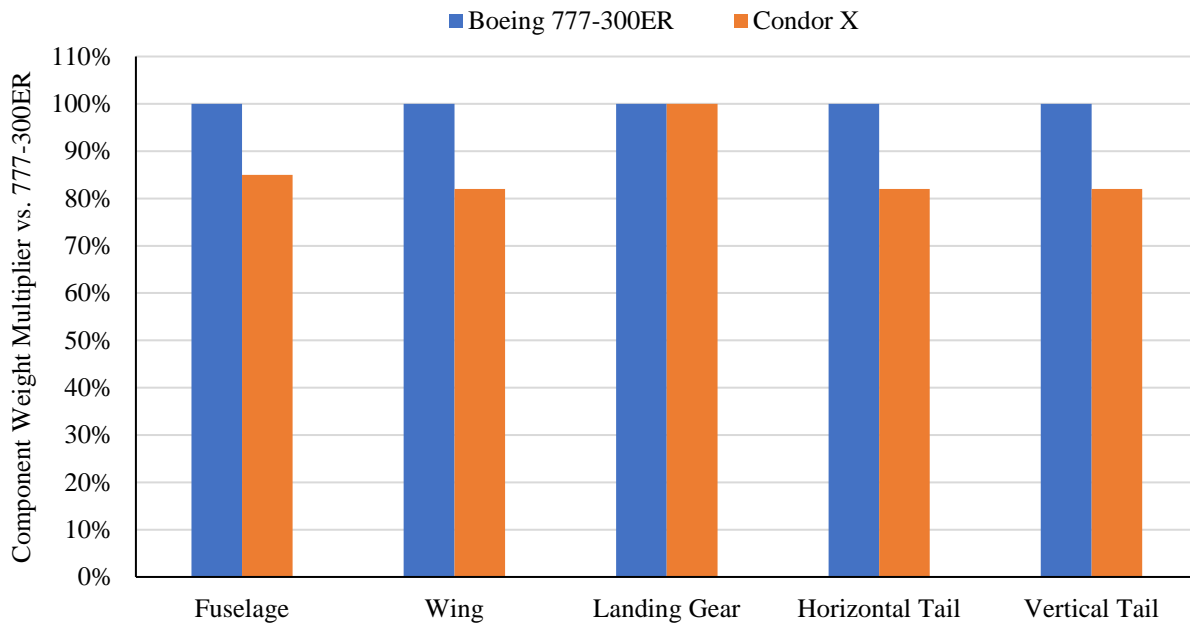
Figure 56. Component weight multiplier comparison between the 777-300ER and the Condor X

Structural Layout

Loads

Based on the V-n diagram in Figure 37, the maximum gust load factor for the Condor X is 3.22. Assuming that this load factor is reached very quickly after takeoff at approximately maximum takeoff weight, (420,373.5 pounds) the maximum aerodynamic load on the structure will be approximately 1,354,000 pounds. An initial estimate for the distribution of this lift force can be made by producing a Trefftz plot in AVL. Figure 57 shows the Trefftz plot produced for a high lift case. Because the lift is concentrated towards the root, most of the load will be transferred directly into the central wing box and from there into the fuselage via keel beams. For that reason, it is imperative that these components are manufactured to the proper yield strength.
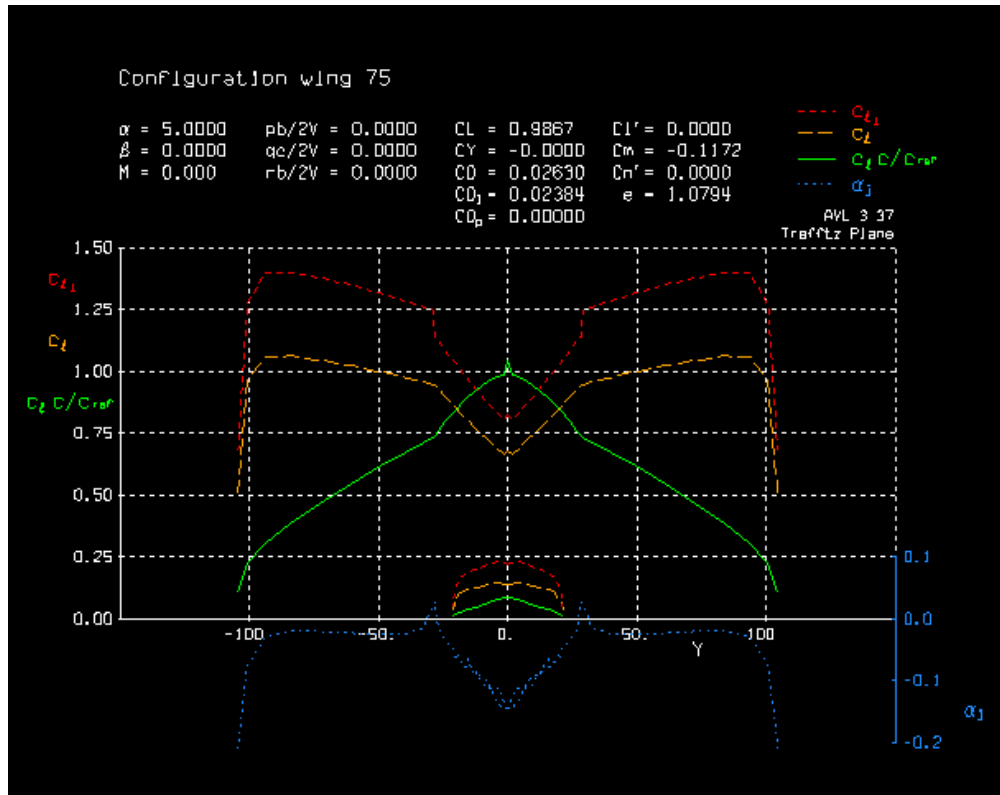
Figure 57. Trefftz plot of Condor X lift distribution at a 5-degree angle of attack

Fuselage

The fuselage structure of the Condor X utilizes a single-barrel design with an outer CFRP skin, which varies between 1 and 2 millimeters (0.04 and 0.08 inches) in thickness. A set of 72 integrated trapezoidal stringers with a pitch of approximately 10 inches runs the length of the fuselage. The skin and stringers will be manufactured and baked in an autoclave together to form a cohesive piece. These stringers have a bottom width of 5 inches, (7 inches including flanges) a top width of 1 inch, and a height of 1.5 inches. They are hollow with an outer thickness of 2.2 millimeters (0.09 inches). The stringers run radially along the entire fuselage except at the window frame locations. In the nose and tail sections, the number of stringers is halved in order to leave room for stringers in the areas where the fuselage is tapered.

The fuselage frames have a c-profile with a thickness of 3 mm and are shaped to bolt directly onto the stringer flanges. The flange width of each frame is 1 inch. These are placed along the fuselage with longitudinal pitch ranging

from 14 to 25.5 inches in order to leave openings for windows and doors. Frames are placed in the center of door openings and cut out at the door locations as necessary to maintain a reasonable frame pitch. The radial thickness of frames is 4.96 inches such that the overall fuselage wall thickness is 5 inches. Floor beams with a thickness of 4.5 inches are placed at the longitudinal location of each frame, which they will be bolted into. For the purposes of preliminary structural design, the frame and stringer dimensions outlined above were based on general values for existing aircraft [55]. A cutout was also placed at the location of the structural wing box. Figure 58 shows a side profile of the fuselage structure.
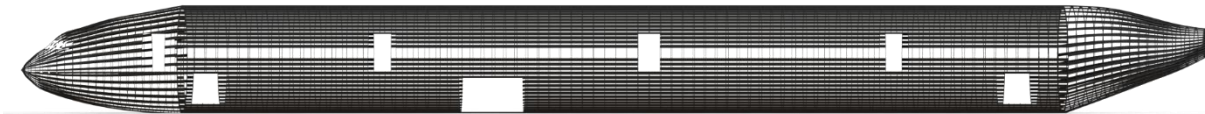
Figure 58. Condor X fuselage structure

Wing

The wing structure consists of two main spars as well as regularly spaced ribs attached to an outer composite skin with a thickness of 7 millimeter (0.28 inches). Z-profile stringers run spanwise along the inside of the skin in between spars to increase stiffness. A central wing box is orthogonal to the fuselage and consists of three spars for increased bending stiffness. The wing box and main structural body of the wing are located such that the landing gear has room to extend and retract behind the structure.

The main spar is located at 25% of the wing chord in order to leave room for slats at the leading edge of the wing and to carry the brunt of the lift force acting on the wing. The rear spar is located at 70% of the wing chord to provide bending stiffness and a direct attachment point for control surfaces and landing gear. The general spar cross-section consists of a 15 millimeter (0.59 inches) thick web attached to the skin with two 5-centimeter (2-inch) thick L-brackets on both the upper and lower surface. Both spar locations are consistent with existing Boeing and Airbus commercial transports [56]. The web thickness is an initial estimate based on a NASA study of the structural loads on the CRM wing, which the Condor X airfoils are based on [57].

The structural ribs remain mostly orthogonal to the leading edge of the wing. The spanwise rib pitch is approximately 24 inches, which is consistent with existing Boeing and Airbus commercial transports [56]. Ribs are cut out in front and behind of the spars in locations where control surfaces exist. An initial rib thickness of 3 millimeters (0.12 inches) was chosen based on the same NASA study used to choose spar web thickness [57]. In order to reduce weight, allow fuel to flow between wing sections, and allow subsystem hydraulic and electrical lines to run along the wing, each rib cross-section includes four circular cut-outs. Figure 59 shows the wing structure.
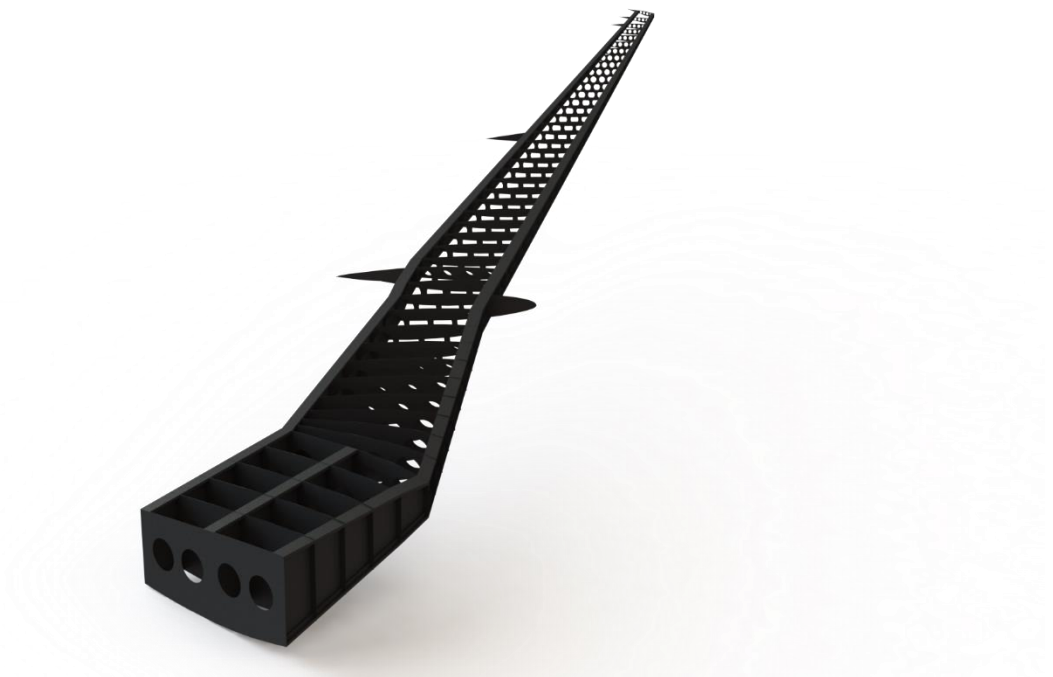
Figure 59. Condor X wing structure

Empennage

The structure of both the vertical and horizontal tail broadly mirrors that of the main wing. The 3 millimeter (0.12 inches) rib thickness and average spanwise rib spacing of approximately 24 inches are the same in the tail as in the wing. However, due to the smaller loads on the tail, the thickness of both the end caps and the web in the front and rear spars was halved in the tail such that the web is 7.5 millimeters (0.30 inches) thick and the L-brackets have a thickness of 2.5 centimeters (1 inch). The Spar locations remained at 25% of the chord for front spars and at

control surface locations for rear spars to allow for direct mounting of control surfaces. Three circular holes were placed in each rib to reduce weight and allow control lines to run along the tail body as was done in the wing. Structural diagrams of both the horizontal and vertical tails are provided in Figure 60 and Figure 61, respectively. Complete diagrams combining all main structural components are shown in Figure 62 and Figure 63.

Figure 60. Condor X horizontal tail structure

Figure 61. Condor X vertical tail structure
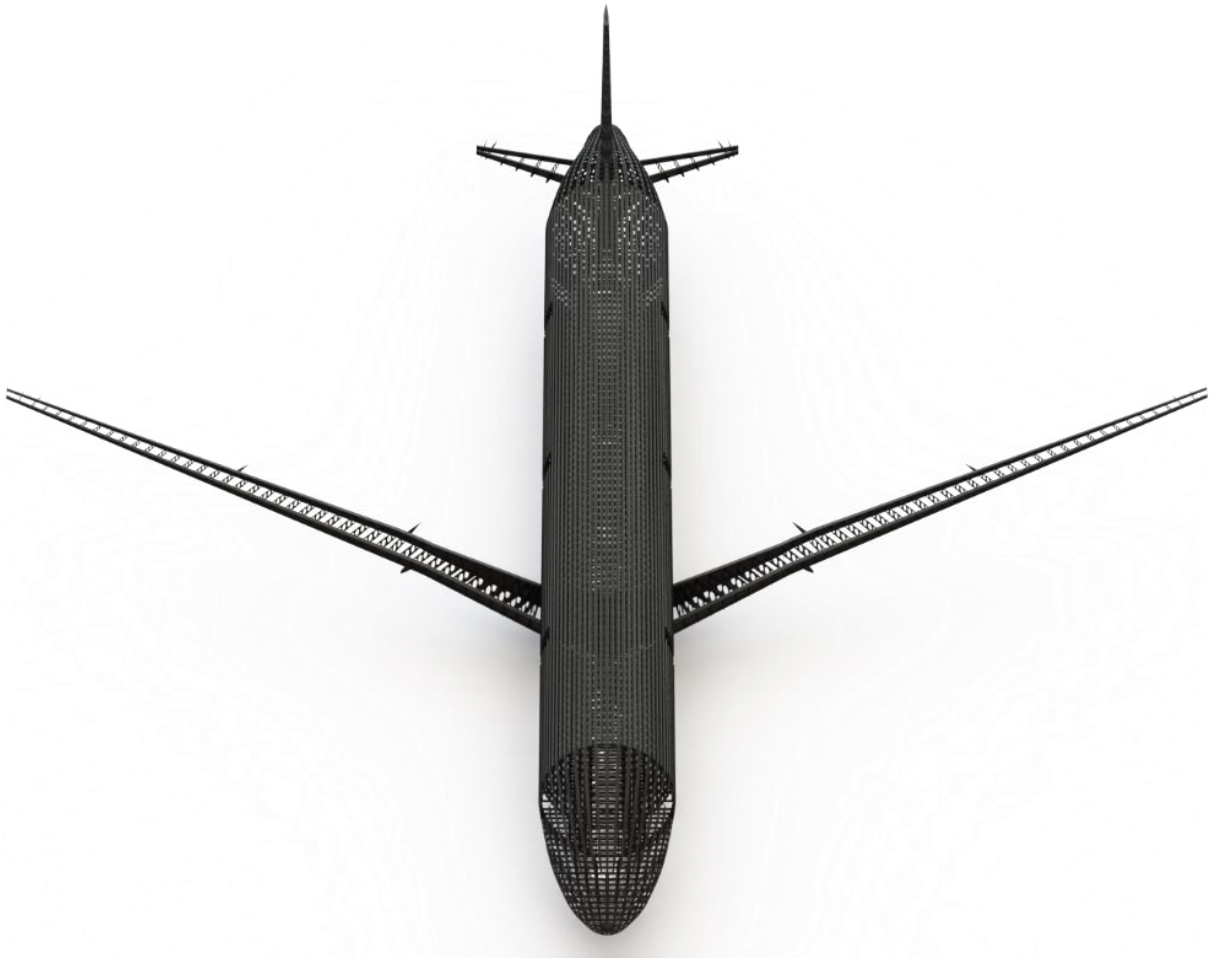
Figure 62. Condor X full structure overhead view

Figure 63. Condor X full structure

Landing Gear

Landing Gear Configuration

The landing gear configuration selection process is straightforward but important to the overall aircraft sizing. The landing gear of an aircraft, in the most critical condition, must bear the entire MTOW of the aircraft if an emergency landing is required promptly after takeoff. As load bearing as they are, they are immensely heavy for their small size, and must be optimized to reduce the aircraft's takeoff weight to increase its overall performance and efficiency. The landing gear configuration in this report is defined as the combination of the number of landing gear, number of bogies (2-tire pairs) for each landing gear and the landing gear placement locations.

With the Condor X designed at around 421,000 pounds MTOW, the simplest option to ensure the landing gear configuration will support the aircraft is to look at other transport aircraft taking off at a similar weight. The closest transport aircraft to the Condor X's weight class is the Boeing 767-400ER at an MTOW of 450,000 pounds [58]. The landing gear configuration of the B767-400ER is as follows: a single bogie nose gear roughly under the

cockpit and two double bogie main landing gears mounted on the inboard section, aft-half of the wings, shown in the Figure 64. This verifies that this configuration will be appropriate for the Condor X, a lighter aircraft.
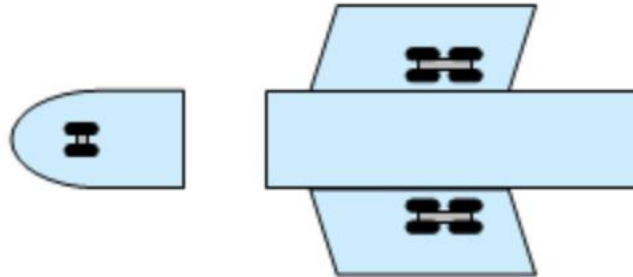

Figure 64. Boeing 767-400ER and selected Condor X undercarriage configuration

However, to optimize the configuration by weight, reducing the number of bogies in the design needs to be investigated. With the nose gear already optimized to the minimum, looking at lighter aircraft for single-bogie main landing gear points to how feasible reducing tire count can be. The heaviest single-bogie main landing gear commercial aircraft leaves the runway at a little over 184,000 pounds [59]. This quickly highlights how unrealistic it is to make the main landing gear of the Condor X have a single bogie, therefore the double bogie configuration was selected.

Rollover Stability

The location of the landing gear directly impacts the on-ground stability of Condor X. The critical condition that influences the placement of the main landing gear away from the centerline is the on-ground rollover stability during taxi, takeoff, and landing. When the aircraft rolls on the ground, one of the main landing gears will lift off the ground and the first part of the aircraft to strike the tarmac is usually the engine nacelle or wing tip. This is the critical condition to design from. The rollover angle is the angle at which the center of gravity moves out of the region between the aircraft's points of contact; this region is shown in Figure 65, and the aircraft is in a stable configuration while the CG remains within the region. The wider the aircraft wheel track (distance between the outermost main landing gear), the larger this region and more inherently stable the aircraft is on its main landing gears. Once the aircraft roll surpasses the rollover angle, the aircraft CG no longer provides a stabilizing moment to get both wheels on the ground but instead works to continue the roll.
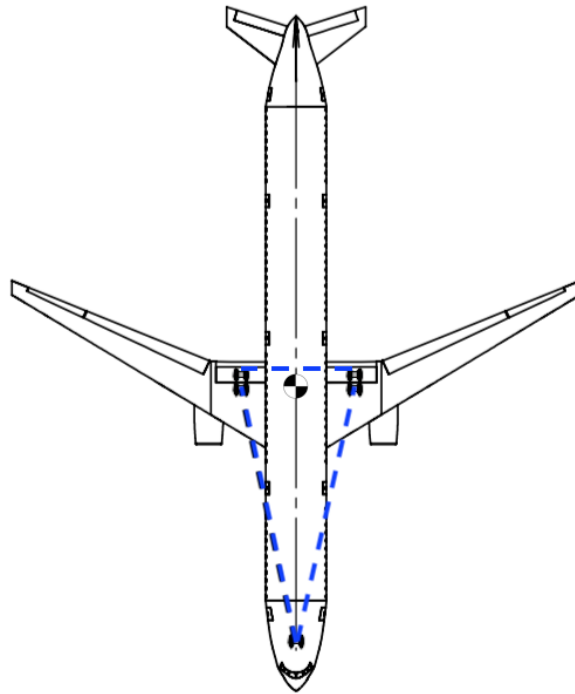
Figure 65. Condor X rollover stability region

Optimally, if the aircraft's engine has not struck the tarmac, the aircraft's CG should stabilize the aircraft and assist rolling it back to all its landing gear. The landing gear wheel track should be large enough to ensure this is the case. However, increasing the wheel track too much results in weight increases in the wing for structural mounts further down the span where it would not otherwise be needed in the wing. Iterating from the centerline, increasing wheel track lengths until a rollover angle is large enough that engine contact will occur before instability, a wheel track of 48 feet was used in the Condor X design. This results in a rollover angle around 42 degrees, while the engine nacelle, with a ground clearance of 131 inches, will strike the ground at a roll of 41 degrees.

Weight and Balance

CG Analysis

The CG location of the Condor X was estimated using the method outlined in Roskam Part V [44] along with individual component/subsystem weights calculated in FLOPS. Passenger CG location however was estimated more thoroughly; all passenger row positions were analyzed individually (along with galleys) to estimate the CG location

of each row, then both passenger classes, and finally the overall CG of all passengers. The overall CG locations can

be found in Table XX. The CG locations are also shown graphically in Figure 66.

Table XX. Center of gravity location of individual aircraft components

| Component	Weight (lb)	X Location (ft)	X Moment (lb-ft)	Z Location (ft)	Z Moment (lb-ft)
Wing	47,800	103.2	4,931,936	16.0	764,800
Horizontal Tail	2,265	212.0	480,180	22.0	49,830
Vertical Tail	2,071	206.0	426,626	32.0	66,272
Fuselage	62,734	100.0	6,273,400	17.0	1,066,478
Main Gear	19,970	108.0	2,156,749	5.0	99,850
Nose Gear	3,524	16.0	56,386	4.0	14,096
Engine	30,291	80.0	2,423,280	12.0	363,492
Surface Controls	3,944	115.0	453,560	17.0	67,048
Aux Power	1,880	205.0	385,400	22.0	41,360
Hydraulics	2,525	108.0	272,700	10.0	25,250
Electrical	3,693	90.0	332,370	15.0	55,395
Avionics/Instruments	2,972	14.0	41,608	16.0	47,552
Furnishings/Eqpt	36,847	102.5	3,776,818	18.0	663,246
Air conditions	3,222	100.0	322,200	24.0	77,328
Icing	314	100.0	31,400	16.0	5,024
Empty	**224,052**	**99.8**	**22,364,612**	**15.2**	**3,407,021**
Crew	2,090	50.0	104,500	20.0	41,800
Passenger Service	7,068	85.0	600,780	19.0	134,292
Cargo Containers	2,161	80.0	172,880	13.0	28,093
Unusable Fuel/Oil	921	87.0	80,127	13.0	11,973
Operating Empty	**236,292**	**98.7**	**23,322,899**	**15.3**	**3,623,179**
Passengers	81,200	121.5	9,869,741	19.0	1,542,800
Baggage	12,180	80.0	974,400	13.0	158,340
Fuel	91,357	100.0	9,135,700	16.0	1,461,712
Gross	**421,029**	**102.8**	**43,302,740**	**16.1**	**6,786,031**
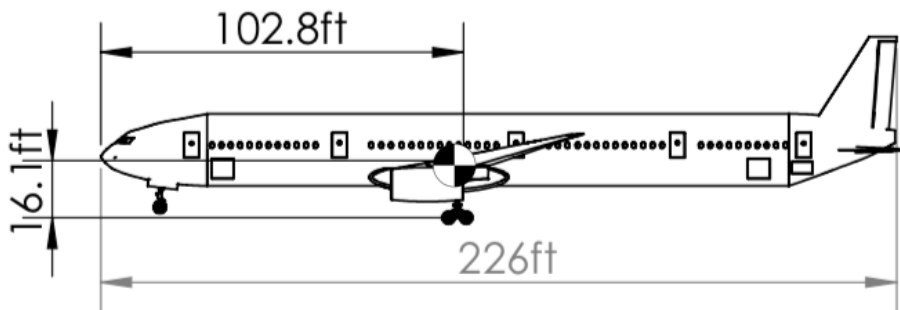
Figure 66. Condor X CG location along the centerline of the aircraft

The parameters in Figure 66 were used alongside the estimated neutral point (discussed later) to iteratively determine the wing and main landing gear position such that the aircraft had sufficient static margin while also satisfying a 15-degree tip-over angle requirement commonly used to account for takeoff rotation and climb out. A static margin of ≥15% at the aft-most CG location was desired to ensure the aircraft would maintain appropriate longitudinal stability. However, the static margin limited to ≤40% so that the aircraft would not require excessive elevator deflection/augmentation to maneuver appropriately. The resulting CG excursion diagrams can be found in Figure 67 and Figure 68. Included in the CG excursion diagram is the main gear contact point, resulting in a longitudinal tip over angle of 15.1 degrees. This exceeds the commonly referenced minimum tip over angle requirement of 15 degrees for takeoff rotation.
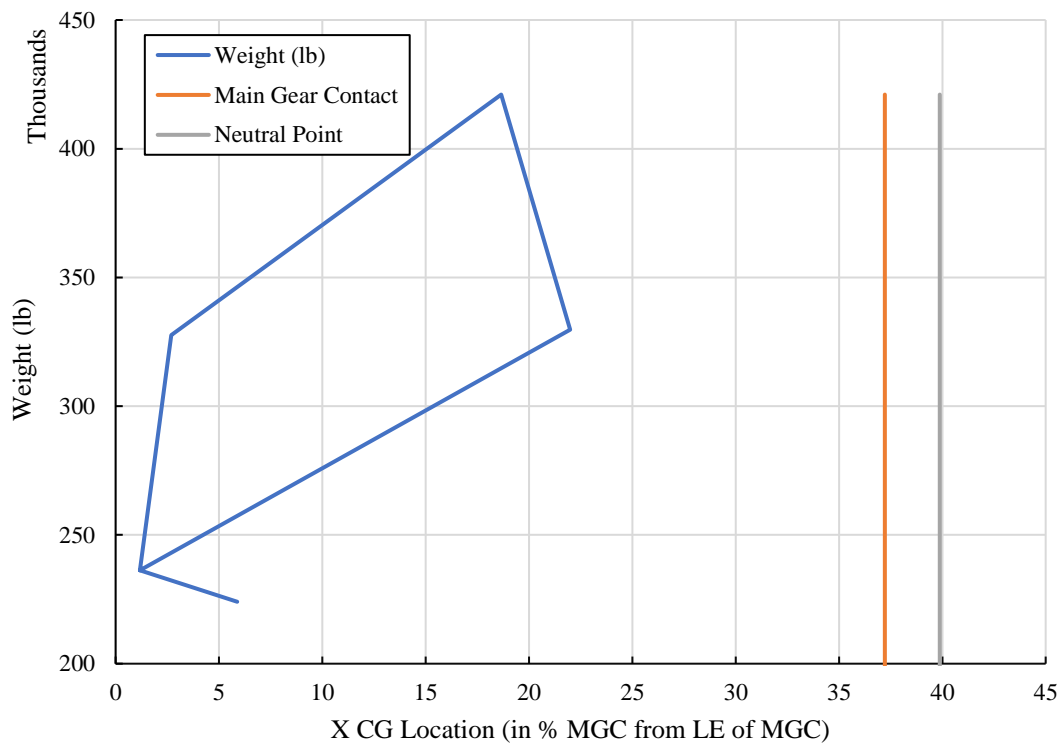

Figure 67. Center of gravity envelope for sizing mission in %MGC (static margin)
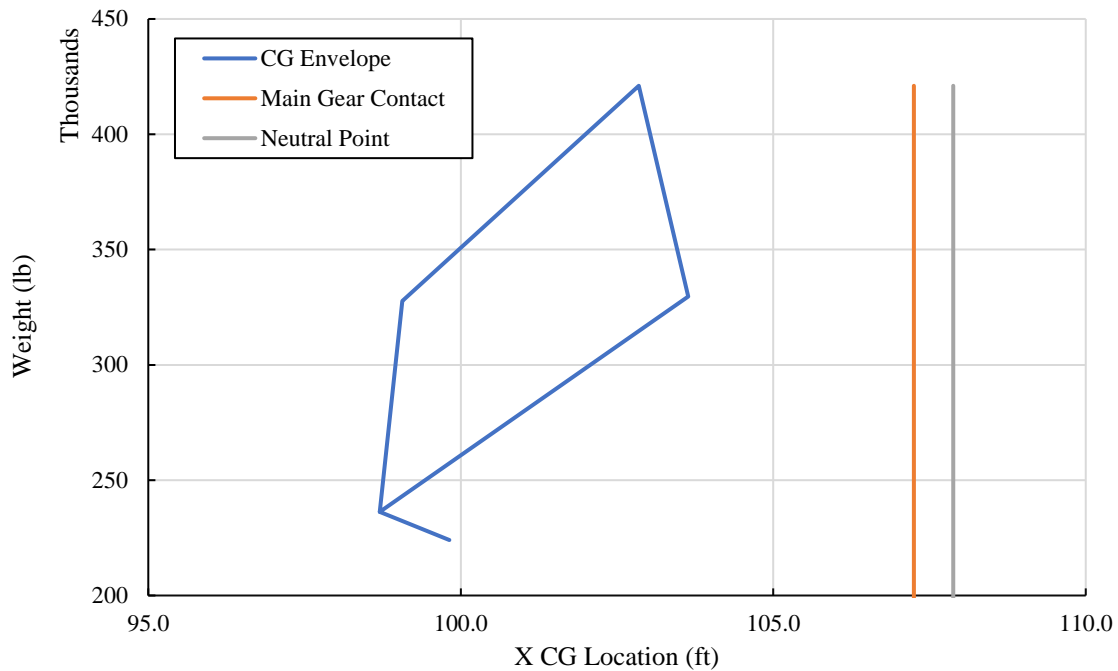
Figure 68. Center of gravity envelope for sizing mission (true location)

Conclusion

The short range, high capacity aircraft designed meets all requirements laid out in the RFP by the AIAA as well as the requirements to be FAA FAR Part 25 certifiable. The resulting aircraft exists in a unique design space compared to all existing aircraft due to its high capacity without the extra weight required to fly long distance. Designing to this specification allows Condor Aviation of fill a niche in which no other aircraft specializes.

To begin preliminary weight sizing, Condor Aviation used FLOPS to iterate from a working model of the Boeing 777-300ER to a novel design more suited to the RFP. Trade studies were implemented to optimize the aircraft's geometry and mission profile. Analyses of propulsion and aerodynamics were conducted to optimize the aircraft for the design mission. New technology in the areas of materials and subsystems were explored to reduce airframe weight. Both a two-class interior layout and a cargo configuration were defined, and a basic structural design was formulated. A cost analysis was performed to help justify the initial business case by comparing the Condor X to competing aircraft. When compared to other aircraft that occupy the same role, the analysis showed that the Condor X is not only

cheaper to produce, but it is also cheaper to operate as well. The Condor X's yearly operating cost is 12 million dollars cheaper when compared to the older 747, and nearly 20 million dollars cheaper than the newer 777.

Condor Aviation believes that the high capacity, short range transport design outlined in this proposal has the potential to fill a large niche in the market occupied by short, high capacity routes which are not currently being flown as efficiently as possible. The state-of-the-art, lightweight, and optimized Condor X is the right choice for airlines new and old to decrease costs and take advantage of expanding domestic air travel markets around the world.

References

[1]   CNN, "World's shortest super jumbo A380 flight," 31 May 2019. [Online]. Available: https://www.cnn.com/travel/article/world-shortest-a380-flight-emirates/index.html. [Accessed 20 January 2020].

[2]   B. o. T. Statistics, "Bureau of Transportation Statistics: Airlines and Airports," [Online]. Available: https://www.bts.gov/topics/airlines-and-airports-0. [Accessed 15 March 2020].

[3]   Airbus, "Global Market Forecast: Cities, Airports, & Aircraft," 2019.

[4]   D. Casey, "Routes Online," 16 September 2018. [Online]. Available: https://www.routesonline.com/news/29/breaking-news/280568/these-are-the-top-100-busiest-routes-on-earth/. [Accessed 5 May 2020].

[5]   L. Harper, "Flight Global," 14 April 2020. [Online]. Available: https://www.flightglobal.com/strategy/iata-deepens-projected-airline-revenue-loss-to-314-billion/137872.article. [Accessed 6 May 2020].

[6]   D. Gates, "Seattle Times," 15 April 2020. [Online]. Available: https://www.seattletimes.com/business/boeing-aerospace/coronavirus-compounds-boeings-crisis-pointing-to-sharp-job-cuts-and-slashed-production/. [Accessed 6 May 2020].

[7]   A. Tangel and R. Wall, "I'm Flying In That? Unloved Turboprop Gets Second Look," Wall Street Journal, 4 February 2019. [Online]. Available: https://www.wsj.com/articles/im-flying-in-that-unloved-turboprop-gets-second-look-11549277255?ns=prod/accounts-wsj. [Accessed 10 April 2020].

[8]   The Boeing Company, 2018 March. [Online]. Available: https://www.boeing.com/resources/boeingdotcom/commercial/airports/acaps/777-9_RevA.pdf. [Accessed February 2020].

[9]   The Boeing Company, May 2015. [Online]. Available: https://www.boeing.com/resources/boeingdotcom/commercial/airports/acaps/777_2lr3er.pdf. [Accessed 2 February 2020].

[10]   L. A. (. McCullers, "Flight Optimization System Release 8.11 User's Guide," Hampton, 2009.

[11]   E. D. Olson, "Semi-Empirical Prediction of Aircraft Low-Speed Aerodynamic Characteristics," NASA Langley Research Center Hampton, VA.

[12]   European Union Aviation Safety Agency, "EASA.IM.E.102: General Electric Company, GEnx Series engines," 13 December 2019. [Online]. Available: https://www.easa.europa.eu/documents/type-certificates/engine-cs-e/easaime102. [Accessed 27 April 2020].

[13] European Union Aviation Safety Agency, "EASA.IM.E.007: General Electric CF6-80E1 Series engines," 25 October 2011. [Online]. Available: https://www.easa.europa.eu/documents/type-certificates/engine-cs-e/easaime007. [Accessed 27 April 2020].

[14] European Union Aviation Safety Agency, "EASA.IM.E.002: General Electric GE90 series engines," 18 December 2019. [Online]. Available: https://www.easa.europa.eu/documents/type-certificates/engine-cs-e/easaime002. [Accessed 27 April 2020].

[15] European Union Aviation Safety Agency, "EASA.IM.E.026: Engine Alliance GP7200 series engines," 4 April 2014. [Online]. Available: https://www.easa.europa.eu/documents/type-certificates/engine-cs-e/easaime026. [Accessed 27 April 2020].

[16] European Union Aviation Safety Agency, "EASA.IM.E.043: Pratt and Whitney PW4000-100 series engines," 7 January 2013. [Online]. Available: https://www.easa.europa.eu/documents/type-certificates/engine-cs-e/easaime043. [Accessed 27 April 2020].

[17] European Union Aviation Safety Agency, "EASA.E.036: Rolls-Royce Deutschland Trent 1000 Series engines," 5 November 2019. [Online]. Available: https://www.easa.europa.eu/documents/type-certificates/engine-cs-e/easae036. [Accessed 27 April 2020].

[18] General Electric Aviation, "Widebody Engine Update: GEnx and GE90," 14 July 2008. [Online]. Available: https://www.geaviation.com/press-release/genx-engine-family/widebody-engine-update-genx-and-ge90. [Accessed 27 April 2020].

[19] R. W. Hess and H. P. Romanoff, "Aircraft Airframe Cost Estimating Relationships: All Mission Types," RAND Corporation, Santa Monica, 1987.

[20] D. P. Raymer, Airfraft Design: A Conceptual Approach, Washington D.C.: AIAA, 1992.

[21] General Electric Aviation, "China Eastern Selects GEnx Engine to Power Its Boeing 787 Dreamliners," 19 June 2017. [Online]. Available: https://www.geaviation.com/press-release/genx-engine-family/china-eastern-selects-genx-engine-power-its-boeing-787-dreamliners. [Accessed 24 April 2020].

[22] S. A. Resetar, J. C. Rogers and R. W. Hess, "Advanced Airframe Structural Materials," RAND Corporation, Santa Monica, 1991.

[23] L. M. Nicolai and G. E. Carichner, Fundamentals of Aircraft and Airship Design, Washington D.C.: AIAA, 2010.

[24] GRA Incorporated, "Economic Values For FAA Investment And Regulatory Decisions, A Guide," GRA Incorporated, Jenkintown, 2007.

[25] U.S. Bureau of Labor Statistics, "Occupational Employment StatisticsOccupational Employment Statistics," U.S. Bureau of Labor Statistics, 31 March 2020. [Online]. Available: https://www.bls.gov/oes/current/oes_nat.htm. [Accessed 24 April 2020].

[26] O. Wyman, "Reported Operating Cost and Utilization of More Than 500 Wide-body Aircraft," Oliver Wyman Group, September 2014. [Online]. Available: https://www.planestats.com/bhsw_2014sep. [Accessed 24 April 2020].

[27] T. Stalnaker, K. Usman and A. Taylor, "Airline Economic Analysis," Oliver Wyman Group, 2016.

[28] "Carbon Dioxide Emissions Coefficients," U.S. Energy Information Administration, 2 February 2016. [Online]. Available: https://www.eia.gov/environment/emissions/co2_vol_mass.php. [Accessed 28 April 2020].

[29] The Boeing Company, [Online]. Available: https://web.archive.org/web/20140724231620/http://www.boeing.com/assets/pdf/commercial/startup/pdf/747-8_perf.pdf. [Accessed 28 April 2020].

[30] European Environment Agency, "Group 8: Other mobile sources and machinery," 20 April 2016. [Online]. Available: https://www.eea.europa.eu/publications/EMEPCORINAIR5/page017.html. [Accessed 28 April 2020].

[31] V. Bhaskara, "UPDATED ANALYSIS: Delta Order for A350; A330neo Hinged on Pricing, Availability," Airways News, 25 November 2014. [Online]. Available: https://web.archive.org/web/20151117045118/http://airwaysnews.com/blog/2014/11/25/analysis-delta-order-for-a350-a330neo-hinged-on-pricing-availability/. [Accessed 28 April 2020].

[32] V. Bhaskara, "ANALYSIS: The Boeing 787-8 and Airbus A330-800neo are Far From Dead," Airways News, 17 March 2016. [Online]. Available: https://web.archive.org/web/20160320082220/http://airwaysnews.com/blog/2016/03/17/boeing-787-8-a330-800neo-far-from-dead/. [Accessed 28 April 2020].

[33] V. Bhaskara, "ANALYSIS: A320neo vs. 737 MAX: Airbus is Leading (Slightly) – Part II," Airways News, 5 February 2016. [Online]. Available: https://web.archive.org/web/20160206082857/http://airwaysnews.com/blog/2016/02/05/a320neo-vs-737-max-pt-ii/. [Accessed 28 April 2020].

[34] Boeing, 2007. [Online]. Available: http://www.boeing.com/resources/boeingdotcom/company/about_bca/startup/pdf/historical/757_passenger.pdf. [Accessed 28 April 2020].

[35] Leeham News and Analysis, "CS300 first flight Wednesday, direct challenge to 737-7 and A319neo," 5 February 2015. [Online]. Available: https://leehamnews.com/2015/02/25/cs300-first-flight-wednesday-direct-challenge-to-737-7-and-a319neo/. [Accessed 4 April 2020].

[36] International Civil Aviation Organization, "Annex 16 to the Convention on International Civil Aviation," March 2017. [Online]. Available: https://www.fzt.haw-hamburg.de/pers/Scholz/materialFM1/ICAO-2017_Annex16_Volume3_CO2CertificationRequirement.pdf. [Accessed 28 April 2018].

[37] Advanced Research Projects Agency–Energy, "METALS Program Overview," Advanced Research Projects Agency–Energy, Washington DC, 2013.

[38] S. Ziadeh, "Carbon Footprint of Pultruded Composite Products Used in Automotive Applications," Tampere University of Technology, Tampere, 2015.

[39] J. C. Vassberg and M. S. Rivers, "Development of a Common Research Model," 2008. [Online]. Available: https://commonresearchmodel.larc.nasa.gov/files/2015/04/AIAA-2008-6919-Vassberg_compliant2.pdf. [Accessed 21 April 2020].

[40] M. S. Rivers, "Experimental Results," 13 June 2017. [Online]. Available: https://commonresearchmodel.larc.nasa.gov/experimental-data/. [Accessed 21 4 2020].

[41] K. Min, R. Plumley and A. Brooks, "Boeing 747," Virginia Tech, 2007. [Online]. Available: http://www.dept.aoe.vt.edu/~mason/Mason_f/B747PresS07.pdf?q=747. [Accessed 21 4 2020].

[42] M. S. Rivers, "IGES Files," 12 September 2017. [Online]. Available: https://commonresearchmodel.larc.nasa.gov/geometry/iges-files/. [Accessed 21 April 2020].

[43] L. A. (. McCullers, "Flight Optimization System," NASA Langley Research Center, Hampton, VA.

[44] J. Roskam, Aircraft Design Part V, Lawrence: Design, Analysis, and Research Corporation, 1999.

[45] "A380 pushes 5000 psi into realm of the common man," Hydraulics and Pneumatics, 30 November 2002. [Online]. Available: https://www.hydraulicspneumatics.com/applications/aerospace/article/21884281/a380-pushes-5000-psi-into-realm-of-the-common-man. [Accessed 4 April 2020].

[46] "RECARO SL3710 Economy Class seat," [Online]. Available: https://www.recaro-as.com/en/aircraft-seats/economy-class/sl3710.html. [Accessed 24 April 2020].

[47] "RECARO CL4400," [Online]. Available: https://www.recaro-as.com/en/aircraft-seats/business-class/cl4400.html. [Accessed 24 April 2020].

[48] P. G. a. M. G. V. Madonna, "Electrical Power Generation in Aircraft: review,," IEEE, Nottingham, 2018.

[49] J. Hale, "Boeing 787 From the Ground Up," *Aeromagazine,* 2006.

[50] MIT OpenCourseWare, "Sandwich Panel Notes," 2015. [Online]. Available: https://ocw.mit.edu/courses/materials-science-and-engineering/3-054-cellular-solids-structure-

properties-and-applications-spring-2015/lecture-notes/MIT3_054S15_L17_trans.pdf. [Accessed 21 April 2020].

[51] "Advanced Composite Use," Boeing, [Online]. Available: https://www.boeing.com/commercial/787/by-design/#/advanced-composite-use. [Accessed 21 April 2020].

[52] C. Fualdes, "Experience and lessons learned of a Composite Aircraft," in *ICA*, Daejeon, 2016.

[53] Airbus, "Composites: Airbus continues to shape the future," 1 August 2017.

[54] G. Gardiner, "Airbus A350 Update: BRaF & FPP," CompositesWorld, 2 January 2012. [Online]. Available: https://www.compositesworld.com/articles/airbus-a350-update-braf-fpp. [Accessed 21 April 2020].

[55] Z. Mikulik and P. Haase, "Composite Damage Metrics and Inspection," EASA, Hamburg, 2012.

[56] M. D. Sensmeier and J. A. Samareh, "A Study of Vehicle Structural Layouts in Post-WWII," NASA, Prescott, 2004.

[57] B. K. Stanford and P. D. Dunning, "Optimal Topology of Aircraft Rib and Spar Structures under," NASA, Hampton, 2014.

[58] C. Brady, "History & Development of the Boeing 737 - NGs," The Boeing 737 Technical Site, 3 August 2000. [Online]. Available: http://www.b737.org.uk/737ng.htm#737-900. [Accessed 26 April 2020].

[59] H. Queen, "Introducing the 767-400 Extended Range Airplane," 1998. [Online]. Available: https://www.boeing.com/commercial/aeromagazine/aero_03/textonly/ps01txt.html.

[60] D. Staff, "High pressure, low weight," Design News, 9 September 2002. [Online]. Available: https://www.designnews.com/aerospace/high-pressure-low-weight/156143108941242. [Accessed 24 April 2020].